

## On the origin of pronounced O<sub>3</sub> gradients in the thunderstorm outflow region during DC3

H. Huntrieser<sup>1</sup>, M. Lichtenstern<sup>1</sup>, M. Scheibe<sup>1</sup>, H. Aufmhoff<sup>1</sup>, H. Schlager<sup>1</sup>, T. Pucik<sup>1,2</sup>, A. Minikin<sup>1</sup>, B. Weinzierl<sup>1,3</sup>, K. Heimerl<sup>1</sup>, D. Fütterer<sup>1</sup>, B. Rappenglück<sup>4</sup>, L. Ackermann<sup>4</sup>, K. E. Pickering<sup>5</sup>, K. A. Cummings<sup>6</sup>, M. I. Biggerstaff<sup>7</sup>, D. P. Betten<sup>7</sup>, S. Honomichl<sup>8</sup>, and M. C. Barth<sup>8</sup>

[1] {Institut für Physik der Atmosphäre, Deutsches Zentrum für Luft- und Raumfahrt (DLR), Oberpfaffenhofen, Germany}

[2] {Masaryk University, Brno, Czech Republic}

[3] {now at: University of Vienna, Faculty of Physics, Vienna, Austria}

[4] {Department of Earth & Atmospheric Sciences, University of Houston, TX, USA}

[5] {Atmospheric Chemistry and Dynamics Laboratory, NASA Goddard Space Flight Center Greenbelt, MD, USA}

[6] {Department of Atmospheric & Oceanic Science, University of Maryland, College Park, MD, USA}

[7] {School of Meteorology, University of Oklahoma, Norman, OK, USA}

[8] {NCAR, Boulder, CO, USA}

Corresponding Author: H. Huntrieser, Institut für Physik der Atmosphäre, Deutsches Zentrum für Luft- und Raumfahrt (DLR) Oberpfaffenhofen, Postfach 1116, D-82230 Weßling, Germany (Heidi.Huntrieser@dlr.de)

This article has been accepted for publication and undergone full peer review but has not been through the copyediting, typesetting, pagination and proofreading process which may lead to differences between this version and the Version of Record. Please cite this article as doi: 10.1002/2015JD024279

## Abstract

Unique in-situ measurements of CO, O<sub>3</sub>, SO<sub>2</sub>, CH<sub>4</sub>, NO, NO<sub>x</sub>, NO<sub>y</sub>, VOC, CN, and rBC were carried out with the German DLR-Falcon aircraft in Central U.S. thunderstorms during the Deep Convective Clouds and Chemistry (DC3) experiment in summer 2012. Fresh and aged anvil outflow (9-12 km) from supercells, mesoscale convective systems, mesoscale convective complexes, and squall lines were probed over Oklahoma, Texas, Colorado, and Kansas. For three case studies (May 30, June 8 and 12) a combination of trace species, radar, lightning, and satellite information, as well as model results, were used to analyze and design schematics of major trace gas transport pathways within and in the vicinity of the probed thunderstorms. The impact of thunderstorms on the O<sub>3</sub> composition in the upper troposphere (UT) / lower stratosphere (LS) region was analyzed. Overshooting cloud tops injected high amounts of biomass burning and lightning-produced NO<sub>x</sub> emissions into the LS, in addition to low O<sub>3</sub> mixing ratios from the lower troposphere. As a dynamical response, O<sub>3</sub>-rich air from the LS was transported downward into the anvil and also surrounded the outflow. The  $\Delta\text{O}_3/\Delta\text{CO}$  ratio was determined in the anvil outflow region. A pronounced in-mixing of O<sub>3</sub>-rich stratospheric air masses was observed in the outflow indicated by highly positive or even negative  $\Delta\text{O}_3/\Delta\text{CO}$  ratios (+1.4 down to -3.9). Photochemical O<sub>3</sub> production ( $\Delta\text{O}_3/\Delta\text{CO} = +0.1$ ) was found to be minor in the recently lofted pollution plumes. O<sub>3</sub> mixing ratios within the aged anvil outflow were mainly enhanced due to dynamical processes.

### Key points:

- Overshooting of Central U.S. severe thunderstorms probed in-situ by aircraft.
- $\Delta\text{O}_3/\Delta\text{CO}$  ratios were determined for fresh and aged (~12-24 h) anvil outflow.
- O<sub>3</sub> enhanced (~20-50 nmol mol<sup>-1</sup>) in the aged anvil outflow mainly due to dynamical processes.

Keywords: thunderstorms, UT/LS, ozone, nitrogen oxides, wildfires

## 1 Introduction

Ozone ( $O_3$ ) plays a key role for the chemical composition in the atmosphere and acts as a prominent greenhouse gas in the upper troposphere (UT) [Myhre *et al.*, 2013]. The main sources of tropospheric ozone are photochemical production and downward transport (entrainment) of  $O_3$ -rich air from the stratosphere [Crutzen, 1995; Stevenson *et al.*, 2006]. Emissions from natural and anthropogenic sources in the boundary layer (BL) (e.g. wildfires and fossil fuel combustion) are rich in  $O_3$  precursors such as carbon monoxide (CO), methane ( $CH_4$ ), and volatile organic compounds (VOCs) and can be uplifted to the UT by warm conveyor belts and/or deep convection [Cooper *et al.*, 2004]. In the UT,  $O_3$  precursors are emitted from lightning-produced  $NO_x$  ( $\triangleq NO + NO_2$ ) (LNO $_x$ ) and aircraft, where LNO $_x$  ( $5 \pm 3$  Tg a $^{-1}$ ) is the most important natural  $O_3$  precursor in the UT [Schumann and Huntrieser, 2007]. In the presence of hydrogen oxides ( $HO_x = HO + HO_2$ ) and NO (also from anthropogenic sources)  $O_3$  can be produced by photochemical oxidation of the precursors [Crutzen, 1970; Fishman *et al.*, 1979]. Due to the increasing lifetime of tropospheric  $NO_x$  with altitude (a few hours in the BL and  $\sim 2$ -3 days in the UT), it is possible to trace thunderstorm outflow  $\sim 1$ -2 days after the thunderclouds have dissipated [Huntrieser *et al.*, 2002].

Due to the large variety of the processes mentioned above, measurements inside and in the vicinity of thunderstorms have shown a wide spectrum of  $O_3$  mixing ratios. Almost zero ozone has been measured in the convective outflow over remote unpolluted regions (e.g. tropical Pacific) because of direct upward transport of low  $O_3$  mixing ratios from the marine BL [Kley *et al.*, 1996; Folkins *et al.*, 2002]. Elevated  $O_3$  in the range of 100 ppbv (or  $nmol\ mol^{-1}$ ) has been observed in the outflow of continental thunderstorms as a result of convective transport of surface polluted air followed by downwind chemistry [Pickering *et al.*, 1990, 1996]. Extreme  $O_3$ -rich transients of a few hundred up to  $\sim 2000$   $nmol\ mol^{-1}$   $O_3$  have been measured in humidified air masses affected by convection over tropical oceanic and rain forest areas possibly because of natural and artificial corona discharges [Zahn *et al.*, 2002; Ridley *et al.*, 2006; Bozem *et al.*, 2014], on the other hand a stratospheric influence has been suggested [Suhre *et al.*, 1997]. Further explanations for this wide  $O_3$  range observed in fresh and aged anvil outflow are discussed below and in Sect. 5. A method to distinguish the

different processes impacting the O<sub>3</sub> composition is described next.

Ozone enhancements observed in the troposphere, whether photochemically produced or transported downward from the stratosphere, are generally distinguished by the sign of the O<sub>3</sub>-CO correlation, as introduced by *Fishman and Seiler* [1983] for aircraft measurements. In the stratosphere, CO decreases with increasing O<sub>3</sub> mixing ratios. Negative O<sub>3</sub>-CO regression slopes characterize the downward transport of stratospheric air masses into the troposphere. Positive slopes have been observed in aged lofted pollution and biomass burning (BB) plumes rich in CO and photochemically produced O<sub>3</sub>, not only in the tropics but also at higher latitudes [*Parrish et al.*, 1993; *Chin et al.*, 1994; *Singh et al.*, 2010; *Jaffe and Wigder*, 2012]. The linear regression slope of the O<sub>3</sub>-CO correlation can also be expressed as  $\Delta O_3/\Delta CO$  ratio in nmol mol<sup>-1</sup>/nmol mol<sup>-1</sup>. Up to now, not much is known about which of the above mentioned processes dominate the O<sub>3</sub> budget and the O<sub>3</sub>-CO correlation within the anvil outflow from thunderstorms. *The main objective of the present study is to analyze processes affecting the O<sub>3</sub> composition in the UT / lower stratosphere (LS) region over the Central United States (U.S.) during the Deep Convective Clouds and Chemistry (DC3) experiment.* More specifically: *Which  $\Delta O_3/\Delta CO$  ratios were observed within and in the vicinity of the probed thunderstorms and how can they be explained?* The DC3 field experiment has been described in detail by *Barth et al.* [2015] and in **HH2016** (which refers to *Huntrieser et al.*, 2016). In the present study details on DC3 are given later in this section and in Sect. 2.

The major processes that may affect the O<sub>3</sub> composition in the thunderstorm outflow region and its range are briefly summarized next: (a) photochemical O<sub>3</sub> production by BB emissions, (b) photochemical O<sub>3</sub> production by LNO<sub>x</sub> emissions, and (c) stratosphere-troposphere exchange.

a) Photochemical O<sub>3</sub> production by BB (and mixed in anthropogenic) emissions:

In general, anthropogenic pollution sources were low in the DC3 thunderstorm inflow regions over the Central U.S. [*Barth et al.*, 2015; *HH2016*]. However, during DC3 some of the largest and most destructive wildfires in New Mexico and Colorado state's history were burning, which strongly influenced air quality in the DC3 thunderstorm inflow and outflow region, as described later (see Sect. 3). In a review article by *Jaffe and Wigder* [2012], *the O<sub>3</sub>-CO regression slope in air masses impacted by wildfires was given a range from -0.1 to +0.9*, however most likely from nearly zero to +0.7, based on many single observations around the

world. In boreal regions, O<sub>3</sub>-CO ratios tend to be low (O<sub>3</sub> enhancement <5 nmol mol<sup>-1</sup>), due to a low nitrogen content in boreal vegetation and low emission rates of urban pollution (O<sub>3</sub> precursors) [Alvarado *et al.*, 2010; Singh *et al.*, 2010]. Furthermore, the cooler temperature and lower insolation in these regions favor slow O<sub>3</sub> production rates. In the mid to upper troposphere (5-9 km) at high northern latitudes, Singh *et al.* [2010] reported a correlation ratio of  $\Delta\text{O}_3/\Delta\text{CO}=+0.1$  in aged BB and urban plumes observed during ARCTAS. A tendency to higher correlation ratios (up to +0.5) has been observed in BB plumes mixed with heavier urban pollution over North America (NA) [Hecobian *et al.*, 2011; Wigder *et al.*, 2013]. In aged BB plumes affected by tropical deep convection, an O<sub>3</sub> formation rate of 7-8 nmol mol<sup>-1</sup> per day has been calculated in case studies and an O<sub>3</sub> enhancement in the range of 30 nmol mol<sup>-1</sup> after 5 days transport has been observed [Pickering *et al.*, 1996; Thompson *et al.*, 1997]. Elevated  $\Delta\text{O}_3/\Delta\text{CO}$  ratios, up to +0.8, have been observed in Asian pollution plumes transported in the UT to NA [Price *et al.*, 2004; Bertschi and Jaffe, 2005; Liang *et al.*, 2007]. Both strong photochemical production due to high pollution levels and mixing processes with stratospheric air masses along isentropic surfaces have been suggested as explanations for these high ratios. A number of observations have shown that the interweaving of stratospheric intrusions with pollution plumes may complicate the fine-scale  $\Delta\text{O}_3/\Delta\text{CO}$  correlations [Parrish *et al.*, 2000; Nowak *et al.*, 2004; Price *et al.*, 2004; Liang *et al.*, 2007].

#### b) Photochemical O<sub>3</sub> production by LNO<sub>x</sub>:

In the literature a wide range of *convective ozone production enhancements ranging up to ~20 nmol mol<sup>-1</sup> per day* have been published (see Table 1 in Morris *et al.*, 2010 and Table 3 in Bozem *et al.*, 2014). However, ozone production rates as high as ~5 nmol mol<sup>-1</sup> per hour, as found in Morris *et al.* [2010] study, may be unrealistic. Model simulations indicate that most of the O<sub>3</sub> production happens within the first 24 h after convection occurs [Barth *et al.*, 2012]. In cases with higher production rates, the presence of anthropogenic pollution and BB emissions, in addition to LNO<sub>x</sub>, seems to play an important role for the enhanced O<sub>3</sub> production in the convective outflow [Real *et al.*, 2010]. Recently the importance of isoprene (emitted from vegetation) for especially high O<sub>3</sub> production rates in modeled LNO<sub>x</sub> plumes has been pointed out [Apel *et al.*, 2012]. For a STERAO-A thunderstorm (Central U.S.) and a EULINOX thunderstorm (southern Germany), where mainly LNO<sub>x</sub> played a role for the O<sub>3</sub> production, DeCaria *et al.* [2005] and Ott *et al.* [2007] calculated O<sub>3</sub> production rates on the order of ~5 and up to 13 nmol mol<sup>-1</sup> per day, respectively. For a tropical thunderstorm over

Suriname, *Bozem et al.* [2014] calculated a production rate of 5-11 nmol mol<sup>-1</sup> O<sub>3</sub> per day based on HO<sub>x</sub> measurements over the tropical rain forest. For two DC3 thunderstorms strongly impacted by BB emissions on June 22, 2012 box model calculations (initialized with measurements in the outflow) by *Apel et al.* [2015] predicted a production rate of 11 and 14 nmol mol<sup>-1</sup> O<sub>3</sub>, respectively, over a two-day period.

c) Stratosphere-troposphere exchange:

Besides the strong influence of BB plumes on the thunderstorm environment during DC3, the interaction with O<sub>3</sub>-rich air masses from the stratosphere was also prominent as already mentioned in *HH2016*. Evidence from aircraft and satellite observations of extratropical convection injecting BL air into the lowermost stratosphere (LMS), e.g. forming filaments 50-100 km in width and several 1000 km in length, has already been reported in previous studies [*Roach*, 1967; *Poulida et al.*, 1996; *Fischer et al.*, 2003; *Hegglin et al.*, 2004; *Ray et al.*, 2004; *Anderson et al.*, 2012; *Homeyer et al.*, 2014]. Besides the deep convective upward transport, traces of downward intrusions of O<sub>3</sub>-rich air masses from the stratosphere into the anvil outflow region have been modeled in a number of studies [*Wang et al.*, 1995; *Stenchikov et al.*, 1996; *Tang and Prather*, 2010; *Homeyer et al.*, 2011; *Tang et al.*, 2011; *Frey et al.*, 2015]. However, this process has infrequently been observed before the DC3 field experiment was conducted. Only a few observations are available [*Dickerson et al.*, 1987; *Poulida et al.*, 1996; *Winterrath et al.*, 1999; *Dye et al.*, 2000; *Hitchman et al.*, 2004; *Homeyer et al.*, 2011]. Different processes have been described in the literature causing a downward intrusion. *Boatman and Auer* [1983] and *Blyth et al.* [1988] introduced the so-called “cloud top entrainment” mechanism: O<sub>3</sub>-rich air masses from above mixes into the upper tropospheric anvil outflow. A distinct rear inflow from the stratosphere was observed in a Mesoscale Convective System (MCS) by *Houze et al.* [1989] based on Doppler radar analyses. Recently *Pan et al.* [2014] presented the first evidence in lidar images of a pronounced downward transport of O<sub>3</sub>-rich stratospheric air masses wrapping around the anvil outflow of a MCS during DC3. Evidence of mixing between polluted convective outflow and stratospheric air in the UT during DC3 was recently also described by *Schroeder et al.* [2014].

As previously stated, the objective of the present study is to investigate if and how the above mentioned processes a), b), and c) affected the O<sub>3</sub> composition in the thunderstorm outflow region during DC3. The airborne in-situ thunderstorm observations presented throughout this

paper will contribute to answer the following questions. (1) *Did deep convection during DC3 substantially impact the O<sub>3</sub> budget in the UT/LS region?* (2) *What processes, coinciding with DC3 deep convection, affect the O<sub>3</sub> budget over the Central U.S.: chemical and/or dynamical processes?* (3) *Which of these processes dominate the O<sub>3</sub> budget in the fresh and aged (0-12/12-24 h) thunderstorm outflow during DC3?*

The DC3 field campaign was carried out from Kansas in May-June 2012. The general experimental set up is described by *Barth et al.* [2015]. An accompanying DC3 study is introduced in *HH2016* where measurements with the German research aircraft of the Deutsches Zentrum für Luft- und Raumfahrt (DLR), a Falcon-20, and one joint flight with the two U.S. aircraft (NASA-DC8 and NSF/NCAR-GV) are presented. In *HH2016* the primary objective is to give an overview of the Falcon measurements and to study emissions from wildfires and LNO<sub>x</sub> within and in the vicinity of the fresh thunderstorm outflow. A secondary objective is to analyze the dynamics of a single storm system and its impact on the O<sub>3</sub> and aerosol composition in the UT/LS region. The analyses are based on vertical profiles of trace species and tracer-tracer correlations (CO-NO<sub>x</sub> and O<sub>3</sub>-NO). The stratosphere-troposphere exchange of O<sub>3</sub> and H<sub>2</sub>O is touched upon, however the exchange of O<sub>3</sub> is highlighted first in the present study.

Here we show detailed analyses based on three Falcon flights during DC3. During these flights the fresh and aged anvil outflow in supercells, Mesoscale Convective Complexes (MCCs), MCSs, and squall lines were probed extensively with the Falcon up to 12 km altitude (for storm definitions see *Maddox*, 1980; *Houze et al.*, 1989; and *Houze*, 2004). A number of trace species, such as sulphur dioxide (SO<sub>2</sub>), CO, O<sub>3</sub>, CH<sub>4</sub>, NO, NO<sub>x</sub>, NO<sub>y</sub>, VOCs, condensation nuclei (CN), and refractory black carbon (rBC) were measured in-situ with the Falcon. On the basis of trace species time series and tracer-tracer correlations (O<sub>3</sub>-CO) the impact on the UT/LS O<sub>3</sub> composition from LNO<sub>x</sub> and BB emissions, and from dynamical processes is analyzed.

The DC3 field experiment and the data products are briefly described in Sect. 2. A general overview of the CO and O<sub>3</sub> composition in selected wildfire plumes and their O<sub>3</sub>-CO correlation are given in Sect. 3. Three detailed thunderstorm case studies are presented in Sect. 4 based on Falcon time series of a variety of trace species and the O<sub>3</sub>-CO correlation within and in the vicinity of the thunderstorm outflow. The May 30, 2012 case focuses on the fresh supercell and MCC outflow over Texas and Oklahoma, whereas the June 8 and 12,

2012 cases focus on the aged MCS and fresh squall line outflow over Colorado and Kansas, respectively. In Sect. 5 the pronounced  $O_3$  gradients observed in the DC3 thunderstorm outflow region are discussed in detail. The summary and conclusions are given in Sect. 6.

## 2 DC3 field experiment and data products

### 2.1 The DC3 field experiment focusing on Falcon measurements

A detailed overview of the DC3 field experiment is given by *Barth et al.* [2015]. For a detailed overview of previous studies on thunderstorms and chemistry over the U.S., and the motivation for the DC3 field experiment, see also *Barth et al.* [2015]. The DC3 field phase was carried out from May 1, to June 30, 2012 with three different aircraft platforms in operation and several ground-based observations. All three research aircraft, the NSF/NCAR Gulfstream-V (GV), NASA-DC8, and DLR-Falcon, were based at the airport in Salina, Kansas (38.8° N, 97.6° W). The Falcon performed mission flights in the time period May 27 to June 17 to Colorado, Wyoming, Nebraska, Missouri, Arkansas, Oklahoma, Texas, and New Mexico. For more details see *HH2016*. The aircraft was equipped with a variety of trace species instruments, see Table 1 herein. Our main target regions over the Central U.S. were fresh and aged (0-12/12-24 h) anvil outflow in the UT up to 12.4 km altitude, and fresh and aged plumes from wildfires in the lower, mid, and upper troposphere. The anvil outflow was probed from different types of convective systems, i.e. supercells, MCCs, MCSs, and squall lines (SQLs).

In the present study, we analyze a variety of in-situ trace species measurements ( $CO$ ,  $O_3$ ,  $SO_2$ ,  $CH_4$ ,  $NO$ ,  $NO_x$ ,  $NO_y$ ,  $CN$ , and  $rBC$ ) sampled by the DLR-Falcon. During each flight several VOC samples were taken. In addition, a video camera was mounted in the Falcon cockpit monitoring the entire flight from start to landing. The videos were partly used to determine the in-cloud time sequences in the anvil outflow and the presence of smoke from wildfires. Further the Falcon was equipped with a standard meteorological measurement system to measure position, altitude, temperature, pressure, humidity and the 3-dimensional wind vector ( $u$ ,  $v$ ,  $w$ ). These data were also needed for the calculation of the potential ( $\Theta$ ) and equivalent-potential temperature ( $\Theta_e$ ). For the computation of  $\Theta_e$  for a water-saturation pseudo-adiabatic process, the formula suggested by *Bolton* [1980] was used for the Falcon data (see also *Huntrieser et al.*, 2007). All flight altitude values refer to pressure height and UTC (Universal Time Coordinated) time. The time difference between UTC and the Central



Daylight Time (CDT) in Salina is +5h (e.g. 06:00 CDT = 11:00 UTC).

## 2.2 Selection of DC3 flight planning tools and post-analysis products

For the flight planning support and post-analysis of the airborne in-situ data, a variety of meteorological products were available from the DC3 field catalog (<http://catalog.eol.ucar.edu/dc3/>).

Different kinds of visible/VIS and infrared/IR satellite products from the Geostationary Environmental Operational Satellite, GEOS-13, were used in the present study, i.e. cloud top heights derived from the thermal-IR cloud top temperatures. Furthermore, GOES East – Aerosol/Smoke Products (GASP) were used for the monitoring of extensive smoke plumes (<http://www.ssd.noaa.gov/PS/FIRE/GASP/>), see also *HH2016*.

The location of the upper tropospheric tracer outflow from thunderstorms (e.g. LNO<sub>x</sub>) was predicted on an hourly basis with the high-resolution Weather Research and Forecasting (WRF) ( $\Delta x=3 \text{ km} \times 3 \text{ km}$ ) model from NCAR ([http://ruc.noaa.gov/wrf/WG11\\_RT/](http://ruc.noaa.gov/wrf/WG11_RT/)), see *Barth et al.* [2012]. The Lagrangian particle dispersion model FLEXPART was run to forecast the location of different natural (CO biomass burning) and anthropogenic pollution sources (CO North America) in the lower/upper troposphere and as a column ( $\Delta x=0.5^\circ \times 0.5^\circ$ ) (<http://transport.nilu.no/flexpart/>), see *Stohl et al.* [2003].

A tropospheric NO<sub>2</sub> product (80 km × 40 km) was available once a day at approximately noon CDT in near-real-time from the morning overpass of the GOME-2 instrument on the MetOp-A satellite. These images were provided by NOAA National Environmental Satellite Data and Information Service (NESDIS) for the monitoring of LNO<sub>x</sub> plumes (same retrieval algorithm as used in *Bucsela et al.*, 2006).

For the monitoring of the flight track during the field missions, the NCAR- Earth Observing Laboratory (EOL) operation tool was successfully used. The GOES-13 satellite images were overlaid by Constant Altitude Plan Position Indicator (CAPPI) images from the Next-Generation Radar (NEXRAD): a network of 160 high-resolution S-band Doppler weather radars operated by the National Weather Service (NWS) (<http://www.roc.noaa.gov/WSR88D/>). Furthermore, the NCAR-EOL operation tool offered the possibility to overlay lightning data from the National Lightning Detection Network (NLDN) and flight track data on the satellite images. The NLDN system is operated by the

Vaisala Thunderstorm Unit [Cummins and Murphy, 2009]; <http://thunderstorm.vaisala.com/>. Similar images as the NCAR-EOL operation tool images are shown in the present study, however in addition O<sub>3</sub> distributions along the flight track have been superimposed.

Detailed radar measurements were performed from the ground in Oklahoma/Texas with the Shared Mobile Atmospheric Research and Teaching (SMART) single and dual polarized C-band Doppler radars (SR1 and SR2) [Biggerstaff *et al.*, 2005]. Multi-Doppler 3DVAR analyses of SMART and other available radar data were used to derive the vertical velocity within the storms. Here X-band dual polarized Doppler radar data from the mobile radar known as NOAA X-POL (NOXP) operated by T. Mansell, NOAA National Severe Storms Laboratory (NSSL) and data from the Dyess Air Force Base (AFB) in Abilene were used. The analysis technique follows Potvin *et al.* [2012].

### **3 Falcon observations in wildfire plumes**

#### **3.1 Influence from wildfires**

Some of the largest and most destructive wildfires in New Mexico (NM) and Colorado state's history were burning during the DC3 field experiment: the Whitewater-Baldy (NM), the Little Bear (NM), and the High Park Fire in Colorado, see Table 3 in *HH2016* and details herein. Pollution layers from these wildfires, elevated in CO, SO<sub>2</sub>, and rBC, were observed during most of the Falcon flights, not only at low altitudes but also in the UT up to ~10 km altitude (see Fig. 2 herein). Occasionally these BB emissions were transported upward in and/or nearby thunderstorms and observed within or just below the anvil outflow region as illustrated in Figs. 16 and 17 herein. In Table 4 in *HH2016*, the most intense BB plumes probed by the Falcon (according to given criteria) and their mean and maximum trace species mixing ratios (CO, SO<sub>2</sub>, and rBC) are listed. Furthermore in this table information on date and time, fire source, distance from fire source, plume height (depth), and plume age is given.

In the present study we use these selected BB plumes from Table 4 in *HH2016* and divide them into thinner layers where a clear O<sub>3</sub>-CO correlation was observed. Their maximum O<sub>3</sub> and CO mixing ratios were determined; see Table 1 and references herein to single O<sub>3</sub>-CO correlation plots presented later in Sect. 4. The selected time sequences for the BB plumes are given in the legend of these correlation plots. In addition, in Table 1 a number of LNO<sub>x</sub> plumes probed on these flights and a further case with anthropogenic pollution (June 8) were included which are discussed later in Sect. 4.

### 3.2 The O<sub>3</sub>-CO correlation in lofted wildfire plumes

Possible reasons for the highly variable O<sub>3</sub> and CO mixing ratios in the selected BB plumes and their O<sub>3</sub>-CO correlation are discussed next. One way to identify cases with photochemical O<sub>3</sub> production or intrusions of O<sub>3</sub>-rich air from the stratosphere is to focus on the O<sub>3</sub>-CO correlation (Sect. 1). In Fig. 1, O<sub>3</sub>-CO correlations from five selected DC3 thunderstorm flights are shown and colored according to flight date. Negative O<sub>3</sub>-CO correlations (stratospheric air masses) were observed during all of these flights; especially pronounced on May 30, June 8 and 12. In contrast, positive O<sub>3</sub>-CO correlations were frequently found in BB plumes from wildfires. CO mixing ratios exceeding ~170 nmol mol<sup>-1</sup> were in general caused by especially pronounced BB plumes. From Fig. 1 it is obvious that rather variable O<sub>3</sub>-CO correlations were observed in the selected BB plumes on May 30, June 11 and June 12. Some examples and explanations will be given below.

The change of O<sub>3</sub> over the change of CO ( $\Delta O_3/\Delta CO$  ratio) is determined by finding the linear regression slope of the O<sub>3</sub>-CO correlation and is summarized for selected BB plumes in Table 1. On May 30, in the dense BB plume probed in the BL (1.2-1.6 km) during the descent to Lubbock (white dots), the  $\Delta O_3/\Delta CO$  ratio (+0.1) indicated a rather low O<sub>3</sub> production rate ~600 km downstream from the New Mexico Whitewater-Baldy Fire. The plume age was determined to be <24 h with on-line HYSPLIT backward trajectories [Draxler and Rolph, 2014; Rolph, 2014] (<http://ready.arl.noaa.gov/HYSPLIT.php>), see also Table 4 in HH2016. Ozone mixing ratios were rather low in the plume and mainly varied between ~50-70 nmol mol<sup>-1</sup>. On June 11, similar conditions were observed in a BB plume lofted to 6-7 km (yellow dots): the  $\Delta O_3/\Delta CO$  ratio (+0.03) was close to zero ~1000 km downstream from the New Mexico Little Bear Fire and the plume age was determined to be ~24-27 h. Ozone mixing ratios were still rather low in the plume and varied between ~50-80 nmol mol<sup>-1</sup>. In contrast, on June 12 (green dots), the  $\Delta O_3/\Delta CO$  ratio (+0.4) was distinctly higher in a lofted BB plume (age ~9 h) probed in the UT (7-10 km) ~600 km downwind from the Colorado High Park Fire and O<sub>3</sub> mixing ratios reached up to ~120 nmol mol<sup>-1</sup>.

The determined  $\Delta O_3/\Delta CO$  ratios in polluted plumes (mainly from BB, LNO<sub>x</sub> excluded) vary between +1.4 and -1.7 as listed in Table 1, with a tendency to distinctly higher positive values above ~8 km and one negative value at ~10 km. In the majority of the BB plumes probed by the Falcon below ~8 km, there is a tendency to a slightly positive correlation on the order of  $\Delta O_3/\Delta CO = +0.1$ . In these plumes O<sub>3</sub> mixing ratios reach up to ~80 nmol mol<sup>-1</sup> compared to

$\sim 70 \text{ nmol mol}^{-1}$  in the background ( $\text{O}_3$  enhancement one day after emission:  $\sim 10 \text{ nmol mol}^{-1}$ ). According to the values presented in Sect. 1, we suggest that photochemical production is the most likely source for  $\text{O}_3$  enhancements observed in our BB plumes below  $\sim 8 \text{ km}$ .

Higher up, at  $\sim 8\text{-}10 \text{ km}$ , a distinct stepwise change and increase of the  $\Delta\text{O}_3/\Delta\text{CO}$  ratio is observed towards values in the range of  $+0.4$  (but also one negative value), indicative of a sudden change in processes influencing this ratio. In these UT-BB plumes,  $\text{O}_3$  mixing ratios are generally in the range of  $90\text{-}130 \text{ nmol mol}^{-1}$  (compared to the background  $\sim 70\text{-}90 \text{ nmol mol}^{-1}$ ), suggesting both in-mixing from the stratosphere and/or photochemical  $\text{O}_3$  production as possible processes. The observed  $\text{O}_3$  enhancements in the UT-BB plumes are however partly higher than expected from photochemical  $\text{O}_3$  production alone ( $<10 \text{ nmol mol}^{-1}$  per day, see Sect. 1). For this reason, the major part of the observed  $\text{O}_3$  enhancements in lofted BB plumes above  $\sim 8 \text{ km}$  in the vicinity of thunderstorms would more likely be consistent with the wrapping of stratospheric intrusions around the thunderstorm outflow as recently observed by *Pan et al.* [2014] for another DC3 thunderstorm. In the next section three Falcon thunderstorm case studies will be analyzed in detail to support the hypothesis stated here.

#### **4. Three Falcon thunderstorm case studies**

In the following, observations during the Falcon flight on May 30, June 8 and 12, 2012 are described and discussed in detail.

##### **4.1 30 May 2012: fresh supercell and MCC outflow over Texas/Oklahoma**

###### **4.1.1 Observations on 30 May 2012**

On May 30, 2012 the Falcon performed two flights. The first flight was mainly dedicated to the smoke plume from the Whitewater-Baldy Fire in New Mexico (see Table 4 in *HH2016*). Emissions from the fire were probed downwind of the source region ( $\sim 400\text{-}700 \text{ km}$ ) between Albuquerque (NM) and Amarillo-Lubbock (TX). The observed BB plume was most pronounced at  $\sim 2\text{-}5 \text{ km}$  altitude (see Figs. 2a-b, e herein). At  $\sim 4 \text{ km}$ , CO mixing ratios reached up to  $540 \text{ nmol mol}^{-1}$  (1 s values not shown). Increasing rBC mass mixing ratios with altitude were also measured from the ground to the mid troposphere (see Fig. 2e herein), with a maximum value at  $\sim 4 \text{ km}$  of  $1508 \text{ ng kg}^{-1}$  (10 s value not shown). This value is similar to rBC mass mixing ratios observed the day before in the same region ( $1477 \text{ ng kg}^{-1}$ , BB plume at  $\sim 1\text{-}4 \text{ km}$ ) (Table 4 herein).

After a brief stop in Ardmore (OK), the second flight was dedicated to thunderstorm probing. Images from GOES East – Aerosol/Smoke Products (GASP) distinctly indicated that the New Mexican smoke plume was advected eastwards in the evening of May 30, crossed the Texas Panhandle and moved into western Oklahoma (Fig. 2a). Similar to the set up the day before (May 29 case in *HH2016*), two intense thunderstorm clusters developed in this area with the dense smoke plume (AOD  $\sim 1.3$ ): a huge MCC with several supercells east of the Texas Panhandle, along the Texas/Oklahoma border, and an isolated supercell near Abilene a few hundred km west of Dallas. Both the probed MCC and the supercell were severe, triggered several tornadoes and had very large hail as reported by the Storm Prediction Center in Norman, Oklahoma.

The thunderstorm systems mentioned above were characterized by high cloud tops with temperatures colder than  $-60$  °C, as indicated in the thermal-IR image from GOES-13 ([http://catalog.eol.ucar.edu/cgi-bin/dc3\\_2012/ops/index](http://catalog.eol.ucar.edu/cgi-bin/dc3_2012/ops/index)). According to the GOES data, the average cloud top height of the anvil outflow deck of the MCC and supercell was  $\sim 11$ - $13$  km, however pronounced overshooting tops reached up to  $\sim 17$ - $18$  km (Fig. 2b). The Mobile GPS Advanced Upper-Air Sounding System (MGAUS) operated by the National Severe Storms Laboratory (NSSL) released a radiosonde in the prestorm environment ( $34.07^\circ$  N,  $99.39^\circ$  W, border TX/OK) around 22 UTC which indicated a primary, secondary, and third tropopause at  $\sim 10.5$ ,  $\sim 12.5$  and  $\sim 15.5$  km, respectively (<http://data.eol.ucar.edu/>). Later radiosonde temperature profiles from Fort Worth (TX) near Dallas ([http://catalog.eol.ucar.edu/cgi-bin/dc3\\_2012/ops/index](http://catalog.eol.ucar.edu/cgi-bin/dc3_2012/ops/index)), Lamont (northern Oklahoma), and Dodge City (south-western Kansas) for May 31 at 00 UTC showed a distinct large-scale double-tropopause structure with a primary and secondary tropopause located at  $\sim 11.5$ - $12.5$  km and at  $\sim 17$  km, respectively (see also Figs. 3b and 9 in *Homeyer et al.*, 2014). A similar heterogeneously structured tropopause was already observed the day before (May 29 case in *HH2016*), which may have facilitated the development of very deep convective cells with overshooting tops.

During the first part of the second flight on May 30, the Falcon headed south-westwards from Ardmore (Fig. 3a), ascending below the MCC outflow (according to the on board video). Thereafter, the aircraft circled counter-clockwise around the supercell located just south of the MCC and crossed its dissipating outflow (Fig. 3b). Thereby highly variable CO, O<sub>3</sub> and NO mixing ratios were observed as shown in the Falcon time series in Figs. 4a-b, mainly impacted by emissions from wildfires, LNO<sub>x</sub>, and stratospheric intrusions as discussed below in more detail.

During the ascent (Fig. 4a, <85500 s), the lower and mid troposphere up to 6 km was polluted by the Whitewater-Baldy smoke plume (CO mixing ratios up to 150 nmol mol<sup>-1</sup>). Above the smoke plume, at ~6-8 km, typical background mixing ratios for both CO and O<sub>3</sub> were observed in the range of 70-80 nmol mol<sup>-1</sup>. Between 8.5-10.4 km, as the aircraft was ascending just below the MCC anvil outflow and partly into the lower boundary of the outflow (Fig. 3a), CO mixing ratios were elevated up to ~130 nmol mol<sup>-1</sup> indicating traces of a lofted BB plume (83819-85250 s, 23:17-23:41 UTC). NO mixing ratios were still low here suggesting that the main MCC outflow (rich in LNO<sub>x</sub>) was not probed during the ascent. Interestingly, O<sub>3</sub> mixing ratios continuously increased with altitude to stratospheric values (up to ~150 nmol mol<sup>-1</sup> at 10.4 km, however still UT according to sounding data) as the aircraft ascended below the MCC outflow along the southern side of the storm. This indicates that the lofted BB plume most likely mixed with O<sub>3</sub>-rich stratospheric air masses surrounding the MCC outflow as discussed later in Sect. 4.1.2.

Evidence for the presence of a pronounced upper-level downward motion within the MCC is available from multi-Doppler 3DVAR radar analyses. In Figs. 5a-b data from the SMART radars and the WSR-88D in Frederick (Oklahoma) on May 30 at 2330 UTC are combined. Two vertical cross sections (east-west and north-south) of the strongest supercell (white arrow in Fig. 3a) embedded within the MCC are shown. Echo tops reached up to ~18 km. Along the edges of the main storm core dominated by strong updrafts (40-50 m s<sup>-1</sup>), downdrafts (15-20 m s<sup>-1</sup>) were particularly well developed on the western and southern side of the core, where the Falcon sampled. The main subsidence extended from 14 km to 10 km with a secondary region of subsidence down to ~8 km altitude. The centers of the maximum up- and downdrafts in the UT/LS region were located in a narrow region less than ~10 km apart, likely promoting a strong mixing of lower stratospheric air masses with tropospheric air masses from the BL not only inside the storm but also just outside the anvil outflow as observed by the Falcon.

At the rear side of the MCC, the Falcon passed the dry line. At a cruising altitude of 10.7 km (Fig. 3a), O<sub>3</sub> mixing ratios were distinctly enhanced (~200 nmol mol<sup>-1</sup>) and CO mixing ratios were low (50-80 nmol mol<sup>-1</sup>) suggesting that the tropopause was located lower in this region (10.4 km) compared to the front side (10.7 km) and that the aircraft penetrated into the lowermost stratosphere (~85000-86500 s, Fig. 4a). The two different tropopause altitudes are clearly visible in the vertical temperature profiles (T, Θ, and Θ<sub>e</sub>) as illustrated in Figs. 6a-b.

After the probing of the MCC, the Falcon headed further south-westwards and probed an isolated supercell (Fig. 3a). The aircraft circled around the isolated supercell and reached its front side (again UT), descending from 10.7 to 9.1 km to probe the dissipating anvil outflow (Fig. 3b). In the vicinity and within the anvil outflow, a rapid change between up- and downdrafts dominated as illustrated by the vertical wind vector component (30 s mean) in Fig. 4b. These time sequences are listed separately in Table 2, according to up- and downdraft dominated areas, to illustrate the major differences observed in a variety of measured trace species (CO, O<sub>3</sub>, SO<sub>2</sub>, and NO) due to dynamical effects.

At ~87000 s (Fig. 4b), the aircraft was first flying just below the supercell outflow, outside of clouds (according to the on board video). NO mixing ratios were not enhanced, however CO mixing ratios were slightly enhanced (~110 nmol mol<sup>-1</sup>) and O<sub>3</sub> mixing ratios were rather low (70-80 nmol mol<sup>-1</sup>) indicating that remnants of pollution were probed (according to FLEXPART most likely lofted BB plume and not anthropogenic pollution, see DC3 field catalog). Unfortunately, rBC measurements are not available for this time sequence. As the Falcon penetrated into the visible anvil outflow between 9.6 to 9.1 km altitude, strong gradients in CO, O<sub>3</sub>, and NO mixing ratios were observed (Fig. 4b). The edges of the dissipating anvil outflow partly had trace gas signatures of downward motion (~87200-87300 and ~87400-87500 s), as also confirmed by the vertical velocity. Ozone mixing ratios were elevated up to ~140 nmol mol<sup>-1</sup>, as typical for the lowermost stratosphere, over a horizontal distance of ~20-40 km. In contrast, within the center of the anvil outflow (~87300-87400 s), O<sub>3</sub> mixing ratios were as low as ~70 nmol mol<sup>-1</sup>, indicating upward motion from lower levels closer to the convective core, as also confirmed by the vertical velocity. Interestingly, the highest CO mixing ratios up to ~160 nmol mol<sup>-1</sup> were observed along the edges of the anvil outflow dominated by downward motion (discussed in more detail in Sect. 4.1.2). The highest NO mixing ratios (8.6 nmol mol<sup>-1</sup>) were observed within the part of the anvil outflow dominated by upward motion (fresh NO production by lightning).

As listed in Table 2, SO<sub>2</sub> mixing ratios within the anvil outflow were ~50 pmol mol<sup>-1</sup> on average (in bold italic) and similar to background conditions (in bold). The background ethane and propane mixing ratios at 9.5 km altitude were low with 247 and 29 pmol mol<sup>-1</sup>, respectively, and the benzene/toluene ratio was 0.2, both indicating rather clean background conditions. Unfortunately, no VOC samples were taken within the anvil outflow during this flight. Due to the high humidity within the anvil outflow, no refractory black carbon (rBC) measurements were available during these flight sequences. Furthermore, CH<sub>4</sub>, NO<sub>x</sub>, and

NO<sub>y</sub> measurements were not available for this entire flight due to technical problems (see Table 2 in *HH2016*).

After passing the supercell, the aircraft continued heading northwestwards at 9.1 km altitude and approached the anvil outflow of the MCC again (Fig. 3b). In the clear air between the supercell and the MCC outflow (~89500 s), O<sub>3</sub> and CO mixing ratios dropped below ~80 and ~90 nmol mol<sup>-1</sup>, respectively, typical background values (Fig. 4a). Thereafter, the lower boundary of the MCC outflow was sampled again (~90000 s), O<sub>3</sub> and CO mixing ratios increased to values around 90-100 and 100-110 nmol mol<sup>-1</sup>, respectively, influenced by the lofted BB plume and most likely mixing with stratospheric air masses as described before. The vertical temperature profiles indicate that stratospheric intrusions reached down to 8.8 and 9.2 km, visible as inversion layers (Figs. 6a-b).

As the Falcon left the MCC outflow, it started to descend for landing in Lubbock. During the first part of the descent in clear air, between 9 and 7 km, both O<sub>3</sub> and CO mixing ratios dropped down to 70-80 nmol mol<sup>-1</sup>, typical background values as observed during the ascent. Below 7 km, the advected BB plume from New Mexico was prominent again, especially pronounced between 3 km and the ground, with enhanced O<sub>3</sub> and CO mixing ratios, ~80-90 and up to ~200 nmol mol<sup>-1</sup> (1 s values), respectively. Compared to the start in Ardmore, the BB plume was much more pronounced around Lubbock, due to the proximity to the source region.

#### **4.1.2 Discussion of 30 May 2012 observations**

From the observations during the second Falcon flight on May 30, it is obvious that especially strong up- and downward motions, within and in the vicinity of the supercell and MCC outflow, efficiently redistributed the chemical composition ratio in the UT/LS region. Schematics of the observations presented in the last subsection are summarized in Fig. 7a for the supercell and in Fig. 7b for the MCC, and discussed in more detail below.

Almost the entire horizontal extent of the supercell outflow (Fig. 3b) was probed from south to north, but mainly the lower boundary near ~9 km, as indicated by the orange shading in Fig. 7a. The entire cloud deck extended from ~9 to 11 km altitude. In the vicinity of the convective core of the supercell, updrafts dominated the vertical transport of CO-rich (BB plume, broad yellow arrow) and low-O<sub>3</sub> air masses from below (broad green arrow). Due to the strong intensity of the supercell (overshooting top), the uplifted BB emissions (from below 3 km according to the background O<sub>3</sub>-CO composition in the LT) penetrated through



the tropopause and mixed with LMS air masses (black-yellow ellipse). O<sub>3</sub>-rich but also CO-rich air masses were transported downwards again along and into the edges of the overshooting top (curved yellow and straight red arrows), as compensation to the strong updrafts in the storm core. Normally the CO mixing ratio rapidly decreases above the tropopause, which should cause a decrease in CO mixing ratios of the air masses transported downward. However, we observed the opposite in this specific case. We assume that a considerable amount of CO was already injected to the LMS earlier by the isolated supercell but also by the nearby overshooting MCC, the latter system was even more intense and higher than the isolated supercell (Fig. 2b). The GOES Aerosol Optical Depth image (Fig. 2a) shows that the center of the strong Whitewater-Baldy smoke plume passed just below the MCC. Most likely a high amount of CO was transported upward to the LMS by this MCC but also by the nearby isolated supercell and mixed with CO-poorer but O<sub>3</sub>-rich air masses. This mixture still enhanced both in CO and O<sub>3</sub> was later brought down again by the storm's downdrafts as seen in our measurements. Our hypothesis on these transport pathways is supported by the multi-Doppler radar analysis described before, where strong up- ( $\sim 50 \text{ m s}^{-1}$ ) and downdrafts ( $\sim 20 \text{ m s}^{-1}$ ) observed within a MCC supercell have the capability to very rapidly ( $\sim 5\text{-}15 \text{ min}$ ) mix tropospheric and stratospheric air masses.

Besides these measurements inside the anvil outflow of the supercell, measurements just outside of the outflow are also illustrated in Fig. 7a. Compared to the UT background, CO and O<sub>3</sub> mixing ratios were higher and lower within this cloud-free air, respectively, indicating that pollution transport from below was efficient, not only inside the storm, but also just outside of the storm (low O<sub>3</sub> indicated by thin green arrows in Fig. 7a). Around 87750 s, within this cloud-free air close to the storm at  $\sim 9 \text{ km}$ , O<sub>3</sub> mixing ratio as low as  $\sim 80 \text{ nmol mol}^{-1}$  and slightly elevated CO mixing ratios ( $\sim 100 \text{ nmol mol}^{-1}$ ) were observed, indicative of pollution transport from the BL. In addition, elevated water vapor mixing ratios ( $0.3\text{-}0.4 \text{ g kg}^{-1}$ ) and relative humidity values ( $\sim 60\%$ ) indicate that these air masses were possibly uplifted from lower levels. Most likely smaller convective cells (towering cumulus along the flanking line) uplift and spread BB emissions just below the anvil outflow (yellow arrows in Fig. 7b), as discussed in *HH2016* and illustrated in Figs. 13, 16, and 17 herein. In the present study Fig. 8 nicely shows that an extended area of pronounced wave clouds was present east of the investigated thunderstorms supporting the uplift of BB emissions. The exceptional high equivalent potential temperature observed at  $\sim 3 \text{ km}$  altitude ( $>350 \text{ K}$ ) may also facilitate the rapid lifting of such BB layers to the UT (Fig. 6b).

In the MCC case (Fig. 7b) the main anvil outflow deck spread slightly higher compared to the supercell case (MCC main ceiling at ~12-13 km, clearly located above the primary tropopause). Stratospheric air masses were likely forced to move downwards as compensation to the powerful upward motion in the MCC penetrating the tropopause. Our in-situ measurements indicate that these stratospheric air masses likely enwrapped the anvil outflow (red curved arrow) similar to the findings by *Pan et al.* [2014] and mixed with CO-rich air masses located just below the MCC outflow (lofted BB plume, yellow arrows).

A further illustrative example of the mixing of the lofted BB plume with air masses of stratospheric origin wrapping around the MCC outflow is presented in Fig. 9a showing the O<sub>3</sub>-CO correlation. For comparison, the correlation in the free tropospheric and stratospheric background is superimposed in gray (from Falcon a-flight on June 8, 2012). As described before, during the westward ascent, just below the MCC outflow, both CO and O<sub>3</sub> mixing ratios increased with altitude between 8.5 and 10.4 km (Fig. 4a). In Fig. 9a positive O<sub>3</sub>-CO correlations ( $\Delta O_3/\Delta CO$  ratio = +0.4) were observed within this lower portion of the BB plume (yellow dots with no or light orange edges), mainly due to mixing with the stratospheric intrusion and not due to photochemical O<sub>3</sub> production. The ratio value alone (also listed in Table 1) is within common ranges reported in BB plumes affected by photochemical O<sub>3</sub> production (Sect. 1). However, the steep increase in O<sub>3</sub> mixing ratios with altitude (Fig. 4a) clearly suggests that O<sub>3</sub>-rich air masses from the LMS are mixed in which explain the enhanced  $\Delta O_3/\Delta CO$  ratio observed. Photochemical O<sub>3</sub> production within the plume is not expected to increase with altitude as the production rate is slower at colder temperatures.

Within the upper portion of the BB plume (~10.4 km), at the rear side of the MCC, a negative O<sub>3</sub>-CO correlation ( $\Delta O_3/\Delta CO$  ratio = -1.7) was observed (yellow dots with thick black edges in Fig. 9a), dominated by the in-mixing of the BB plume into the LMS. South of the MCC, as the aircraft ascended up to 10.7 km and circled counter-clockwise around the supercell, the aircraft penetrated into the troposphere again, indicating that the local tropopause was slightly higher in this region (tilted tropopause between thunderstorm front and rear side supporting the troposphere-stratosphere exchange) (Figs. 6a-b). The anvil outflow of the supercell (characterized by elevated NO) was probed next which was located distinctly lower, at 9.1-9.4 km (Fig. 4b). Mixing of the outflow with both stratospheric and BB impacted air masses was prominent (for illustration see Fig. 7a), which caused a positive O<sub>3</sub>-CO correlation, as shown in Fig. 9b. During the descent from 9.4 to 9.1 km, the regression slope was steeper

( $\Delta\text{O}_3/\Delta\text{CO}$  ratio = +1.4) (red dots without black edges) compared to the correlation at the cruise altitude of 9.1 km ( $\Delta\text{O}_3/\Delta\text{CO}$  ratio = +0.5) (red dots with black edges), due to increasing influence of stratospheric air masses and decreasing influence of the ingested BB plume at the higher level. The high CO mixing ratios ( $\sim 160 \text{ nmol mol}^{-1}$ ) observed within the anvil outflow indicate that BB emissions were most likely ingested into the supercell from the top of the BL at  $\sim 3 \text{ km}$  (according to CO and  $\Theta_e$  values in Figs. 4a and 6b, respectively). In addition, the observed elevated  $\text{O}_3$  mixing ratios ( $\sim 140 \text{ nmol mol}^{-1}$ ) suggest that air masses were simultaneously transported downward from the tropopause region (10.4-10.7 km or above) into the anvil (values too high values for photochemical  $\text{O}_3$  production).

In Table 2, average trace gas conditions in the supercell outflow (bold italic) and typical background mixing ratios (bold) are listed. Both CO and  $\text{O}_3$  mixing ratios were on average distinctly enhanced in the anvil outflow by 11 and  $5 \text{ nmol mol}^{-1}$ , respectively, compared to the background composition. In summary, like the lofted BB plume in Fig. 9a, the observed  $\text{O}_3$  enhancement within the LNO<sub>x</sub> plume (Fig. 9b) was mainly caused by downward mixing of  $\text{O}_3$ -rich air masses from the LMS and not due to photochemical  $\text{O}_3$  production. The highly variable  $\Delta\text{O}_3/\Delta\text{CO}$  ratios with altitude observed in the probed LNO<sub>x</sub> plume also suggest a major dynamical and not photochemical influence. The observed trace gas gradients in the time series have larger amplitudes than expected from chemical processes only. As discussed in Sect. 1 such chemical processes are also much slower.

## **4.2 12 June 2012: fresh squall line outflow over Colorado/Kansas**

### **4.2.1 Observations on 12 June 2012**

On June 12, 2012 a pronounced smoke plume from the High Park Fire in Colorado (see Tables 3-4 in *HH2016*) spread south-eastward along the border between Colorado and Kansas according to the FLEXPART lower tropospheric BB tracer analyses (CO) (Fig. 10). In addition, BB emissions from the wildfires in New Mexico likely spread north-eastward to the same region.

An elongated squall line ( $\sim 700 \text{ km}$  anvil length) with cold cloud tops ( $< -60 \text{ }^\circ\text{C}$ ) developed in the convergence zone of these smoke plumes along the border between Kansas, Oklahoma, and Colorado ([http://catalog.eol.ucar.edu/cgi-bin/dc3\\_2012/ops/index](http://catalog.eol.ucar.edu/cgi-bin/dc3_2012/ops/index)), the target area for the Falcon flight on June 12. The average cloud top height was in the range of 12-13 km, with overshooting tops up to 14-15 km (Fig. 11). The cloud tops were not as high as observed

during the previously presented flight (May 30). The 00 UTC radiosoundings from Dodge City (south-western KS) and Amarillo (Texas Panhandle) both indicate that the primary tropopause was located at 11.1 km ([http://catalog.eol.ucar.edu/cgi-bin/dc3\\_2012/ops/index](http://catalog.eol.ucar.edu/cgi-bin/dc3_2012/ops/index)). In addition, in Dodge City a secondary tropopause was prominent at 11.8 km. Both tropopause heights are located slightly below the average cloud top height (~12-13 km), which indicates that the main cloud deck likely penetrated into the LMS.

After take-off in Salina, the aircraft headed south-westward and remained in the lower troposphere (~3-5 km) to probe the smoke plume from the High Park (and NM) fire and the inflow region of the squall line (Figs. 12a-b). Within this lower portion of the advected smoke layer (~79500 s), the highest CO mixing ratios (~160 nmol mol<sup>-1</sup>) were observed at 3.3 km altitude, whereas O<sub>3</sub> mixing ratios were rather low, in the range of 60 nmol mol<sup>-1</sup>, indicating no pronounced photochemical O<sub>3</sub> production (Fig. 13a). In addition, SO<sub>2</sub> and CH<sub>4</sub> mixing ratios were enhanced with ~0.5 nmol mol<sup>-1</sup>, 1.90 μmol mol<sup>-1</sup>, respectively (Figs. 13c-d).

As the aircraft reached the squall line, it started to ascend below the anvil outflow, thereby also heading northward towards a smaller, isolated thunderstorm cell (Fig. 12a). In the mid troposphere between 5 and 7 km, low CO and O<sub>3</sub> mixing ratios in the range of 80-90 nmol mol<sup>-1</sup> and 50-60 nmol mol<sup>-1</sup>, respectively, were observed as typical for the background (Fig. 13a). During the previous flight (May 30) described in the last subsection, the same type of layer with low CO and O<sub>3</sub> mixing ratios was observed between 6 and 8 km. On June 12, the layer above 7 km and below 9.7 km was characterized by strongly elevated CO and O<sub>3</sub> mixing ratios, up to 190 and 120 nmol mol<sup>-1</sup>, respectively (~82500-84000 s). The vertical (equivalent)-potential temperature profiles indicate that an air mass layer located at ~3-4 km altitude, characterized by elevated Θ<sub>e</sub> temperatures (~335 K), would have the potential to be uplifted to these altitudes in the UT (Figs. 14a-b).

The aircraft then (after 84000 s) started to probe the north-eastern edge of the squall line outflow during stepwise ascent from 9.7 to 11.9 km altitude. Thereby the aircraft was cruising between the squall line, background air and the smaller, isolated thunderstorm cell in the north (Figs. 12a-b). Within the anvil outflow (Fig. 13b: ~84500-85000 and ~86000-87000 s), elevated CO and low O<sub>3</sub> mixing ratios were observed, in the range of 120 and 70 nmol mol<sup>-1</sup>, respectively, indicating upward transport from lower altitudes below ~4 km. In addition, NO and NO<sub>x</sub> mixing ratios were distinctly enhanced within the anvil outflow (Figs.

13a-c), mainly due to in-situ production by lightning. Along the northern edge of the anvil outflow, the lofted BB plume was most prominent in a layer between ~7 and 9.7 km. Above ~8 km and up to 9.7 km (~82500-84000 s) O<sub>3</sub> mixing ratios were in addition enhanced. As in the previous thunderstorm case described, no significantly elevated NO and NO<sub>x</sub> mixing ratios were observed within this lofted BB. Most likely the BB emissions were not uplifted inside the storm cell but near the active thunderstorm by flanking convection (see visible satellite images 1 km resolution, [http://catalog.eol.ucar.edu/cgi-bin/dc3\\_2012/ops/index](http://catalog.eol.ucar.edu/cgi-bin/dc3_2012/ops/index)), as also illustrated for the previous case in Fig. 8a). The high SO<sub>2</sub> and CH<sub>4</sub> mixing ratios observed within the UT-BB plume (~0.6 nmol mol<sup>-1</sup> and 1.89 μmol mol<sup>-1</sup>), similar to the composition observed at the beginning of the flight in the LT-BB plume (~0.5 nmol mol<sup>-1</sup> and 1.90 μmol mol<sup>-1</sup>), support this assumption of direct uplift to the UT outside of the squall line not affected by any wash-out processes prevalent inside the storm. However, interestingly rBC mass mixing ratios were low within the UT-BB plume (maximum <30 ng kg<sup>-1</sup>, mean ~12 ng kg<sup>-1</sup>) (see Fig. 2e in *HH2016*). This observation indicates that perhaps other processes, e.g. sedimentation, possibly lowered the rBC mass mixing ratio in the UT-BB plume. Within the lofted plume on June 12, water vapor measurements are available between 7 and 9 km altitude (82500-82860 s). The relative humidity was highly variable between ~10-100%, however most frequently values between 40% and 70% were measured and elevated H<sub>2</sub>O mixing ratios in the range of ~0.3 g kg<sup>-1</sup>, indicative of transport from lower levels. CO mixing ratios were elevated (100-180 nmol mol<sup>-1</sup>) as expected in a plume generated from BB, but also ozone-rich stratospheric air masses (up to ~120 nmol mol<sup>-1</sup>) mixed into the plume.

At ~85000-86000 s, as the aircraft left the anvil outflow at ~11 km to turn for the next higher flight level, the BB plume was not prominent anymore but O<sub>3</sub> mixing ratios were clearly enhanced (~140 nmol mol<sup>-1</sup>) and CO mixing ratios decreased down to ~90 nmol mol<sup>-1</sup> (Fig. 13a). At the next higher level along the anvil edge (~12 km, ~87000-87500 s) the influence from the LMS was even more distinct with elevated O<sub>3</sub> mixing ratios over a horizontal distance of ~50 km with mixing ratios up to ~260 nmol mol<sup>-1</sup> and CO mixing ratios as low as ~80 nmol mol<sup>-1</sup>. In addition, NO and NO<sub>x</sub> mixing ratios were still distinctly elevated during this time sequence inside the anvil outflow.

#### **4.2.2 Discussion of 12 June 2012 observations**

A schematic of the major air mass transport pathways based on observations from June 12, 2012 is shown in Fig. 15 (colored arrows). One side of the storm system was probed during

stepwise ascent from 9.7 to 11.9 km altitude as indicated by the orange shaded area.

Within the center of the anvil outflow, low O<sub>3</sub> and elevated CO mixing ratios (70 and 120 nmol mol<sup>-1</sup>, respectively) were observed indicating upward transport from lower altitudes below ~4 km, as illustrated by the green and yellow arrows near the storm core. In contrast, along the edges of the anvil outflow and at the highest flight level in the anvil outflow (~11.9 km, ~87000-87500 s) a clear mixing of elevated NO<sub>x</sub> (mainly LNO<sub>x</sub>) with O<sub>3</sub>-rich stratospheric air masses (~260 nmol mol<sup>-1</sup>) was observed. The highest flight level in the anvil outflow was located above the primary/secondary tropopause (~11.1/11.8 km) giving evidence of detrainment of LNO<sub>x</sub> into the LMS.

Elevated O<sub>3</sub> mixing ratios were still measured down to ~8 km when the aircraft left the anvil outflow and started the steep descent for landing. Air masses of lower stratospheric origin not only mixed with the top and edges of the anvil outflow (straight red arrows) but also surrounded it as a stratospheric intrusion (curved red arrow). This latter air mass transport pathway is similar to the observations by *Pan et al.* [2014] as seen in O<sub>3</sub> lidar images. However, since lidar measurements are not available inside thick clouds such as thunderstorms, the direct downward injection of O<sub>3</sub>-rich air masses into the anvil edges and upward injection of anvil-LNO<sub>x</sub> into the LMS was not observed by *Pan et al.* [2014].

As in the previous flight described (Fig. 7b), here we also observed that just outside and beneath the anvil outflow a lofted BB plume (curved yellow arrow in Fig. 15) mixed with the stratospheric intrusion (~8-9.7 km). The O<sub>3</sub> mixing ratio in the lofted BB plume was much higher (twice as high) as observed before in the LT-BB plume at ~5 km (~60 nmol mol<sup>-1</sup>), which excludes that the major O<sub>3</sub> enhancement was due to photochemical O<sub>3</sub> production.

To illustrate the strong influence of the squall line on the chemical composition in the UT/LS also the O<sub>3</sub>-CO correlation in BB and LNO<sub>x</sub> plumes was determined as shown in Fig. 16. Just below and outside of the anvil outflow, the lofted BB plume (yellow dots) mixed with a stratospheric intrusion (~8-10 km), causing a positive regression slope ( $\Delta\text{O}_3/\Delta\text{CO}$  ratio = +0.4) in the same range as observed in the May 30 case (Table 1). The anvil outflow at 9.7-11.0 km (red dots with black edges) was characterized by a mixture of O<sub>3</sub>- and CO-rich air masses from the stratosphere and wildfires, indicating partly negative and partly positive O<sub>3</sub>-CO correlations. The in-mixing partly took place along the boundaries of the anvil outflow, as indicated in Figs. 13a and 15. Higher up within the anvil outflow (11.0-11.9 km) an increased in mixing of stratospheric air masses with altitude was observed (red dots without

black edges), causing a negative O<sub>3</sub>-CO correlation ( $\Delta O_3/\Delta CO$  ratio = -3.9).

In Table 3, trace species mixing ratios within the squall line is compared to the background. Elevated CO and low O<sub>3</sub> mixing ratios within the anvil outflow (~120 and ~ 80 nmol mol<sup>-1</sup>) compared to the background (~100 and ~130 nmol mol<sup>-1</sup>) indicate that the anvil outflow above ~10 km was surrounded by lower stratospheric air masses. SO<sub>2</sub> mixing ratios within the anvil outflow (~10-20 pmol mol<sup>-1</sup>) were distinctly lower compared to the background (~40-80 pmol mol<sup>-1</sup>) and the BL (>100 pmol mol<sup>-1</sup>) suggesting efficient wash-out processes within the squall line (see also Fig. 13d). In contrast, CH<sub>4</sub> mixing ratios were slightly elevated by ~10 nmol mol<sup>-1</sup> within the anvil outflow compared to the background due to ingested wildfire emissions (see also Fig. 13c). Within the anvil outflow peak NO (NO<sub>x</sub>) mixing ratios, 3.1 (4.1) nmol mol<sup>-1</sup>, were observed at 11.0 km. Enhanced anvil-NO<sub>x</sub> was present above the primary tropopause (11.1 km) indicating injection into the LMS. The presence of ingested wildfire emissions within the anvil outflow is also supported by the enhanced ethane and propane mixing ratios (1073 and 615 pmol mol<sup>-1</sup>) compared to the BL (443 and 410 pmol mol<sup>-1</sup>) and the background from the previous flight on May 30 (247 and 29 pmol mol<sup>-1</sup>), see also Table 2. Unfortunately, no VOC background measurements were available from the flight on June 12. Within the anvil outflow, the benzene/toluene ratio (=0.3) was distinctly lower compared to the BL (=1.7) and similar to background values (=0.2) observed on May 30, indicating no pronounced influence from fresh anthropogenic emissions in the BL. In addition, on June 12 low rBC mass mixing ratios (<20 ng kg<sup>-1</sup>) were observed in the background.

The results from this second thunderstorm case study, June 12 (Fig. 15), support the findings from the first presented DC3 Falcon case from May 30 (Figs. 7a-b): (1) emissions from wildfires (high in CO) are ingested into the thunderstorm near the cloud base, (2) the storm produces an overshooting top, possibly facilitated by the large-scale double(triple)-tropopause structure, (3) the overshooting top injects high amounts of BB emissions and LNO<sub>x</sub> into the LMS in addition to low O<sub>3</sub> mixing ratios from the BL, (4a) as a dynamical response, O<sub>3</sub>-rich air from the LMS is transported downward into the edges of the anvil outflow and (4b) surrounds the outflow like an umbrella (stratospheric intrusion), (5a) in addition, a rapid uplift of “less diluted” emissions from wildfires from the LT to the UT is frequently observed outside of thunderstorms, most likely transported upward in towering cumulus clouds along the storm’s flanking line, (5b) this lofted BB plume mixes with the stratospheric intrusion surrounding the anvil outflow.

Several of these major air mass transport pathways (1-5) have by chance been observed in previous thunderstorm studies as described in Sect. 1. However, in this study we report for the first time on observations in different types of thunderstorm systems during one field campaign supported by a unique variety of airborne and ground-based measurements. Furthermore, during DC3 the influence of smoke plumes and stratospheric air masses on the thunderstorm environment was much more pronounced than during previous U.S. thunderstorm field experiments. Wildfire emissions were useful tracers to construct a general picture of trace gas transport pathways within and nearby DC3 thunderstorms. Air mass pathways as (4a), (4b), (5a), and (5b) have rarely been observed and described before. However, they indicate a distinct influence of O<sub>3</sub>-rich air masses from the LMS on the UT-O<sub>3</sub> composition inside and nearby thunderstorms besides the more well-known influence of low O<sub>3</sub> air transported from the BL. In the next subsection observations in aged thunderstorm outflow (~12-24 h) even more distinctly highlight the pronounced air mass exchange in the UT/LS region caused by thunderstorms.

### **4.3 8 June 2012: aged MCS outflow over Colorado/Kansas**

#### **4.3.1 Observations on 8 June 2012**

In the evening on June 7, scattered severe convection developed over eastern Colorado that moved eastward and lasted until the next morning on June 8. In the night the scattered convection and their anvils merged to a kind of MCS in the general sense (not as strict as defined by Houze *et al.*, 1989). On June 8, the Falcon performed two flights to investigate the remnants of the MCS. The two flight patterns were similar, covering the major extension of the MCS remnants (~700 km wide) that spread across Kansas. In addition, the background air composition ahead and behind of the remnants was probed. The focus here is on the first Falcon flight around noon local time.

The GOES thermal-IR image for cloud top temperatures from the previous evening ([http://catalog.eol.ucar.edu/cgi-bin/dc3\\_2012/ops/index](http://catalog.eol.ucar.edu/cgi-bin/dc3_2012/ops/index)) indicates that in agreement with the other two presented case studies the MCS cloud tops reached temperatures below -60 °C. However, in this case the temperatures were slightly colder and extended over a larger area indicating that the main cloud deck reached even higher altitudes. During the mature stage of the MCS, an embedded storm cell close to Denver developed into a strong supercell with very high radar reflectivity (65-70 dBZ) (not shown), producing large hail and several



tornadoes. At this time the average cloud top height in Fig. 17a reached as high as ~13-14 km (higher, wider, and more homogeneous compared to the previous two cases in Figs. 2b and 11). Between 18 and 00 UTC, the primary tropopause was located slightly lower at ~11-13 km according to the closest radiosoundings from Denver in eastern Colorado and Dodge City in south-western Kansas ([http://catalog.eol.ucar.edu/cgi-bin/dc3\\_2012/ops/index](http://catalog.eol.ucar.edu/cgi-bin/dc3_2012/ops/index)). These observations indicate that parts of the main cloud deck of the intense MCS very likely crossed the tropopause and mixed with air masses in the LMS.

During the flight the day after the mature MCS activity, thin cirrus clouds over western Kansas not only gave evidence of MCS cloud remnants (Fig. 17b), but NCAR WRF forecasts of the column LNO<sub>x</sub> tracer (8-16 km) were also used to determine the position of the MCS remnants and to guide the aircraft. The forecasts for 11 and 16 UTC (Figs. 18a-b) predicted that the remnants (enhanced in LNO<sub>x</sub>) spread eastwards over Kansas and merged with less pronounced remnants of a second, weaker thunderstorm system over Texas and Oklahoma. At 16 UTC the major LNO<sub>x</sub> plume from the aged MCS outflow is located west of Salina. The Falcon in-situ observations of O<sub>3</sub> in this area indicate highly variable mixing ratios between ~60-150 nmol mol<sup>-1</sup> in the UT (Fig. 17b). Ahead (east) of the LNO<sub>x</sub> plume a broad area with strongly enhanced O<sub>3</sub> mixing ratios (>150 nmol mol<sup>-1</sup>) was observed which was caused by a pronounced stratospheric intrusion.

Besides model forecasts and airborne measurements, satellite measurements of NO<sub>2</sub> from GOME-2 were also available for the region of interest (Fig. 19). At 17 UTC, GOME-NO<sub>2</sub> data show that Kansas was entirely covered with enhanced tropospheric NO<sub>2</sub> vertical column densities up to  $7-8 \times 10^{15}$  molec cm<sup>-2</sup>, most likely produced by lightning ~12-24 h earlier. Within the remnants of the MCS, the Falcon observed NO enhancements in the range of 0.5-1 nmol mol<sup>-1</sup> between ~9 and 11.6 km altitude (~63000-65000 s and ~66000-67000 s) (Figs. 20a-b). In addition, NO<sub>y</sub> mixing ratios were clearly enhanced (~2-3 nmol mol<sup>-1</sup>) and the low NO/NO<sub>y</sub> ratios (0.2-0.3) indicate that the LNO<sub>x</sub> emissions were aged (Figs. 20c-d). Furthermore, CH<sub>4</sub> mixing ratios reached up to 1.86 μmol mol<sup>-1</sup> and SO<sub>2</sub> mixing ratios were mostly <100 pmol mol<sup>-1</sup>. Highly variable CO (~60-110 nmol mol<sup>-1</sup>) and O<sub>3</sub> (~80-280 nmol mol<sup>-1</sup>) mixing ratios were also observed within the aged outflow, most likely caused by dynamical processes. The maximum cruising altitude within the remnants of the MCS (11.6 km) coincide with the broad tropopause according to the vertical temperature profile from the Falcon (Figs. 21a-b) and the 12 UTC radiosounding from Topeka in north-eastern Kansas ([http://catalog.eol.ucar.edu/cgi-bin/dc3\\_2012/ops/index](http://catalog.eol.ucar.edu/cgi-bin/dc3_2012/ops/index)).

### 4.3.2 Discussion of 8 June 2012 observations

Based on the Falcon trace gas time series in Fig. 20a, major pathways for the most likely trace gas transport within and near the active MCS are illustrated in Fig. 22. Almost the entire vertical and horizontal (E-W) extension of the MCS remnant was probed, as indicated by the orange shaded area (most complete probing compared to the two previous cases in Figs. 7a and 15).

On June 8, remnants of the MCS characterized by low  $O_3$  and high CO mixing ratios (transport from below) were located near areas with elevated  $O_3$  and low CO mixing ratios (transport from above) as indicated in the time series in Fig. 20a and in Fig. 22 by the different colored and directed arrows in the orange shaded area. The highly variable CO and  $O_3$  mixing ratios observed at this altitude within the aged MCS outflow indicate a mixing and cross layering of lower stratospheric and upper tropospheric air masses in the broad tropopause transition zone.

In general, CO mixing ratios were not as enhanced as in the previously presented cases. The most likely BL pollution source in this case was anthropogenic pollution from Dallas and northern Texas, and not emissions from wildfires (results from FLEXPART analyses not shown here, see DC3 field catalog). As indicated in Fig. 22, pollution was ingested near the cloud base of the MCS (yellow and green arrows), but was also present outside of the MCS and mixed with a stratospheric intrusion reaching as far downward as  $\sim 7$  km (yellow and red curved arrows). The time sequence of the flight through the latter layer is presented in Fig. 18b. Above this mixed polluted layer, a second polluted layer was observed, however not mixed with stratospheric air masses. Low NO mixing ratios indicate that these two layers were most likely not processed inside the MCS.

On the other hand, elevated NO mixing ratios were observed within the entire aged MCS outflow probed between 8.8 and 11.6 km (outflow depth  $>2.8$  km) (Figs. 20a, 22). Near the upper boundary of the aged outflow (11.6 km), highly variable  $O_3$  mixing ratios (up to  $280 \text{ nmol mol}^{-1}$ ) coincided with elevated NO indicating mixing with lower stratospheric air masses (broad, red arrows in Fig. 22). In addition, as indicated in Fig. 18a ( $\sim 67000$  s) the lower boundary of the aged outflow ( $\sim 8-9$  km) likely mixed with a stratospheric intrusion (up to  $170 \text{ nmol mol}^{-1}$ ) wrapped around the outflow (red curved arrow in Fig. 22). In agreement, the vertical temperature profiles indicate an inversion layer at 8.6 km (Figs. 21a-b).

During the flight on June 8 the exchange of tropospheric and stratospheric air masses in the

aged MCS outflow region was not the only striking process, but also the strong influence of the MCS on the particle concentration in the UT/LS region. In Fig. 23 time series of a variety of particle concentrations (CPC, rBC, and FSSP-100) are shown for the first flight on June 8. Within the aged MCS outflow at 11.6 km and during the descent through the outflow (both areas highlighted in yellow), the FSSP-100 concentrations are generally low indicating almost cloud free conditions. In addition, the rBC mass mixing ratios are rather low ( $<10 \text{ ng kg}^{-1}$ ), most likely due to wash-out processes. In contrast, high numbers of condensation nuclei CPC  $>5 \text{ nm}$  and  $>14 \text{ nm}$  are present (up to  $20,000\text{-}30,000 \text{ particles STP cm}^{-3}$ ). These concentrations partly exceed the concentrations observed in the BL and are most likely produced in-situ (by dynamical effects and from precursors as  $\text{SO}_2$  and VOCs, see below). The measurements in the aged outflow indicate that new ultra-fine particles are formed, since CPC  $>5 \text{ nm}$  partly exceeds the value for CPC  $>14 \text{ nm}$ . The low concentration of non-volatile particles ( $\sim 100 \text{ particles STP cm}^{-3}$ ) supports the suggestion of in-situ production prevailing over the upward particle transport from the BL. Of all Falcon DC3-flights in the vicinity of thunderstorms, this is the only flight that shows clear evidence of new particle formation.

Next the  $\Delta\text{O}_3/\Delta\text{CO}$  ratio in the lofted pollution layers ( $\sim 7\text{-}8 \text{ km}$ ) and in the aged MCS outflow ( $\sim 9\text{-}12 \text{ km}$ ) mentioned above is discussed for the Falcon flight on June 8. The influence of the stratospheric intrusion on the polluted layers probed during the ascent from Salina is shown in Fig. 24a (see also Figs. 20b, 22). The  $\Delta\text{O}_3/\Delta\text{CO}$  ratio was enhanced (+1.4) in the lower pollution layer located at  $6.6\text{-}7.2 \text{ km}$  due to mixing with a stratospheric intrusion. Within the core of this layer a negative  $\Delta\text{O}_3/\Delta\text{CO}$  ratio (-0.4) was observed, as typical for stratospheric influenced air masses. In contrast, the second lofted pollution layer located above the first one at  $7.4\text{-}7.9 \text{ km}$  was not impacted by the stratospheric intrusion. The observed  $\Delta\text{O}_3/\Delta\text{CO}$  ratio (+0.1) in this plume agrees with observations in lofted BB plumes ( $<7 \text{ km}$ ) not mixed with stratospheric air masses and suggests only a weak photochemical  $\text{O}_3$  production,  $\sim 5\text{-}10 \text{ nmol mol}^{-1}$  (see Fig. 24a and Table 1). Within the aged MCS outflow ( $\sim 63000\text{-}65000 \text{ s}$  and  $\sim 66000\text{-}67000 \text{ s}$ ) in Fig. 18a, distinct negative  $\Delta\text{O}_3/\Delta\text{CO}$  ratios (-3.8 and -3.4, respectively) were observed in the lower boundary ( $8.8\text{-}10.7 \text{ km}$ ), as well as in the upper boundary (at  $11.6 \text{ km}$ ) of the aged outflow (Fig. 24b). Here the mixing of the aged MCS outflow with air masses from the LMS was prominent throughout the entire anvil outflow region, as illustrated in Fig. 22 in the orange shaded area by the different colored arrows.

A summary of the chemical composition ratio observed in the aged MCS outflow on June 8 compared to the background is given in Table 4. The day after the major convective activity CO mixing ratios at ~10-12 km altitude were only slightly enhanced by ~10 nmol mol<sup>-1</sup>. In contrast, O<sub>3</sub> mixing ratios were distinctly enhanced compared to the background by ~20-50 nmol mol<sup>-1</sup> on average over a wide horizontal distance of up to ~200 km, indicating a distinct downward mixing of O<sub>3</sub>-rich air masses from the LMS and simultaneously in-mixing of tropospheric air masses (rich in CO and low in O<sub>3</sub>) into the LMS. CH<sub>4</sub> mixing ratios were slightly enhanced (up to 1.85 μmol mol<sup>-1</sup>) compared to the background due to upward transport of pollution. As in the previous cases, SO<sub>2</sub> mixing ratios were low (~30 pmol mol<sup>-1</sup>) within the aged outflow due to efficient wash-out effects. In agreement to our observations, high scavenging efficiencies in the range of 80% have been observed by *Yang et al.* [2015] in other DC3 thunderstorms on May 29 and 30, 2012. In addition, H<sub>2</sub>SO<sub>4</sub> was most likely formed from SO<sub>2</sub> and acted as a precursor for the formation of new particles (Fig. 23).

On June 8, the influence from LNO<sub>x</sub> was still observable in the aged MCS outflow with mean NO and NO<sub>y</sub> mixing ratios in the range of 0.5 and 2.5 nmol mol<sup>-1</sup>, respectively, both well enhanced above typical background values (Table 4). In addition, the high ethane and propane mixing ratios (>1200 pmol mol<sup>-1</sup>) and benzene/toluene ratio (1.0) indicate a prominent influence of anthropogenic pollution transported upward from the BL to the anvil outflow region. The rBC mass mixing ratio was low (5-7 ng kg<sup>-1</sup>) within the aged MCS outflow compared to the background (11-16 ng kg<sup>-1</sup>), most likely influenced by efficient wash-out processes. In comparison, the concentration of condensation nuclei >5 nm and >14 nm was much larger in the aged outflow (~10,000-30,000 particles STP cm<sup>-3</sup>) compared to the background (~500-1000 particles STP cm<sup>-3</sup>) as a result of new particle formation.

The last presented case study from June 8 clearly shows that tropospheric and stratospheric air masses are efficiently mixed in the aged MCS outflow region (Fig. 22). The irreversible in-mixing of UT air masses with O<sub>3</sub>-rich air masses in the LMS is prominent at least up to 11.6 km altitude. Here elevated NO mixing ratios (on average ~0.5-1 nmol mol<sup>-1</sup>) from LNO<sub>x</sub> was observed to coincide with stratospheric O<sub>3</sub> mixing ratios up to 278 nmol mol<sup>-1</sup>. In contrast, the cause for the elevated O<sub>3</sub> mixing ratios observed within the aged anvil outflow in the UT is most likely in-mixing from the LMS. Any pronounced contribution from photochemical O<sub>3</sub> production is not obvious in our observations within the aged thunderstorm outflow after 12-24 h, due to the dominance of the dynamical contribution from the LMS. The observed O<sub>3</sub> enhancement (~20-50 nmol mol<sup>-1</sup> on average) in the UT is far too high and

the  $\Delta\text{O}_3/\Delta\text{CO}$  ratios (-3.4/-3.8) are far too low to result from photochemical production alone (~5-20 nmol mol<sup>-1</sup> per day and a positive correlation expected, see Sect. 1). Perhaps the duration with daylight (~6 hours) was too short to produce significant O<sub>3</sub> amounts. From our measurements it is however not possible to investigate if a smaller contribution to the observed O<sub>3</sub> enhancement was generated by photochemical O<sub>3</sub> production, since HO<sub>x</sub> measurements were not available on the Falcon. A MCS case study including HO<sub>x</sub> measurements on the DC8 during DC3 is in preparation by C. Cantrell (private communication, 2015).

## 5 Discussion of observed ozone enhancements within thunderstorms

In the introduction, present knowledge on major processes responsible for O<sub>3</sub> enhancements in thunderstorm outflow were summarized, i.e. *photochemical O<sub>3</sub> production and stratospheric downward mixing*. The presented case studies from DC3 indicate that the latter process was most dominant in Central U.S. thunderstorms investigated by the Falcon during May-June 2012. This result is not surprising given that the sampling was conducted in convection that had been exposed to less than ~6 hours of sunlight, likely not long enough for much O<sub>3</sub> production to occur.

A further mechanism responsible for O<sub>3</sub> enhancements within thunderstorms has been discussed by Zahn *et al.* [2002]. During a number of commercial “Civil Aircraft for Regular Investigation of the Atmosphere Based on an Instrument Container” (CARIBIC) flights, “ozone-rich transients” (up to ~2000 nmol mol<sup>-1</sup>) over a horizontal distance of 5-80 km were occasionally observed in the vicinity of deep convection, which were attributed to “measurement artifacts” (trigger electrical “corona” discharges on the aircraft fuselage or sampling inlets). During DC3, we observed this type of brief O<sub>3</sub> enhancements (without accompanying CO signature) due to a triggered flash during one Falcon flight on June 6, 2012 (see Falcon flight reports: [http://catalog.eol.ucar.edu/dc3\\_2012/missions/missions.html](http://catalog.eol.ucar.edu/dc3_2012/missions/missions.html)).

In the past, “ozone-rich transients” have also frequently been observed during “Measurements of Ozone and Water Vapor by In-service Aircraft” (MOZAIC) flights over the equatorial Atlantic Ocean, as reported by Suhre *et al.* [1997]. About 1/3 of all flights showed signatures of enhanced O<sub>3</sub> (~100-500 nmol mol<sup>-1</sup>, also 5-80 km wide at 10-12 km), occasionally coinciding with enhanced water vapor, turbulence and wind changes when the

aircraft passed under a thunderstorm anvil at a distance of at least 15-30 km from convective towers. *Suhre et al.* [1997] suggested that a stratospheric influence, “the downward turbulent transfer through the tropopause caused by convection”, was the main cause for the observed O<sub>3</sub> enhancements. When precipitation streaks loaded with ice particles fall from an overshooting anvil, water vapor and O<sub>3</sub>-rich air may be transported downward through the tropopause region into the UT. The continuous evaporative cooling of the ice particles causes a rapidly downward moving air mass and a reduction of its potential temperature. This microphysical process would produce “cold” downdrafts. However, detailed radar measurements in squall-line systems by *Biggerstaff and Houze* [1993] have shown that the upper-level downdrafts are “warm” and dynamically induced compared to the microphysically forced “cold” downdrafts at lower-levels between the surface and ~5 km. They proposed that the upper-level downdrafts were caused by gravity waves as a result of the strong convective updrafts. Model simulations by *Wang et al.* [2003] have also shown that gravity wave breaking at the top of deep convective systems in the mid-latitudes may cause an air mass exchange between stratosphere and troposphere. *We believe that such a dynamical mechanism, as suggested by e.g. Biggerstaff and Houze [1993] and Wang et al. [2003], may explain the O<sub>3</sub> enhancements in the vicinity of thunderstorms that we observed during DC3.* Also coexisting signatures in other trace gases during DC3, e.g. CO and CH<sub>4</sub> support the presence of a dynamical mechanism. This type of downdraft structure has commonly been observed by radar measurements in supercells in the past [*Payne et al.*, 2010] and is similar to the upper-level rear-flank downdraft in the *Lemon and Doswell* [1979] conceptual model of supercell storms.

Compared to most other studies, where O<sub>3</sub> enhancements from thunderstorms were more or less accidentally observed during commercial flights (e.g. CARIBIC and MOZAIC) or during single research flights (Sect. 1), the gain of the DC3 experiment was the selective targeting of different thunderstorm types in different developing stages over a wide area over the Central U.S. supported by a variety of airborne in-situ trace species measurements, dense ground-based networks of radar and lightning detection systems, and satellite data. Thus, the measured O<sub>3</sub> enhancements from thunderstorms could more easily be assigned to certain regions of the thunderstorms and its outflow, and were found to extend over wide areas (~20-200 km) and to coexist with pronounced gradients in other trace gases.

To our knowledge, the study presented here is the first one of its kind where a general picture of the major transport paths within and in the vicinity of Central U.S. thunderstorms is

obtained as schematics (Figs. 7, 15, 22) based on such a comprehensive data set: (1) *The wrapping of stratospheric air around the anvil outflow* in our schematic pictures based on Falcon measurements is also confirmed by O<sub>3</sub> lidar measurements on board the NASA-DC8 aircraft during DC3 [Pan et al., 2014] and has been suggested to result from radiated gravity waves initiated when the strong convective updrafts deform the tropopause upward [Hitchman et al., 2004]. (2) *The direct injection of O<sub>3</sub>-rich stratospheric air masses into the UT anvil outflow* in our schematic pictures based on Falcon measurements has only rarely been observed in the past. Our case study from May 30 indicates that the vigorous nature of a supercell and MCC thunderstorm may connect polluted layers located in the LT with the ~10 km distant LMS, thereby reversing the chemical composition ratio in the UT/LS region. Until now our present knowledge about cross-tropopause tracer transport was mainly based on results from model studies with e.g. WRF and cloud-resolving models. These studies indicate that overshooting tops have the potential to inject large amount of LT air into the LMS [e.g. Mullendore et al., 2005; Homeyer et al., 2014] and in the opposite direction [e.g. Frey et al., 2015].

The three case studies we presented herein and in *HH2016* give enough evidence to propose that: “*in May-June in the UT/LS region over the Central U.S. a pronounced exchange of tropospheric and lowermost stratospheric air masses is present which is influenced by the frequent occurrence of intense thunderstorms*”. One main question is, if the observed O<sub>3</sub> enhancements in the aged anvil outflow during DC3 significantly contribute to maintain the recurring UT-O<sub>3</sub> maximum as observed by Li et al. [2005] in a stationary anticyclone centered over the southeastern U.S. later in summer during the NA monsoon. Until recently, the downward mixing of O<sub>3</sub> rich air from the stratosphere and ozone precursors (NO<sub>x</sub> and VOCs) transported upward from the BL by convection were found to only play a minor role and O<sub>3</sub> production by aged LNO<sub>x</sub> was found to play the dominant role in this anticyclone [Choi et al., 2005; Cooper et al., 2006, 2007; Choi et al., 2008; Cooper et al., 2009; Zhao et al., 2009; Allen et al., 2010, 2012]. In a sensitivity test, Cooper et al. [2007] increased global LNO<sub>x</sub> emissions from 2.2 Tg a<sup>-1</sup> to 6.6 Tg a<sup>-1</sup> in their ECHAM5/MESSy1 chemistry general circulation model during the 2006 summer monsoon and achieved a better agreement between ozone measurements and model results supporting the importance of LNO<sub>x</sub> for O<sub>3</sub> production in the stationary anticyclone. However, for some regions (e.g. at 10-11 km above Huntsville, Alabama) the discrepancies between ozone observations and model results were still large. Cooper et al. [2007] suggested that the presence of aged ozone-rich stratospheric

air masses in the UT region could contribute to this discrepancy, however the spatial model resolutions implemented in the UT/LS region was too coarse to study this transport in detail. Further simulations with global models over NA in summer have shown large discrepancies in quantifying UT-O<sub>3</sub> and -NO<sub>x</sub> produced by lightning compared to observations [Pfister *et al.*, 2008; Hudman *et al.*, 2009; Jourdain *et al.*, 2010]. Wang *et al.* [2013] pointed out that present model predictions for UT-O<sub>3</sub> over NA are generally too low and still differ by ~20-25 nmol mol<sup>-1</sup> compared to measurements with ozonesondes. First recent CTM results by Tang *et al.* [2011] suggest that the cause of the persistent ozone maximum observed in summer over northern mid-latitude continents (e.g. over the Central U.S.) is a deep convective stratosphere-troposphere exchange (STE) flux. Only a small number of all convective events penetrate into the LMS but these events may induce a pronounced downward O<sub>3</sub>-flux as reaction of the tropopause upward deformation [Tang and Prather, 2010]. In addition, high-resolved simulations of the meteorology and chemistry with the WRF-Chem model by Barth *et al.* [2012] and Homeyer *et al.* [2014] suggest that the entrainment of O<sub>3</sub>-rich air from the stratosphere may play a major role for the UT-O<sub>3</sub> maximum observed during the NA monsoon. Our measurements in a number of thunderstorms during DC3 support these more recent results and give evidence of a more pronounced influence from the stratosphere on the convective outflow in specific regions, such as the Central U.S., at least during specific periods (May-June). Later during the NA monsoon (June-August) the tropopause height is increasing and most convective systems are less severe which would most likely cause a less pronounced O<sub>3</sub> contribution from the stratosphere and a larger contribution from LNO<sub>x</sub> as suggested by Cooper *et al.* [2007].

## 6 Summary and Conclusions

A unique data set on chemistry and dynamics within and in the vicinity of Central U.S. thunderstorms sampled during the DC3 field experiment in summer 2012 was presented. We focused on in-situ trace species measurements (CO, O<sub>3</sub>, SO<sub>2</sub>, CH<sub>4</sub>, NO, NO<sub>x</sub>, NO<sub>y</sub>, VOC, CN, and black carbon) carried out by the German DLR-Falcon aircraft in fresh (<12 h) and aged (~12-24 h) anvil outflow (~9-12 km altitude) from different thunderstorm types (MCS, MCC, supercells, and squall lines) over Oklahoma, Texas, Colorado, and Kansas. A combination of trace gas time series and correlations (O<sub>3</sub>-CO), radar, lightning, and satellite information, as well as model results from WRF and FLEXPART, were used to analyze and design schematics of major trace gas transport pathways within and in the vicinity of the probed



thunderstorms to study the impact of thunderstorms on the UT/LS O<sub>3</sub> composition. On most thunderstorm days, dense smoke plumes from huge wildfires in New Mexico and Colorado were also present. These wildfire emissions in the vicinity of the probed thunderstorms, characterized by pronounced trace gas gradients, were useful tracers to construct a general picture of trace gas transport pathways within and nearby thunderstorms.

The analyses indicate that the investigated thunderstorms influenced the chemical composition ratio of the UT/LS region over the Central U.S. significantly in accordance with first findings presented in *HH2016*. A distinct redistribution and production of trace gases, especially CO, O<sub>3</sub> and NO<sub>x</sub>, was observed in the UT/LS region. Within and in the vicinity of thunderstorms, O<sub>3</sub>-poor (CO-rich) air from the LT was transported upward to the UT, as known from previous thunderstorm studies. However, compared to past thunderstorm campaigns (see e.g. Table 10 in *Schumann and Huntrieser, 2007; Huntrieser et al., 1998, 2002, 2008, 2009, 2011*), the frequency and intensity of events with O<sub>3</sub>-poor (CO-rich) air penetrating the tropopause into the LMS, and simultaneously O<sub>3</sub>-rich air transported downward from the LMS to the UT was especially high during DC3. On a regular basis, the probed DC3 storms developed overshooting tops promoting the stratosphere-troposphere exchange of air masses. Furthermore, the results from three DC3 case studies gave sufficient evidence that the in-mixing of O<sub>3</sub>-rich air masses from the LMS (and not photochemical O<sub>3</sub> production) was the major source of elevated O<sub>3</sub> mixing ratios observed within and in the vicinity of fresh and aged anvil outflow:

- On the Falcon flight on May 30, 2012 in the center of the fresh anvil outflow from an overshooting supercell, where also the highest lightning-NO mixing ratios were observed (8.6 nmol mol<sup>-1</sup>), O<sub>3</sub> mixing ratios as low as ~70 nmol mol<sup>-1</sup> were observed at ~9 km altitude, indicating upward transport from lower levels (LT). In contrast, along the boundaries of the anvil outflow a mixture of O<sub>3</sub>-rich air masses (up to ~140 nmol mol<sup>-1</sup>) from the LMS and CO-rich air masses (up to ~160 nmol mol<sup>-1</sup>) from BB emissions (Whitewater-Baldy Fire) was observed. In addition, on May 30, we observed that the fresh anvil outflow from a nearby overshooting MCC was surrounded by a stratospheric intrusion similar to the observations by *Pan et al. [2014]*; in our case lofted BB emissions (CO ~120 nmol mol<sup>-1</sup>) located below the MCC outflow (~8-10.5 km) mixed with O<sub>3</sub>-rich air masses from the LMS (O<sub>3</sub> ~150 nmol mol<sup>-1</sup>). In summary, our observations indicate that the major impact on the UT/LS O<sub>3</sub> composition within and in the vicinity of the investigated supercell and MCC outflow must have been caused by dynamical (and not photochemical) processes, because the observed

trace gas gradients have larger amplitudes than expected from photochemical processes only. In addition, this was further supported by measurements of the vertical velocity by aircraft and from multi-Doppler radar analyses.

- On the Falcon flight on June 12, 2012 in the fresh outflow from a squall line, low O<sub>3</sub> mixing ratios in the range of 70 nmol mol<sup>-1</sup> were observed throughout the center of the outflow layer between ~9.5-12 km altitude in conjunction with elevated CO mixing ratios in the range of 120 nmol mol<sup>-1</sup> from BB emissions (High Park Fire) transported upward from the LT. At the highest flight level (~12 km), both air masses of LT origin as well as LMS origin (~260 and ~80 nmol mol<sup>-1</sup> O<sub>3</sub> and CO, respectively) were observed next to each other in the anvil outflow in conjunction with lightning-produced NO in the range of 1-3 nmol mol<sup>-1</sup>. In addition, a stratospheric intrusion was wrapped around the overshooting anvil outflow and reached down to ~9 km with O<sub>3</sub> mixing ratios as high as ~120 nmol mol<sup>-1</sup>. Just below the anvil outflow (~8-9.5 km), lofted BB emissions (CO ~180 nmol mol<sup>-1</sup>) mixed with the stratospheric intrusion.

- On the Falcon flight on June 8, 2012 in the aged outflow (~12-24 h) from scattered severe convection organized to a MCS, anthropogenic pollution with CO mixing ratios exceeding ~100 nmol mol<sup>-1</sup> was transported upward from the LT and mixed with O<sub>3</sub>-rich air masses (>200 nmol mol<sup>-1</sup>) at ~11.5 km altitude. Observed O<sub>3</sub> enhancements (~20-50 nmol mol<sup>-1</sup> on average) were far too high and ΔO<sub>3</sub>/ΔCO ratios (down to -3.8) far too low to result from photochemical production (~5-20 nmol mol<sup>-1</sup> per day and a positive correlation expected) and instead the in-mixing of O<sub>3</sub>-rich stratospheric air masses was suggested to cause these enhancements. In addition, enhanced NO mixing ratios produced by lightning (~0.5-1 nmol mol<sup>-1</sup>) mixed with these O<sub>3</sub>-rich air masses. Furthermore, a stratospheric intrusion with O<sub>3</sub> mixing ratios as high as ~170 nmol mol<sup>-1</sup> was wrapped around the lower boundary of the MCS outflow and reached down to 8-9 km altitude. The highly variable CO and O<sub>3</sub> mixing ratios observed within the aged MCS outflow were most likely caused by mixing and layering of lower stratospheric and upper tropospheric air masses. Of all Falcon DC3-flights in the vicinity of thunderstorms, this is the only flight that shows clear evidence of new particle formation. Results from past field experiments have shown that new particle formation is a common process observed in the vicinity of deep convection due to convective lifting and formation from precursors such as SO<sub>2</sub> [Thornton *et al.*, 1997; de Reus *et al.*, 1999; Wang *et al.*, 2000; Huntrieser *et al.*, 2002].

Our findings from the above mentioned case studies can be summarized as follows (see also schematics of major trace gas pathways in Figs. 7, 15, and 22):

- a rapid uplift of “less diluted” emissions from wildfires (high in CO, SO<sub>2</sub>, and rBC) from the LT to the UT is frequently observed in the vicinity of thunderstorms, most likely transported upward in towering cumulus clouds along the storm’s flanking line,
- emissions from wildfires are also ingested into the thunderstorm near the cloud base,
- DC3 thunderstorms frequently produce an overshooting top, possibly facilitated by the large-scale double(triple)-tropopause structure,
- the overshooting top injects high amounts of BB emissions (mainly CO) and LNO<sub>x</sub> into the LMS in addition to low O<sub>3</sub> mixing ratios from the LT,
- as a dynamical response (most likely gravity waves), O<sub>3</sub>-rich air from the lowermost stratosphere is transported downward directly into the anvil outflow and in addition surrounds the outflow like an umbrella (stratospheric intrusion),
- the lofted BB plume mixes with the stratospheric intrusion surrounding the anvil outflow.

In comparison to the described, pronounced trace gas exchange in the UT/LS region initiated by dynamical processes, no clear signatures of photochemical O<sub>3</sub> production was observed within the anvil outflow probed during the presented DC3 Falcon flights. The exposure to daylight (<6 h) was probably too short. We expect that sufficient UT-HO<sub>x</sub> is available for the production, but the observed production rate (<10 nmol mol<sup>-1</sup>) in the lofted BB and anthropogenic plumes is negligible in comparison to the dynamical processes (>> 10 nmol mol<sup>-1</sup>) observed in the anvil outflow region. The major part of the probed thunderstorms over the Central U.S. developed over regions with low mixing ratios of anthropogenic O<sub>3</sub> precursors in the BL, which is assumed to cause the lack of pronounced O<sub>3</sub> production signatures:

- Rather low O<sub>3</sub> enhancements (<10 nmol mol<sup>-1</sup>) and production signatures ( $\Delta O_3/CO = +0.03$  to  $+0.14$ ) were observed in “less undiluted” BB and anthropogenic plumes lofted to the LT-MT (~1-7 km) altitude in the vicinity, but outside of the investigated thunderstorms.
- Occasionally these pollution plumes (elevated in  $\Theta_e$ ) were even lofted to the UT (~7-

10 km) both inside and outside of the thunderstorms and frequently mixed with stratospheric intrusions wrapped around the anvil outflow ( $\Delta\text{O}_3/\text{CO} = -1.7$  to  $+1.4$ ).

- Even more pronounced  $\Delta\text{O}_3/\text{CO}$  ratios (between  $-3.9$  and  $+1.4$ ) were observed higher up in the anvil outflow region ( $\sim 9$ - $12$  km), due to a stronger and more direct exchange of air masses between the LT and UT/LS region.

In summary, DC3 thunderstorms over the Central U.S. seem to act as huge cooking pots, mixing a cocktail of polluted BL air (here especially enhanced in CO from wildfires) with  $\text{O}_3$ -rich lower stratospheric air and emitting this mixture (together with high amounts of LNO<sub>x</sub>) over a surprisingly wide area in the UT/LS region and on a surprisingly regular basis during DC3. We would expect that this aged thunderstorm outflow may have a large impact on the UT/LS composition in general and may contribute to the recurring UT- $\text{O}_3$  maximum observed in a stationary anticyclone centered over the southeastern U.S. in summer by *Li et al.* [2005]. In addition, the aged thunderstorm outflow may impact the UT/LS composition downwind of the U.S. (e.g. North Atlantic), as already observed by e.g. *Brunner et al.* [1998] and *Jeker et al.* [2000]. Besides the wide horizontal spreading of the thunderstorm outflow during DC3, the frequent development of overshooting cloud tops was also striking. In these cases a large-scale multiple-tropopause structure was present, which may facilitate the development of overshooting tops [*Homeyer et al.*, 2014].

It is expected that the impact of thunderstorms on the  $\text{NO}_x$  and  $\text{O}_3$  composition in the UT/LS region will increase in the near future as a response to climate change. Especially within the perspective of increasing global temperatures, frequency of severe thunderstorms and wildfire activity [*Simmonds et al.*, 2005; *Brooks et al.*, 2013; *Turetsky et al.*, 2011; *Romps et al.*, 2014], we recommend further combined, high-resolved model studies, airborne in-situ and lidar measurements in the UT/LS region, and ground-based radar measurements on this important topic. The analyses presented here and in *HH2016* show that the frequent occurrence of deep and severe convection over the Central U.S. is a preferred target region for these kinds of studies. The impact of smoke aerosols on the intensification of Central U.S. thunderstorms also needs to be addressed in more detail in future studies.

## Acknowledgements

The DC3 field campaign was established by a collaborative effort of NCAR, NASA, the U.S. university community, NOAA, and DLR. The National Science Foundation (NSF), NASA, NOAA and DLR were the primary funders for DC3. NCAR is supported by the NSF. Detailed information on the scientific goals and a link to the field data is available from the DC3 web site, [https://www.eol.ucar.edu/field\\_projects/dc3](https://www.eol.ucar.edu/field_projects/dc3). We greatly acknowledge the excellent collaboration with the DC3 principal investigators and all the support the DLR team received during the field phase from: M. C. Barth (NCAR), C. A. Cantrell (University of Colorado), W. H. Brune (The Pennsylvania State University), S. A. Rutledge (Colorado State University), and J. H. Crawford (NASA/LaRC). Furthermore, the logistical support from NCAR-EOL by V. Salazar, J. Moore, G. Stossmeister, and B. Baeuerle is greatly appreciated. We thank the Falcon pilots (R. Welser and P. Weber), A. Hausold for the logistics, the engineers and scientists of the DLR flight department for the excellent support during the field phase. We express our gratitude to the DLR colleagues who supported the trace gas and aerosol measurements: J. Kim, A. Reiter, A. Roiger, H. Ziereis and the financial support from the Deutsche Forschungsgemeinschaft (DFG, project number MI 583/4-1). Furthermore, the ETH Zurich (T. Peters) is greatly acknowledged for providing the NO instrument, J. Brioude (NOAA) for providing FLEXPART model products, and S. Kondragunta (NOAA/NESDIS) for providing GOME-2 NO<sub>2</sub> retrieval products. The GOES data was provided by NCAR/EOL under sponsorship of the National Science Foundation (<http://data.eol.ucar.edu/>). We thank L. L. Pan and C. R. Homeyer (NCAR Boulder) for fruitful discussions. Finally, we are grateful to A. Roiger (DLR) and the three anonymous reviewers for their helpful comments and suggestions, which greatly helped to improve the manuscript.

## References

- Allen, D., Pickering, K. E., Duncan, B., and Damon, M.: Impact of lightning NO emissions on North American photochemistry as determined using the Global Modeling Initiative (GMI) model, *J. Geophys. Res.*, 115, D22301, doi:10.1029/2010JD014062, 2010.
- Allen, D. J., Pickering, K. E., Pinder, R. W., Henderson, B. H., Appel, K. W., and Prados, A.: Impact of lightning-NO on eastern United States photochemistry during the summer

of 2006 as determined using the CMAQ model, *Atmos. Chem. Phys.*, 12, 1737-1758, doi:10.5194/acp-12-1737-2012, 2012.

Alvarado, M. J., Logan, J. A., Mao, J., Apel, E., Riemer, D., Blake, D., Cohen, R. C., Min, K.-E., Perring, A. E., Browne, E. C., Wooldridge, P. J., Diskin, G. S., Sachse, G. W., Fuelberg, H., Sessions, W. R., Harrigan, D. L., Huey, G., Liao, J., Case-Hanks, A., Jimenez, J. L., Cubison, M. J., Vay, S. A., Weinheimer, A. J., Knapp, D. J., Montzka, D. D., Flocke, F. M., Pollack, I. B., Wennberg, P. O., Kurten, A., Crouse, J., Clair, J. M. St., Wisthaler, A., Mikoviny, T., Yantosca, R. M., Carouge, C. C., and Le Sager, P.: Nitrogen oxides and PAN in plumes from boreal fires during ARCTAS-B and their impact on ozone: an integrated analysis of aircraft and satellite observations, *Atmos. Chem. Phys.*, 10, 9739-9760, doi:10.5194/acp-10-9739-2010, 2010.

Anderson, J. G., Wilmouth, D. M., Smith, J. B., and Sayres, D. S.: UV dosage levels in summer: Increased risk of ozone loss from convectively injected water vapor, *Science* 337, 835, doi:210.1126/science.1222978, 2012.

Apel, E. C., Olson, J. R., Crawford, J. H., Hornbrook, R. S., Hills, A. J., Cantrell, C. A., Emmons, L. K., Knapp, D. J., Hall, S., Mauldin III, R. L., Weinheimer, A. J., Fried, A., Blake, D. R., Crouse, J. D., Clair, J. M. St., Wennberg, P. O., Diskin, G. S., Fuelberg, H. E., Wisthaler, A., Mikoviny, T., Brune, W., and Riemer, D. D.: Impact of the deep convection of isoprene and other reactive trace species on radicals and ozone in the upper troposphere, *Atmos. Chem. Phys.*, 12, 1135-1150, doi:10.5194/acp-12-1135-2012, 2012.

Apel, E. C., Hornbrook, R. S., Hills, A. J., Blake, N. J., Barth, M. C., Weinheimer, A., Cantrell, C., Rutledge, S. A., Basarab, B., Crawford, J., Diskin, G., Homeyer, C. R., Campos, T., Flocke, F., Fried, A., Blake, D. R., Brune, W., Pollack, I., Peischl, J., Ryerson, T., Wennberg, P. O., Crouse, J. D., Wisthaler, A., Mikoviny, T., Huey, G., Heikes, B., O'Sullivan, D., and Riemer, D. D.: Upper tropospheric ozone production from lightning NO<sub>x</sub>-impacted convection: smoke ingestion case study from the DC3 campaign, *J. Geophys. Res.*, accepted, doi: 10.1002/2014JD022121, 2015.

Barth, M. C., Lee, J., Hodzic, A., Pfister, G., Skamarock, W. C., Worden, J., Wong, J., and Noone, D.: Thunderstorms and upper troposphere chemistry during the early stages of the 2006 North American Monsoon, *Atmos. Chem. Phys.*, 12, 11003-11026, doi:10.5194/acp-12-11003-2012, 2012.

- Barth, M. C., Brune, W. H., Cantrell, C. A., Rutledge, S., Crawford, J., Huntrieser, H., Carey, L., Mac Gorman, D., Weisman, M., et al.: The Deep Convective Clouds and Chemistry (DC3) Field Campaign, *Bull. Am. Meteorol. Soc.*, doi: 10.1175/BAMS-D-13-00290.1, 2015.
- Bertschi, I. T., and Jaffe, D. A.: Long-range transport of ozone, carbon monoxide, and aerosols to the NE Pacific troposphere during the summer of 2003: Observations of smoke plumes from Asian boreal fires, *J. Geophys. Res.*, 110, D05303, doi:10.1029/2004JD005135, 2005.
- Biggerstaff, M. I., and Houze, Jr., R. A.: Kinematics and microphysics of the transition zone of the 10-11 June, 1985 squall-line system. *J. Atmos. Sci.*, 50, 3091-3110, doi: [http://dx.doi.org/10.1175/1520-0469\[1993\]050<3091:KAMOTT>2.0.CO;2](http://dx.doi.org/10.1175/1520-0469[1993]050<3091:KAMOTT>2.0.CO;2), 1993.
- Biggerstaff, M. I., Wicker, L. J., Guynes, J., Ziegler, C. L., Straka, J. M., Rasmussen, E. N., Doggett, A., Carey, L. D., Schroeder, J. L., and Weiss, C.: The Shared Mobile Atmospheric Research and Teaching radar: A collaboration to enhance research and teaching. *Bull. Amer. Meteor. Soc.*, 86, 1263–1274, doi: <http://dx.doi.org/10.1175/BAMS-86-9-1263>, 2005.
- Blyth, A. M., Cooper, W. A., and Jensen, J. B.: A study of the source of entrained air in Montana cumuli, *J. Atmos. Sci.*, 45, 3944–3964, doi: [http://dx.doi.org/10.1175/1520-0469\[1988\]045<3944:ASOTSO>2.0.CO;2](http://dx.doi.org/10.1175/1520-0469[1988]045<3944:ASOTSO>2.0.CO;2), 1988.
- Boatman, J. F. and Auer, A. H.: The role of cloud top entrainment in cumulus clouds, *J. Atmos. Sci.*, 40, 1517-1534, doi:[http://dx.doi.org/10.1175/1520-0469\[1983\]040<1517:TROCTE>2.0.CO;2](http://dx.doi.org/10.1175/1520-0469[1983]040<1517:TROCTE>2.0.CO;2), 1983.
- Bolton, D.: The computation of equivalent potential temperature, *Mon. Wea. Rev.*, 108, 1046-1053, doi: [http://dx.doi.org/10.1175/1520-0493\[1980\]108<1046:TCOEPT>2.0.CO;2](http://dx.doi.org/10.1175/1520-0493[1980]108<1046:TCOEPT>2.0.CO;2), 1980.
- Bozem, H., Fischer, H., Gurk, C., Schiller, C. L., Parchatka, U., Koenigstedt, R., Stickler, A., Martinez, M., Harder, H., Kubistin, D., Williams, J., Eerdeken, G., and Lelieveld, J.: Influence of corona discharge on the ozone budget in the tropical free troposphere: a case study of deep convection during GABRIEL, *Atmos. Chem. Phys. Discuss.*, 14, 5233-5270, doi:10.5194/acpd-14-5233-2014, 2014.
- Brooks, H. E.: Severe thunderstorms and climate change, *Atmos. Res.*, 123, 129-138,

doi:10.1016/j.atmosres.2012.04.002, 2013.

Brunner, D., Staehelin, J., and Jeker, D.: Large-scale nitrogen oxide plumes in the tropopause region and implications for ozone, *Science*, 282, 1305-1309, doi:10.1126/science.282.5392.1305, 1998.

Bucseles, E., Celarier, E., Wenig, M., Gleason, J. F., Veeffkind, P., Boersma, K. F., and Brinksma, E.: Algorithm for NO<sub>2</sub> vertical column retrieval from the Ozone Monitoring Instrument, *IEEE Trans. Geosci. Remote Sens.*, 44, 1245-1258, doi:10.1109/TGRS.2005.863715, 2006.

Chin, M., Jacob, D. J., Munger, J.W., Parrish, D. D., and Doddridge, B. G.: Relationship of ozone and carbon monoxide over North America and its implication for ozone production and transport, *J. Geophys. Res.*, 99, 14565–14573, doi:10.1029/94JD00907, 1994.

Choi, Y., Wang, Y., Zeng, T., Martin, R. V., Kurosu, T. P., and Chance, K.: Evidence of lightning NO<sub>x</sub> and convective transport of pollutants in satellite observations over North America, *Geophys. Res. Lett.*, 32, L02805, doi:10.1029/2004GL021436, 2005.

Choi, Y., Wang, Y., Zeng, T., Cunnold, D., Yang, E., Martin, R., Chance, K., Thouret, V., and Edgerton, E.: Springtime transitions of NO<sub>2</sub>, CO, and O<sub>3</sub> over North America: Model evaluation and analysis, *J. Geophys. Res.*, 113, D20311, doi:10.1029/2007JD009632, 2008.

Cooper, O. R., Forster, C., Parrish, D., Trainer, M., Dunlea, E., Ryerson, T., Hübler, G., Fehsenfeld, F., Nicks, D., Holloway, J., de Gouw, J., Warneke, C., Roberts, J. M., Flocke, F., and Moody, J.: A case study of trans-Pacific warm conveyor belt transport: The influence of merging airstreams on trace gas import to North America, *J. Geophys. Res.*, 109, D23S08, doi:10.1029/2003JD003624, 2004.

Cooper, O. R., Stohl, A., Trainer, M., Thompson, A. M., Witte, J. C., Oltmans, S. J., Morris, G., Pickering, K. E., Crawford, J. H., Chen, G., Cohen, R. C., Bertram, T. H., Wooldridge, P., Perring, A., Brune, W. H., Merrill, J., Moody, J. L., Tarasick, D., Nédélec, P., Forbes, G., Newchurch, M. J., Schmidlin, F. J., Johnson, B. J., Tirquety, S., Baughcum, S. L., Ren, X., Fehsenfeld, F. C., Meagher, J. F., Spichtinger, N., Brown, C. C., McKeen, S. A., McDermid, I. S., and Leblanc, T.: Large upper tropospheric ozone enhancements above midlatitude North America during summer:



- In situ evidence from the IONS and MOZAIC ozone measurement network, *J. Geophys. Res.*, 111, D24S05, doi:10.1029/2006JD007306, 2006.
- Cooper, O. R., Trainer, M., Thompson, A. M., Oltmans, S. J., Tarasick, D. W., Witte, J. C., Stohl, A., Eckhardt, S., Lelieveld, J., Newchurch, M. J., Johnson, B. J., Portmann, R. W., Kalnajs, L., Dubey, M. K., Leblanc, T., McDermid, I. S., Forbes, G., Wolfe, D., Carey-Smith, T., Morris, G. A., Lefer, B., Rappenglück, B., Joseph, E., Schmidlin, F., Meagher, J., Fehsenfeld, F. C., Keating, T. J., Van Curen, R. A., and Minschwaner, K.: Evidence for a recurring eastern North America upper tropospheric ozone maximum during summer, *J. Geophys. Res.*, 112, D23304, doi:10.1029/2007JD008710, 2007.
- Cooper, O. R., Eckhardt, S., Crawford, J. H., Brown, C. C., Cohen, R. C., Bertram, T. H., Wooldridge, P., Perring, A., Brune, W. H., et al.: Summertime buildup and decay of lightning NO<sub>x</sub> and aged thunderstorm outflow above North America, *J. Geophys. Res.*, 114, D01101, doi:10.1029/2008JD010293, 2009.
- Crutzen, P. J.: The influence of nitrogen oxides on the atmospheric ozone content, *Quart. J. Roy. Meteor. Soc.*, 96, 320-325, doi:10.1002/qj.49709640815, 1970.
- Crutzen, P. J.: Overview of tropospheric chemistry: developments during the past quarter century and a look ahead, in: *Faraday Discussions on Atmospheric Chemistry – Measurements, Mechanics and Models*, Royal Soc. Chemistry, Vol. 100, 1–21, Cambridge, doi:10.1039/FD9950000001, 1995.
- Cummins, K. L., and Murphy, M. J.: An overview of lightning locating systems: History, techniques, and data uses, with an in-depth look at the U.S. NLDN, *IEEE Trans. Electromagn. Compat.*, 51(3), 499–518, 2009.
- DeCaria, A. J., Pickering, K. E., Stenchikov, G. L., and Ott, L. E.: Lightning-generated NO<sub>x</sub> and its impact on tropospheric ozone production: a three-dimensional modeling study of a Stratosphere–Troposphere Experiment: Radiation, Aerosols and Ozone (STERAO-A) thunderstorm, *J. Geophys. Res.*, 110, 13, doi:10.1029/2004jd005556, 2005.
- de Reus, M., Ström, J., Hoor, P., Lelieveld, J., and Schiller, C.: Particle production in the lowermost stratosphere by convective lifting of the tropopause, *J. Geophys. Res.*, 104, 23935-23940, doi: 10.1029/1999JD900774, 1999.

- Dickerson, R. R., Huffman, G. J., Luke, W. T., Nunnermacker, L. J., Pickering, K. E., Leslie, A. C. D., Lindsey, C. G., Slinn, W. G. N., Kelly, T. J., Delany, A. C., Greenberg, J. P., Zimmerman, P. R., Boatman, J. F., Ray, J. D., and Stedman, D. H.: Thunderstorms: An important mechanism in the transport of air pollutants, *Science*, 235, 460-465, doi: 10.1126/science.235.4787.460, 1987.
- Draxler, R. R., and Rolph, G. D.: HYSPLIT (HYbrid Single-Particle Lagrangian Integrated Trajectory) Model access via NOAA ARL READY Website (<http://ready.arl.noaa.gov/HYSPLIT.php>). NOAA Air Resources Laboratory, Silver Spring, MD, 2014.
- Dye, J. E., Ridley, B. A., Skamarock, W., Barth, M., Venticinque, M., Defer, E., Blanchet, P., Thery, C., Laroche, P., Baumann, K., Hubler, G., Parrish, D. D., Ryerson, T., Trainer, M., Frost, G., Holloway, J. S., Matejka, T., Bartels, D., Fehsenfeld, F. C., Tuck, A., Rutledge, S. A., Lang, T., Stith, J., and Zerr, R.: An overview of the Stratospheric-Tropospheric Experiment: Radiation, Aerosols, and Ozone (STERAO)-Deep Convection experiment with results for the July 10, 1996 storm, *J. Geophys. Res.*, 105(D8), 10023–10045, doi:10.1029/1999JD901116, 2000.
- Fischer, H., de Reus, M., Traub, M., Williams, J., Lelieveld, J., de Gouw, J., Warneke, C., Schlager, H., Minikin, A., Scheele, R., and Siegmund, P.: Deep convective injection of boundary layer air into the lowermost stratosphere at midlatitudes, *Atmos. Chem. Phys.*, 3, 739-745, doi:10.5194/acp-3-739-2003, 2003.
- Fishman, J., and Seiler, W.: Correlative nature of ozone and carbon monoxide in the troposphere: Implications for the tropospheric ozone budget, *J. Geophys. Res.*, 88, 3662-3670, doi: 10.1029/JC088iC06p03662, 1983.
- Fishman, J., Solomon, S., and Crutzen, P. J.: Observational and theoretical evidence in support of a significant in situ photochemical source of tropospheric ozone, *Tellus*, 31, 432-446, doi:10.1111/j.2153-3490.1979.tb00922.x, 1979.
- Folkens, I., Braun, C., Thompson, A. M., and Witte, J.: Tropical ozone as an indicator of deep convection, *J. Geophys. Res.*, 107, 4184, doi:10.1029/2001JD001178, 2002.
- Frey, W., Schofield, R., Hoor, P., Kunkel, D., Ravegnani, F., Ulanovsky, A., Viciani, S., D'Amato, F., and Lane, T. P.: The impact of overshooting deep convection on local transport and mixing in the tropical upper troposphere/lower stratosphere (UTLS),

- Atmos. Chem. Phys. Discuss., 15, 1041-1091, doi:10.5194/acpd-15-1041-2015, 2015.
- Hecobian, A., Liu, Z., Hennigan, C. J., Huey, L. G., Jimenez, J. L., Cubison, M. J., Vay, S., Diskin, G. S., Sachse, G. W., Wisthaler, A., Mikoviny, T., Weinheimer, A. J., Liao, J., Knapp, D. J., Wennberg, P. O., Kürten, A., Crouse, J. D., Clair, J. St., Wang, Y., and Weber, R. J.: Comparison of chemical characteristics of 495 biomass burning plumes intercepted by the NASA DC-8 aircraft during the ARCTAS/CARB-2008 field campaign, *Atmos. Chem. Phys.*, 11, 13325-13337, doi:10.5194/acp-11-13325-2011, 2011.
- Hegglin, M. I., Brunner, D., Wernli, H., Schwierz, C., Martius, O., Hoor, P., Fischer, H., Parchatka, U., Spelten, N., Schiller, C., Krebsbach, M., Weers, U., Staehelin, J., and Peter, Th.: Tracing troposphere-to-stratosphere transport above a mid-latitude deep convective system, *Atmos. Chem. Phys.*, 4, 741-756, doi:10.5194/acp-4-741-2004, 2004.
- Hitchman, M. H., Buker, M. L., Tripoli, G. J., Pierce, R. B., Al-Saadi, J. A., Browell, E. V., and Avery, M. A.: A modeling study of an East Asian convective complex during March 2001, *J. Geophys. Res.*, 109, D15S14, doi:10.1029/2003JD004312, 2004.
- Homeyer, C. R., Bowman, K. P., Pan, L. L., Zondlo, M. A., and Bresch, J. F.: Convective injection into stratospheric intrusions, *J. Geophys. Res.*, 116, D23304, doi:10.1029/2011JD016724, 2011.
- Homeyer, C. R., Pan, L. L., and Barth, M. C.: Transport from convective overshooting of the extratropical tropopause and the role of large-scale lower stratosphere stability, *J. Geophys. Res. Atmos.*, 119, 2220–2240, doi:10.1002/2013JD020931, 2014.
- Houze, R. A., Jr., Rutledge, S. A., Biggerstaff, M. I., and Smull, B. F.: Interpretation of Doppler weather radar displays in midlatitude mesoscale convective systems. *Bull. Amer. Meteor. Soc.*, 70, 608-619, doi:10.1175/1520-0477[1989]0702.0.CO;2, 1989.
- Houze, R. A.: Mesoscale convective systems, *Rev. Geophys.*, 42, RG4003, doi:10.1029/2004RG000150, 2004.
- Hudman, R. C., Murray, L. T., Jacob, D. J., Turquety, S., Wu, S., Millet, D. B., Avery, M., Goldstein, A. H., and Holloway, J.: North American influence on tropospheric ozone and the effects of recent emission reductions: Constraints from ICARTT observations, *J. Geophys. Res.*, 114, D07302, doi:10.1029/2008JD010126, 2009.

- Huntrieser, H., Schlager, H., Feigl, C., and Höller, H.: Transport and production of NO<sub>x</sub> in electrified thunderstorms: Survey of previous studies and new observations at mid-latitudes, *J. Geophys. Res.*, 103, 28247-28264, doi:10.1029/98JD02353, 1998.
- Huntrieser, H., Feigl, C., Schlager, H., Schröder, F., Gerbig, C., van Velthoven, P., Flatøy, F., Théry, C., Petzold, A., Höller, H., and Schumann, U.: Airborne measurements of NO<sub>x</sub>, tracer species and small particles during the European Lightning Nitrogen Oxides Experiment, *J. Geophys. Res.*, 107, 4113, doi:10.1029/2000JD000209, 2002.
- Huntrieser, H., Schlager, H., Roiger, A., Lichtenstern, M., Schumann, U., Kurz, C., Brunner, D., Schwierz, C., Richter, A., and Stohl, A.: Lightning-produced NO<sub>x</sub> over Brazil during TROCCINOX: airborne measurements in tropical and subtropical thunderstorms and the importance of mesoscale convective systems, *Atmos. Chem. Phys.*, 7, 2987-3013, doi:10.5194/acp-7-2987-2007, 2007.
- Huntrieser, H., Schumann, U., Schlager, H., Höller, H., Giez, A., Betz, H.-D., Brunner, D., Forster, C., Pinto Jr., O., and Calheiros, R.: Lightning activity in Brazilian thunderstorms during TROCCINOX: implications for NO<sub>x</sub> production, *Atmos. Chem. Phys.*, 8, 921-953, doi:10.5194/acp-8-921-2008, 2008.
- Huntrieser, H., Schlager, H., Lichtenstern, M., Roiger, A., Stock, P., Minikin, A., Höller, H., Schmidt, K., Betz, H.-D., Allen, G., Viciani, S., Ulanovsky, A., Ravegnani, F., and Brunner, D.: NO<sub>x</sub> production by lightning in Hector: first airborne measurements during SCOUT-O3/ACTIVE, *Atmos. Chem. Phys.*, 9, 8377-8412, doi:10.5194/acp-9-8377-2009, 2009.
- Huntrieser, H., Schlager, H., Lichtenstern, M., Stock, P., Hamburger, T., Höller, H., Schmidt, K., Betz, H.-D., Ulanovsky, A., and Ravegnani, F.: Mesoscale convective systems observed during AMMA and their impact on the NO<sub>x</sub> and O<sub>3</sub> budget over West Africa, *Atmos. Chem. Phys.*, 11, 2503-2536, doi:10.5194/acp-11-2503-2011, 2011.
- Huntrieser, H., Lichtenstern, M., Scheibe, M., Aufmhoff, H., Schlager, H., Pucik, T., Minikin, A., Weinzierl, B., Heimerl, K., Pollack, I. B., Peischl, J., Ryerson, T. B., Weinheimer, A. J., Honomichl, S., Ridley, B. A., Biggerstaff, M. I., Betten, D. P., Hair, J. W., Butler, C. F., Schwartz, M. J., and Barth, M. C.: Injection of lightning-produced NO<sub>x</sub>, water vapor, wildfire emissions, and stratospheric air to the UT/LS as observed from DC3 measurements, *J. Geophys. Res.*, submitted,

doi:10.1002/2015JD024273, 2016.

Jaffe, D., A., and Wigder, N. L.: Ozone production from wildfires: A critical review, *Atmos. Environ.*, 51, 1-10, doi:<http://dx.doi.org/10.1016/j.atmosenv.2011.11.063>, 2012.

Jeker, D. P., Pfister, L., Thompson, A. M., Brunner, D., Pickering, K. E., Boccippio, D. J., Wernli, H., Kondo, Y., and Staehelin, J.: Measurements of nitrogen oxides at the tropopause - attributions to convection and correlation with lightning, *J. Geophys. Res.*, 105, 3679-3700, doi:10.1029/1999JD901053, 2000.

Jourdain, L., Kulawik, S. S., Worden, H. M., Pickering, K. E., Worden, J., and Thompson, A. M.: Lightning NO<sub>x</sub> emissions over the USA constrained by TES ozone observations and the GEOS-Chem model, *Atmos. Chem. Phys.*, 10, 107-119, doi:10.5194/acp-10-107-2010, 2010.

Kley, D., Crutzen, P. J., Smit, H. G. J., Vömel, H., Oltmans, S. J., Grassl, H., and Ramanathan, V.: Observations of near-zero ozone concentrations over the convective Pacific: Effects on air chemistry, *Science*, 274, 230-233, doi:10.1126/science.274.5285.230, 1996.

Lemon, L. R., and Doswell III, C. A.: Severe thunderstorm evolution and meso-cyclone structure as related to tornadogenesis, *Mon. Wea. Rev.*, 107, 1184-1197, doi:[http://dx.doi.org/10.1175/1520-0493\[1979\]107<1184:STEAMS>2.0.CO;2](http://dx.doi.org/10.1175/1520-0493[1979]107<1184:STEAMS>2.0.CO;2), 1979.

Li, Q., Jacob, D. J., Park, R., Wang, Y., Heald, C. L., and Hudman, R.: North American pollution outflow and the trapping of convectively lifted pollution by upper-level anticyclone, *J. Geophys. Res.*, 110, D10301, doi:10.1029/2004JD005039, 2005.

Liang, Q., Jaeglé, L., Hudman, R. C., Turquety, S., Jacob, D. J., Avery, M. A., Browell, E. V., Sachse, G. W., Blake, D. R., Brune, W., Ren, X., Cohen, R. C., Dibb, J. E., Fried, A., Fuelberg, H., Porter, M., Heikes, B. G., Huey, G., Singh, H. B., and Wennberg, P. O.: Summertime influence of Asian pollution in the free troposphere over North America, *J. Geophys. Res.*, doi:10.1029/2006JD007919, 112, D12S11, doi:10.1029/2006JD007919, 2007.

Maddox, R.A: Mesoscale convective complexes, *Bull. Amer. Meteor. Soc.*, 61, 1374-1387, doi:[http://dx.doi.org/10.1175/1520-0477\[1980\]061<1374:MCC>2.0.CO;2](http://dx.doi.org/10.1175/1520-0477[1980]061<1374:MCC>2.0.CO;2), 1980.

Morris, G. A., Thompson, A. M., Pickering, K. E., Chen, S., Bucsela, E. J., and Kucera, P. A.: Observations of ozone production in a dissipating tropical convective cell during

- TC4, Atmos. Chem. Phys., 10, 11189-11208, doi:10.5194/acp-10-11189-2010, 2010.
- Mullendore, G. L., Durran, D. R., and Holton, J. R.: Cross-tropopause tracer transport in midlatitude convection, J. Geophys. Res., 110, D06113, doi:10.1029/2004JD005059, 2005.
- Myhre, G., D. Shindell, F.-M. Bréon, W. Collins, J. Fuglestedt, J. Huang, D. Koch, J.-F. Lamarque, D. Lee, B. Mendoza, T. Nakajima, A. Robock, G. Stephens, T. Takemura, and H. Zhang: Anthropogenic and Natural Radiative Forcing. In: *Climate Change 2013: The Physical Science Basis. Contribution of Working Group I to the Fifth Assessment Report of the Intergovernmental Panel on Climate Change* [Stocker, T.F., D. Qin, G.-K. Plattner, M. Tignor, S.K. Allen, J. Boschung, A. Nauels, Y. Xia, V. Bex and P.M. Midgley (eds.)]. Cambridge University Press, Cambridge, United Kingdom and New York, NY, USA, pp. 659–740, doi:10.1017/CBO9781107415324.018, 2013.
- Nowak, J. B., Parrish, D. D., Neuman, J. A., Holloway, J. S., Cooper, O. R., Ryerson, T. B., Kicks Jr., D. K., Flocke, F., Roberts, J. M., Atlas, E., de Gouw, J. A., Donnelly, S., Dunlea, E., Hübler, G., Huey, L. G., Schauffler, S., Tanner, D. J., Warneke, C., and Fehsenfeld, F. C., Gas-phase chemical characteristics of Asian emission plumes observed during ITCT 2K2 over the eastern North Pacific Ocean, J. Geophys. Res., 109, D23S19, doi:10.1029/2003JD004488, 2004.
- Ott, L. E., Pickering, K. E., Stenchikov, G. L., Huntrieser, H., and Schumann, U.: Effects of lightning NO<sub>x</sub> production during the July 21 European Lightning Nitrogen Oxides Project storm studied with a three-dimensional cloud-scale chemical transport model, J. Geophys. Res., 112, D05307, doi:10.1029/2006JD007365, 2007.
- Pan, L. L., Homeyer, C. R., Honomichl, S., Ridley, B., Weisman, M., Barth, M., Hair, J. W., Fenn, M. A., Butler, C., Diskin, G. S., Crawford, J. H., Ryerson, T. B., Pollack, I., Peischl, J., and Huntrieser, H.: Thunderstorms enhance tropospheric ozone by wrapping and shedding stratospheric air, Geophys. Res. Lett., doi: 10.1002/2014GL061921, ISSN 0094-8276, 2014.
- Parrish, D. D., Holloway, J. S., Trainer, M., Murphy, P. C., Forbes, F. L., and Fehsenfeld, F. C.: Export of North American pollution ozone to the North Atlantic Ocean, Science, 259, 1436–1439, doi:10.1126/science.259.5100.1436, 1993.
- Parrish, D. D., Holloway, J. S., Jakoubek, R., Trainer, M., Ryerson, T. B., Hübler, G.,

- Fehsenfeld, F. C., Moody, J. L., and Cooper, O. R.: Mixing of anthropogenic pollution with stratospheric ozone: A case study from the North Atlantic wintertime troposphere, *J. Geophys. Res.*, 105, 24363-24374, doi:10.1029/2000JD900291, 2000.
- Payne, C. D., Schuur, T. J., MacGorman, D. R., Biggerstaff, M. I., Kuhlman, K. M., and Rust, W. D.: Polarimetric and Electrical Characteristics of a Lightning Ring in a Supercell Storm, *Mon. Wea. Rev.*, 138, 2405-2425, doi: 10.1175/2009MWR3210.1, 2010.
- Pfister, G. G., Emmons, L. K., Hess, J. F., Thompson, A. M., and Yorks, J. E.: Analysis of the summer 2004 ozone budget over the United States using Intercontinental Transport Experiment Ozone Sonde Network Study (IONS) observations and Model of Ozone and Related Tracers (MOZART-4) simulations, *J. Geophys. Res.*, 113, D23306, doi:10.1029/2008JD010190, 2008.
- Pickering, K. E., Thompson, A. M., Dickerson, R. R., Luke, W. T., McNamara, D. P., Greenberg, J. P., and Zimmerman, P. R.: Model calculations of tropospheric ozone production potential following observed convective events, *J. Geophys. Res.*, 95, 14049-14062, doi:10.1029/JD095iD09p14049, 1990.
- Pickering, K. E., Thompson, A. M., Wang, Y., Tau, W. K., McNamara, D. P., Kirchoff, V. W. J. H., Heikes, B. G., Sachse, G. W., Bradshaw, J. D., Gregory, G. L., and Blake, D. R.: Convective transport of biomass burning emissions over Brazil during TRACE A, *J. Geophys. Res.*, 101, 23993-24012, doi:10.1029/96JD00346, 1996.
- Potvin, C. K., Betten, D., Wicker, L. J., Elmore, K. L., and Biggerstaff, M. I.: 3DVAR versus traditional dual-Doppler wind retrievals of a simulated supercell thunderstorm, *Mon. Wea. Rev.*, 140, 3487-3494, doi:http://dx.doi.org/10.1175/MWR-D-12-00063.1, 2012.
- Poulida, O., Dickerson, R. R., and Heymsfield, A.: Stratosphere-troposphere exchange in a midlatitude mesoscale convective complex. Part 1: Observations, *J. Geophys. Res.*, 101, 6823-6836, doi:10.1029/95JD03523, 1996.
- Price, H. U., Jaffe, D. A., Cooper, O. R., and Doskey, P. V.: Photochemistry, ozone production, and dilution during long-range transport episodes from Eurasia to the northwest United States, *J. Geophys. Res.*, 109, D23S13, doi:10.1029/2003JD004400, 2004.
- Ray, E. A., Rosenlof, K. H., Richard, E. C., Hudson, P. K., Cziczo, D. J., Loewenstein, M.,

- Jost, H.-J., Lopez, J., Ridley, B., Weinheimer, A., Montzka, D., Knapp, D., Wofsy, S. C., Daube, B. C., Gerbig, C., Xueref, I. and Herman, R. L.: Evidence of the effect of summertime midlatitude convection on the subtropical lower stratosphere from CRYSTAL-FACE tracer measurements, *J. Geophys. Res.*, 109, D18304, doi:10.1029/2004JD004655, 2004.
- Real, E., Orlandi, E., Law, K. S., et al.: Cross-hemispheric transport of central African biomass burning pollutants: implications for downwind ozone production, *Atmos. Chem. Phys.*, 10, 3027-3046, doi:10.5194/acp-10-3027-2010, 2010.
- Ridley, B. A., Avery, M. A., Plant, J. V., Vay, S. A., Montzka, D. D., Weinheimer, A. J., Knapp, D. J., Dye, J. E., and Richard, E. C.: Sampling of chemical constituents in electrically active convective systems: Results and cautions, *J. Atmos. Chem.*, 54, 1–20, doi:10.1007/s10874-005-9007-5, 2006.
- Roach, W. T.: On the nature of the summit areas of severe storms in Oklahoma, *Q. J. R. Meteorol. Soc.*, 93, 318-336, doi:10.1002/qj.49709339704, 1967.
- Rolph, G. D.: Real-time Environmental Applications and Display sYstem (READY) Website (<http://ready.arl.noaa.gov>). NOAA Air Resources Laboratory, Silver Spring, MD, 2014.
- Romps, D. M., Seeley, J. T., Vollaro, D., and Molinari, J.: Projected increase in lightning strikes in the United States due to global warming, *Science*, 346, 851-854, doi:10.1126/science.1259100, 2014.
- Schroeder, J. R., Pan, L. L., Ryerson, T., Diskin, G., Hair, J., Meinardi, S., Simpson, I., Barletta, B., Blake, N., and Blake, D. R.: Evidence of mixing between polluted convective outflow and stratospheric air in the upper troposphere during DC3, *J. Geophys. Res.*, 119, 11477-11491, doi:10.1002/jgrd.v119.19, 2014.
- Schumann, U. and Huntrieser, H.: The global lightning-induced nitrogen oxides source, *Atmos. Chem. Phys.*, 7, 3823-3907, doi:10.5194/acp-7-3823-2007, 2007.
- Simmonds, P. G., Manning, A. J., Derwent, R. G., Ciais, P., Ramonet, M., Kazan, V., and Ryall, D.: A burning question. Can recent growth rate anomalies in the greenhouse gases be attributed to large-scale biomass burning events? *Atmos. Environ.*, 39, doi:10.1016/j.atmosenv.2005.02.018, 2005.
- Singh, H. B., Anderson, B. E., Brune, W. H., Cai, C., Cohen, R. C., Crawford, J. H., Cubison,



- M. J., Czech, E. P., Emmons, L., Fuelberg, H. E., Huey, G., Jacob, D. J., Jimenez, J. L., Kaduwela, A., Kondo, Y., Mao, J., Olson, J. R., Sachse, G. W., Vay, S. A., Weinheimer, A., Wennberg, P. O., Wisthaler, A., and the ARCTAS Science Team: Pollution influences on atmospheric composition and chemistry at high northern latitudes: Boreal and California forest fire emissions, *Atmos. Environ.*, 44, 4553-4564, doi:<http://dx.doi.org/10.1016/j.atmosenv.2010.08.026>, 2010.
- Stenchikov, G., Dickerson, R., Pickering, K., Ellis, Jr. W., Doddridge, B., Kondragunta, S., Poulida, O., Scala, J., and Tao, W.-K.: Stratosphere-troposphere exchange in a mid-latitude mesoscale convective complex: Part 2, numerical simulations. *J. Geophys. Res.*, 101, doi:10.1029/95JD02468, 6837-6851, 1996.
- Stevenson, D. S., Dentener, F. J., Schultz, M. G., et al.: Multimodel ensemble simulations of present-day and near-future tropospheric ozone, *J. Geophys. Res.*, 111, D08301, doi:10.1029/2005JD006338, 2006.
- Stohl, A., Forster, C., Eckhardt, S., Spichtinger, N., Huntrieser, H., Heland, J., Schlager, H., Wilhelm, S., Arnold, F., and Cooper, O.: A backward modeling study of intercontinental pollution transport using aircraft measurements, *J. Geophys. Res.*, 108, 4370, doi:10.1029/2002JD002862, 2003.
- Suhre, K., Cammas, J.-P., Nedelec, P., Rosset, R., Marenco, A., and Smit, H. G. J.: Ozone-rich transients in the upper equatorial Atlantic troposphere, *Nature*, 388, 661-663, doi:10.1038/41749, 1997.
- Tang, Q. and Prather, M. J.: Correlating tropospheric column ozone with tropopause folds: the Aura-OMI satellite data, *Atmos. Chem. Phys.*, 10, 9681-9688, doi:10.5194/acp-10-9681-2010, 2010.
- Tang, Q., Prather, M. J., and Hsu, J.: Stratosphere-troposphere exchange ozone flux related to deep convection, *Geophys. Res. Lett.*, 38, L03806, doi:10.1029/2010GL046039, 2011.
- Thompson, A. M., Tao, W. K., Pickering, K. E., Scala, J. R., and Simpson, J.: Tropical deep convection and ozone formation, *Bull. Amer. Meteor. Soc.*, 78, 1043-1054, doi:10.1029/95JD03523, 1997.
- Thornton, D. C., Bandy, A. R., Blomquist, B. W., Bradshaw, J. D., and Blake, D. R.: Vertical transport of sulfur dioxide and dimethyl sulfide in deep convection and its role in new

- particle formation, *J. Geophys. Res.*, 102, 28501-28510, doi:10.1029/97JD016471997.
- Turetsky, M. R., Kane, E. S., Harden, J.W., Ottman, R. D., Maines, K. L., Hoy, E., and Kashschke, E. S.: Recent acceleration of biomass burning and carbon losses in Alaskan forests and peatlands, *Nature Geosci.*, 4, 27–31, doi:10.1038/NGEO1027, 2011.
- Wang, C., Crutzen, P. J., Ramanathan, V., and Williams, S. F.: The role of a deep convective storm over the tropical Pacific Ocean in the redistribution of atmospheric chemical species, *J. Geophys. Res.*, 100, 11509–11516, doi:10.1029/95JD01173, 1995.
- Wang, Y., Liu, S. C., Anderson, B. E., Kondo, Y., Gregory, G. L., Sachse, G. W., Vay, S. A., Blake, D. R., Singh, H. B., and Thompson, A. M.: Evidence of convection as a major source of condensation nuclei in the northern midlatitude upper troposphere, *Geophys. Res. Lett.*, 27, 369-372, doi: 10.1029/1999GL010930, 2000.
- Wang, P. K.: Moisture plumes above thunderstorm anvils and their contributions to cross-tropopause transport of water vapor in midlatitudes, *J. Geophys. Res.*, 108, 4194, doi:10.1029/2002JD002581, 2003.
- Wang, L., Newchurch, M. J., Pour-Biazar, A., Kuang, S., Khan, M., Liu, X., Koshak, W., and Chance, K.: Estimating the influence of lightning on upper tropospheric ozone using NLDN lightning data and CMAQ model, *Atmos. Environ.*, 67, 219-228, doi:http://dx.doi.org/10.1016/j.atmosenv.2012.11.001, 2013.
- Wigder, N. L., and Jaffe, D. A.: Ozone and particulate matter enhancements from regional wildfires observed at Mount Bachelor during 2004-2011, *Atmos. Environ.*, 75, 24-31, doi:10.1016/j.atmosenv.2013.04.026, 2013.
- Winterrath, T., Kurosui, T. P., Richter, A., and Burrows, J. P.: Enhanced O<sub>3</sub> and NO<sub>2</sub> in Thunderstorm Clouds: Convection or Production?, *Geophys. Res. Lett.*, 26, 1291-1294, doi: 10.1029/1999GL900243, 1999.
- Yang, Q., et al.: Aerosol transport and wet scavenging in deep convective clouds: A case study and model evaluation using a multiple passive tracer analysis approach, *J. Geophys. Res.*, 120, doi:10.1002/2015JD023647, 2015.
- Zahn, A., Brenninkmeijer, C. A. M., Crutzen, P. J., Parrish, D. D., Sueper, D., Heinrich, G., Güsten, H., Fischer, H., Hermann, M., and Heintzenberg, J.: Electrical discharge

source for tropospheric “ozone-rich transients”, *J. Geophys. Res.*, 107, 4638, doi:10.1029/2002JD002345, 2002.

Zhao, C., Wang, Y., Choi, Y., and Zeng, T.: Summertime impact of convective transport and lightning NO<sub>x</sub> production over North America: modeling dependence on meteorological simulations, *Atmos. Chem. Phys.*, 9, 4315-4327, doi:10.5194/acp-9-4315-2009, 2009.

Accepted Article

**Table 1.**  $\Delta O_3/\Delta CO$  ratios in selected layers impacted by anthropogenic pollution, biomass burning emissions from wildfires and lightning-produced  $NO_x$  (LNO<sub>x</sub>) during DC3 (in *italic/bold*: plumes not/strongly mixed with stratospheric air masses) (based on Table 4 in *HH2016*).

DC3 Flight Number, Date, Flight a or b	Source	Figure Number (incl. data range)	Pressure Altitude, km	Max. CO Mixing Ratio, nmol mol <sup>-1</sup>	Max. O <sub>3</sub> Mixing Ratio, nmol mol <sup>-1</sup>	Mix With Stratospheric Air Masses?	$\Delta O_3/\Delta CO$ Ratio
F#4 300512b	Baldy/Whitewater fire (NM)	1	<i>1.2-1.6</i>	<i>200</i>	<i>80</i>	<i>No</i>	<i>+0.10</i>
	Baldy/Whitewater fire (NM)	9a	8.5-8.7	130	90	Yes	+0.38
	Baldy/Whitewater fire (NM)	9a	9.9-10.4	120	100	Yes	+0.39
	Baldy/Whitewater fire (NM)	9a	<b>at 10.4</b>	<b>120</b>	<b>150</b>	<b>Yes</b>	<b>-1.67</b>
	LNO <sub>x</sub> & Baldy/Whitewater fire (NM)	9b	at 9.1	160	130	Yes	+0.49
	LNO <sub>x</sub> & Baldy/Whitewater fire (NM)	9b	9.1-9.4	130	140	Yes	+1.42
F#8 080612a	Anthropogenic pollution (TX)	24a	6.6-7.2	120	110	Yes	+1.44
	Anthropogenic pollution (TX)	24a	<i>7.4-7.9</i>	<i>120</i>	<i>70</i>	<i>No</i>	<i>+0.14</i>
	LNO <sub>x</sub> & Anthropogenic pollution (TX)	24b	<b>8.8-10.7</b>	<b>110</b>	<b>160</b>	<b>Yes</b>	<b>-3.75</b>
	LNO <sub>x</sub> & Anthropogenic pollution (TX)	24b	<b>at 11.6</b>	<b>110</b>	<b>280</b>	<b>Yes</b>	<b>-3.44</b>
F#11 110612b	Little Bear fire (NM)	1	5.8-6.9	720	80	<i>No</i>	<i>+0.03</i>
F#12 120612a	High Park fire (CO)	16	7.1-9.6	180	120	Yes	+0.44
	High Park fire (CO)	16	7.9-9.7	190	120	Yes	+0.38
	LNO <sub>x</sub> & High Park fire (CO)	16	<b>11.0-11.9</b>	<b>130</b>	<b>260</b>	<b>Yes</b>	<b>-3.87</b>

**Table 2.** Trace gas and particle (here only SP2) measurements in the anvil outflow on May 30, 2012 (separated according to anvil regions with up- or downdrafts, and the mean over the entire anvil outflow in *italic*). Mean mixing ratios and standard deviations are given. Minimum and maximum mixing ratios are given in brackets. In addition, mean background mixing ratios outside the anvil outflow are given in **bold**. The arrows indicate if the anvil mixing ratios are higher ( $\uparrow$ ) or lower ( $\downarrow$ ) than the background mixing ratios.

DC3 Flight Number, Date, Flight a or b, Anvil Time	Pressure Altitude, km	CO Mixing Ratio, nmol mol <sup>-1</sup>	O <sub>3</sub> Mixing Ratio, nmol mol <sup>-1</sup>	SO <sub>2</sub> Mixing Ratio, pmol mol <sup>-1</sup>	CH <sub>4</sub> Mixing Ratio, nmol mol <sup>-1</sup>	NO Mixing Ratio, nmol mol <sup>-1</sup>	NO <sub>x</sub> Mixing Ratio, nmol mol <sup>-1</sup>	NO <sub>y</sub> Mixing Ratio, nmol mol <sup>-1</sup>	Ethane/Propane, pmol mol <sup>-1</sup> / pmol mol <sup>-1</sup>	Benzene/Toluene, pmol mol <sup>-1</sup> / pmol mol <sup>-1</sup>	rBC* Mass Mixing Ratio, ng kg <sup>-1</sup>
F#4 300512b (86852-87133s) <i>upward</i>	10.3	103±3 (97/110)	82±5 (69/92)	45±22 (8/101)	-	0.2±0.1 (0.1/0.5)	-	-	-	-	-
F#4 300512b (87134-87323s) <i>downward</i>	9.2	117±10 (99/135)	108±17 (75/142)	33±16 (8/69)	-	1.2±0.6 (0.2/2.3)	-	-	-	-	-
F#4 300512b (87324-87440s) <i>upward</i>	9.1	103±2 (100/107)	80±13 (67/114)	55±17 (19/82)	-	2.7±1.8 (0.4/8.6)	-	-	-	-	-
F#4 300512b (87441-87577s) <i>downward</i>	9.1	130±19 (103/161)	113±11 (92/129)	72±29 (14/131)	-	2.3±0.4 (1.1/3.2)	-	-	-	-	-
F#4 300512b (87578-87838s) <i>upward</i>	9.1	98±6 (89/120)	82±7 (76/100)	52±25 (6/117)	-	0.05±0.01 (0.03/0.08)	-	-	-	-	-
<i>F#4 300512b (86852-87838s)</i>	<b>9.5 (9.1-10.7)</b>	<b>↑108±14</b>	<b>↑91±17</b>	<b>50±25</b>	-	<b>↑1.0±1.3</b>	-	-	-	-	-
<b>Background (83988-84040s)</b>	<b>9.4-9.6</b>	<b>97±2</b>	<b>86±4</b>	<b>50±24</b>	-	<b>0.05±0.03</b>	-	-	<b>247/29 =8.5</b>	<b>5/27 =0.2</b>	-

\*rBC=refractory Black Carbon.

**Table 3.** Trace gas and particle (here only SP2) measurements in the anvil outflow on June 12, 2012 (separated according to anvil regions with up- or downdrafts, and the mean over the entire anvil outflow in italic). Mean mixing ratios and standard deviations are given. Minimum and maximum mixing ratios are given in brackets. In addition, mean background mixing ratios outside the anvil outflow are given in bold. The arrows indicate if the anvil mixing ratios are higher ( $\uparrow$ ) or lower ( $\downarrow$ ) than the background mixing ratios.

DC3 Flight Number, Date, Flight a or b, Anvil Time	Pressure Altitude, km	CO Mixing Ratio, nmol mol <sup>-1</sup>	O <sub>3</sub> Mixing Ratio, nmol mol <sup>-1</sup>	SO <sub>2</sub> Mixing Ratio, pmol mol <sup>-1</sup>	CH <sub>4</sub> Mixing Ratio, ng mol <sup>-1</sup>	NO Mixing Ratio, nmol mol <sup>-1</sup>	NO <sub>x</sub> Mixing Ratio, nmol mol <sup>-1</sup>	NO <sub>y</sub> Mixing Ratio, nmol mol <sup>-1</sup>	Ethane/Propane, pmol mol <sup>-1</sup> /pmol mol <sup>-1</sup>	Benzene/Toluene, pmol mol <sup>-1</sup> /pmol mol <sup>-1</sup>	rBC* MassMixing Ratio, ng kg <sup>-1</sup>
F#12 120612a (84536-85260 s) <i>upward</i>	10.3 (9.7-11.0)	120±3 (113/126)	73±4 (65/85)	18±13 (1/71)	1854±3 (1849/1861)	0.6±0.2 (0.2/1.1)	1.1±0.5 (0.2/2.8)	-	-	-	-
<i>F#12 120612a (84210-85400 s)</i>	<i>10.4</i>	<i>↑121±3</i>	<i>↓82±14</i>	<i>↓25±20</i>	<i>↑1854±3</i>	<i>↑0.7±0.5</i>	<i>↑1.2±0.6</i>	-	-	-	-
<b>Background (87939-87965 s)</b>	<b>10.3 (10.2-10.4)</b>	<b>106±1</b>	<b>120±1</b>	<b>75±20</b>	<b>1844±1</b>	-	-	-	-	-	<b>17±5</b>
F#12 120612a (85996-86999 s) <i>upward</i>	11.6 (11.0-11.9)	123±2 (117/129)	72±4 (60/80)	13±9 (1/38)	1851±3 (1845/1860)	1.5±0.4 (0.8/3.1)	2.0±0.5 (0.7/4.1)	-	1073/615 =1.7**	16/64 =0.3***	-
<i>F#12 120612a (85910-87650 s)</i>	<i>11.6</i>	<i>↑119±10</i>	<i>↓91±39</i>	<i>↓14±10</i>	<i>↑1845±16</i>	<i>↑1.5±0.5</i>	<i>↑1.9±0.6</i>	-	-	-	-
<b>Background (87659-87832 s)</b>	<b>11.3</b>	<b>97±6</b>	<b>137±8</b>	<b>38±17</b>	<b>1833±4</b>	<b>0.2±0.1</b>	<b>0.5±0.1</b>	-	-	-	<b>19±10</b>

\*rBC=refractory Black Carbon.

\*\*Compare to BL over Salina: 443/410=1.1

\*\*\*Compare to BL over Salina: 35/21=1.7

**Table 4.** Trace gas and particle (here only SP2) measurements in the anvil outflow on June 8, 2012 (separated according to anvil regions with aged outflow, and the mean over the entire anvil outflow in *italic*). Mean mixing ratios and standard deviations are given. Minimum and maximum mixing ratios are given in brackets. In addition, mean background mixing ratios outside the anvil outflow are given in **bold**. The arrows indicate if the anvil mixing ratios are higher ( $\uparrow$ ) or lower ( $\downarrow$ ) than the background mixing ratios.

DC3 Flight Number, Date, Flight a or b, Anvil Time	Pressure Altitude, km	CO Mixing Ratio, nmol mol <sup>-1</sup>	O <sub>3</sub> Mixing Ratio, nmol mol <sup>-1</sup>	SO <sub>2</sub> Mixing Ratio, pmol mol <sup>-1</sup>	CH <sub>4</sub> Mixing Ratio, nmol mol <sup>-1</sup>	NO Mixing Ratio, nmol mol <sup>-1</sup>	NO <sub>x</sub> Mixing Ratio, nmol mol <sup>-1</sup>	NO <sub>y</sub> Mixing Ratio, nmol mol <sup>-1</sup>	Ethane/Propane, pmol mol <sup>-1</sup> /pmol mol <sup>-1</sup>	Benzene/Toluene, pmol mol <sup>-1</sup> /pmol mol <sup>-1</sup>	rBC* Mass Mixing Ratio, ng kg <sup>-1</sup>
<i>F#8 080612a (62540-64635 s) aged outflow</i>	<i>11.6</i>	$\uparrow 98 \pm 8$ (64/114)	$\uparrow 127 \pm 30$ (88/278)	$\uparrow 35 \pm 15$ (1/94)	$\uparrow 1839 \pm 15$ (1773/1863)	$\uparrow 0.7 \pm 0.2$ (0.1/2.9)	-	$\uparrow 2.5 \pm 0.3$ (1.5/5.0)	1930/1357 =1.4	26/86 =0.3	$\downarrow 5 \pm 5$ (0/39)
<b>Background** (64636-65638 s)</b>	<b>11.6</b>	<b>84<math>\pm</math>3</b>	<b>77<math>\pm</math>13</b>	<b>20<math>\pm</math>20</b>	<b>1825<math>\pm</math>4</b>	<b>0.1<math>\pm</math>0.06</b>	-	<b>1.2<math>\pm</math>0.1</b>	<b>478/124</b> <b>=3.9</b>	<b>6/91</b> <b>=0.1</b>	<b>11<math>\pm</math>8</b>
<i>F#8 080612a (65921-67251 s) aged outflow</i>	<i>9.9</i>	$\downarrow 100 \pm 4$ (86/111)	$\uparrow 97 \pm 20$ (76/158)	$\downarrow 32 \pm 13$ (1/72)	$\uparrow 1848 \pm 7$ (1818/1859)	$\uparrow 0.4 \pm 0.1$ (0.1/1.0)	-	$\uparrow 2.3 \pm 0.3$ (1.6/3.2)	1737/1243 =1.4	25/25 =1.0	$\downarrow 7 \pm 4$ (1/23)
<b>Background (59286-59366 s)</b>	<b>9.8-10.0</b>	<b>99<math>\pm</math>2</b>	<b>81<math>\pm</math>2</b>	<b>76<math>\pm</math>16</b>	<b>1838<math>\pm</math>1</b>	<b>0.2<math>\pm</math>0.01</b>	-	<b>1.5<math>\pm</math>0.03</b>	-	-	<b>16<math>\pm</math>7</b>

\*rBC=Refractory Black Carbon.

\*\*Background: both CO and O<sub>3</sub> mixing ratios are low indicating a mixture of tropospheric and stratospheric air masses.

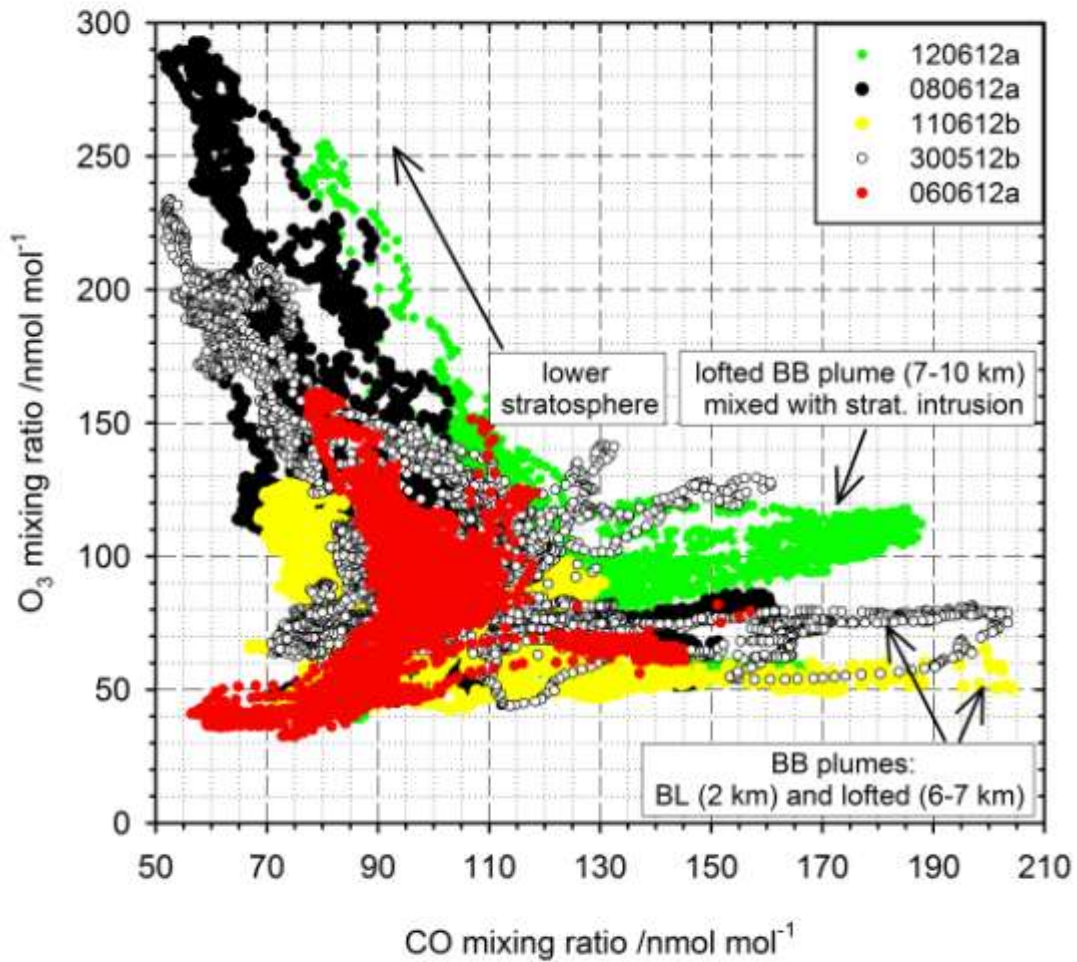


**Figure 1.** O<sub>3</sub>-CO correlations for five selected DC3 flights where BB plumes (indicated) and thunderstorm outflow were probed (color-coded according to date: ddmmyy). For a better overview, the x-axis was cut at 210 nmol mol<sup>-1</sup>, however on the flight 110612b measured CO mixing ratios in the BB plume exceeded ~700 nmol mol<sup>-1</sup>.

Accepted



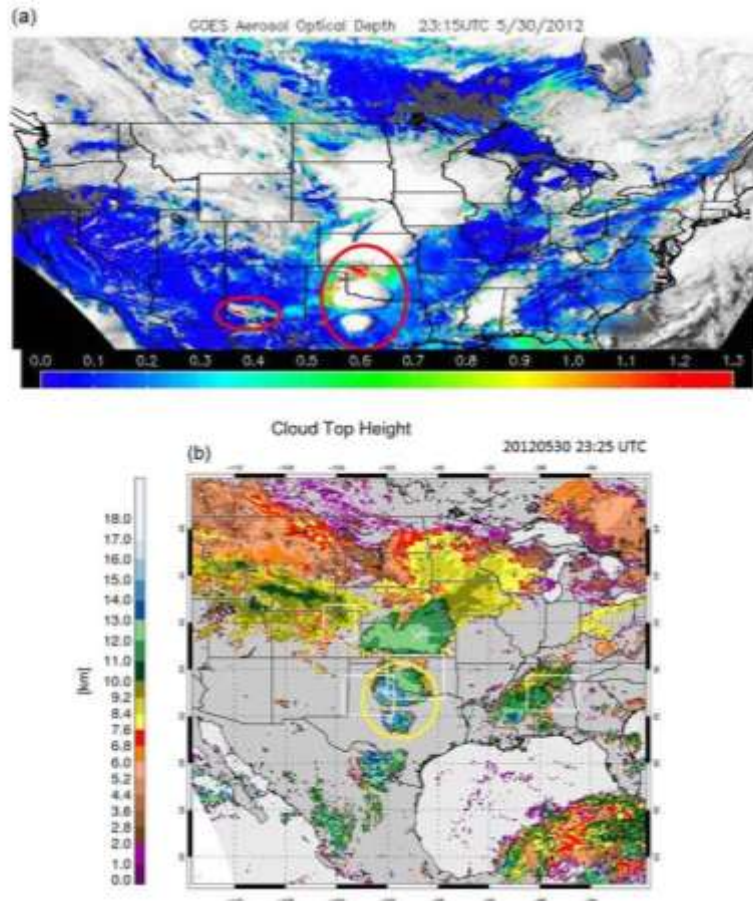


**Figure 2.** GOES Aerosol Optical Depth (AOD) over U.S. and Canada on May 30, 2012 at 23:15 UTC **(a)**. The left red circle indicates the source region of the Whitewater-Baldy fire (New Mexico) and the right red circle shows the area of aircraft operations (MCC and supercell over Texas/Oklahoma probed by the Falcon aircraft). Cloud top heights (in km) derived from GOES data on May 30, 2012 at 23:25 UTC **(b)** (© NCAR/EOL). The yellow circle shows the area of the Falcon operations (supercell and MCC probed). The white squares mark the selected DC3 operation areas and the white cross the campaign base in Salina (KS).

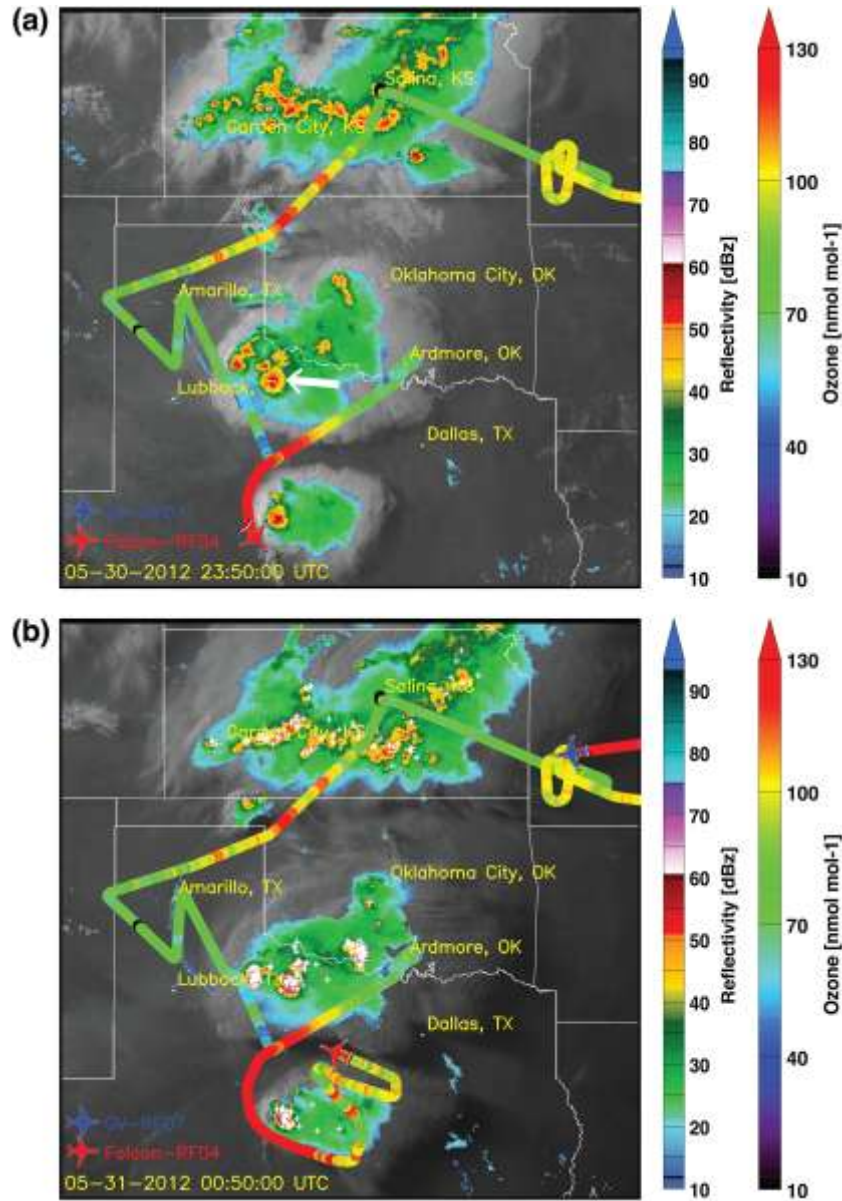


**Figure 3.** Flight tracks of the Falcon (red aircraft) in the evening on May 30, 2012 at 23:50 UTC (a) and May 31 at 00:50 UTC (b) to probe a smoke plume near Lubbock (TX), and after a brief stop in Ardmore (OK) to probe a MCC and an isolated supercell storm over Texas/Oklahoma (blue aircraft: GV). The flight tracks (color-coded according to O<sub>3</sub> mixing ratios along the flight) are superimposed on a GOES IR satellite image (grey), NEXRAD radar reflectivity (colored clouds), and NLDN lightning data (white/pink plus/minus sign for positive/negative flashes). The white arrow marks a storm cell shown in more detail in Figs. 5a-b. The smoke plume from the New Mexico Whitewater-Baldy Fire is visible near Lubbock.

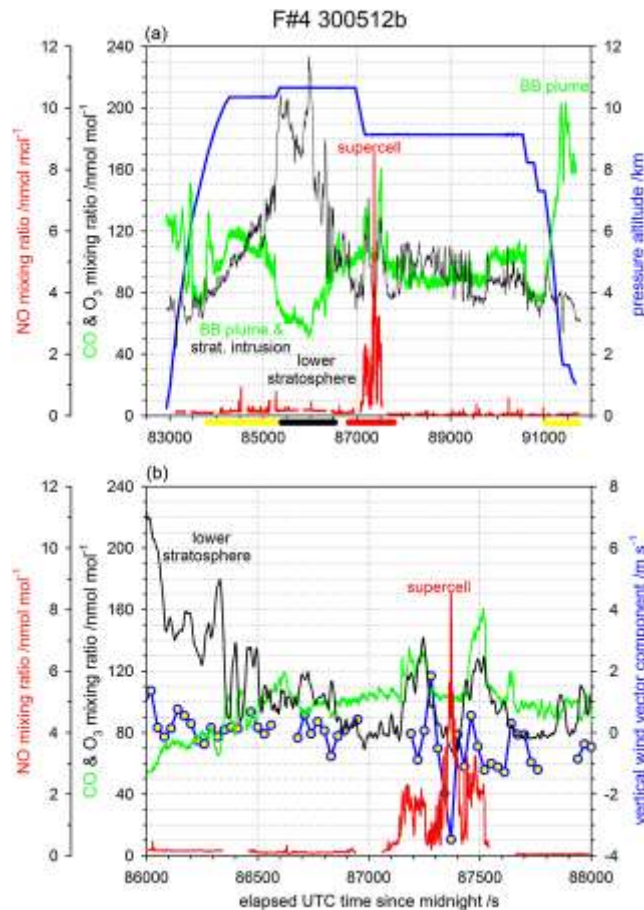


**Figure 4.** Time series of NO, CO, O<sub>3</sub>, pressure altitude (all 1 s values) and vertical wind vector component (30 s mean) for the Falcon flight on May 30, 2012: complete flight (a), and selected time period from 86000-88000 s (b). Positive vertical wind component values indicate downward motion. Colored bars in (a) indicate selected time sequences of the flights with different air masses: BB plume (yellow), lower stratosphere (black), and fresh supercell outflow (red); see also Figs. 9a-b.

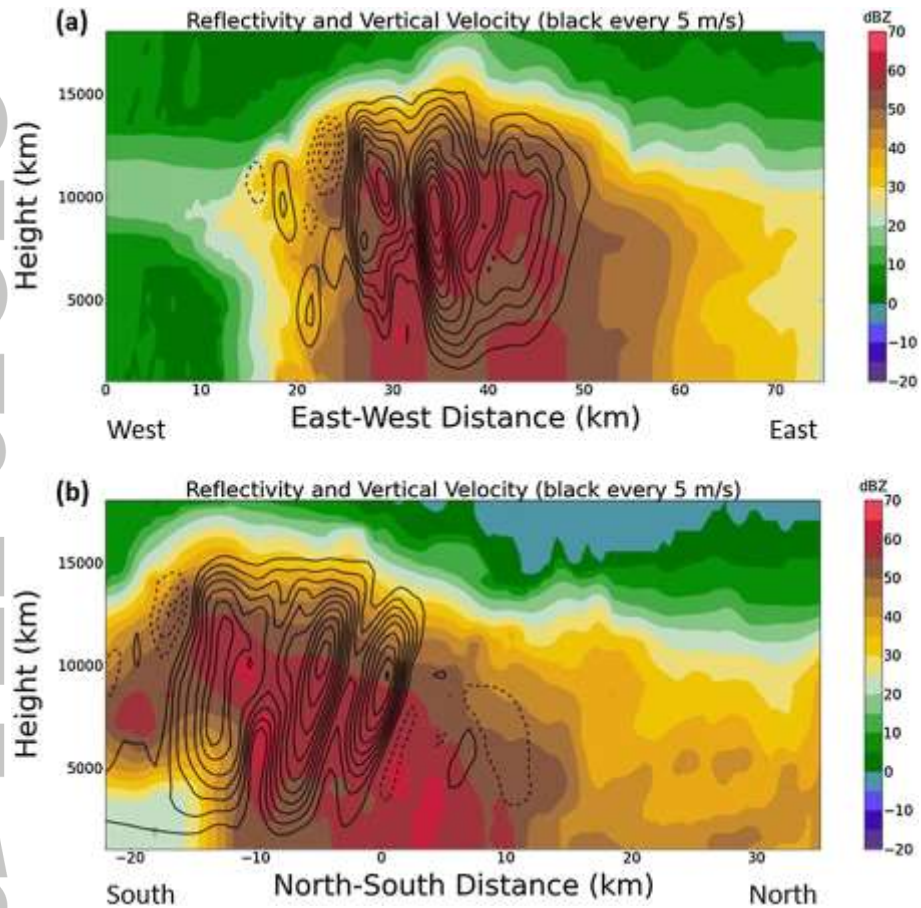


**Figure 5.** Radar reflectivity (dBZ) (colored) and vertical velocity (black isolines every 5  $\text{m s}^{-1}$ , upward solid and downward dashed) obtained from multi-Doppler 3DVAR analysis of data from the SMART and NOXP radars on May 30, 2012 at 2330 UTC. Vertical cross sections in (a) east-west and (b) north-south direction of the strongest supercell embedded in the MCC probed by the Falcon in Fig. 3a marked by a white arrow. The grid center is the location of the SR1 radar ( $33.9^\circ \text{ N}$ ,  $100.3^\circ \text{ W}$ ).

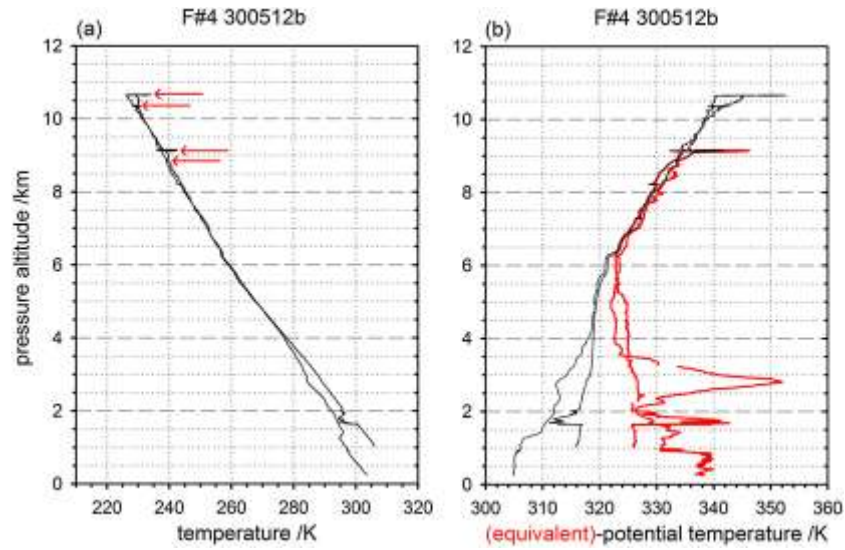


**Figure 6.** Vertical profiles of temperature (a), and (equivalent)-potential temperature (b) derived from Falcon measurements on May 30, 2012. The red arrows indicate two different tropopause levels at 10.4 and 10.7 km, and stratospheric intrusions at 8.8 and 9.2 km.

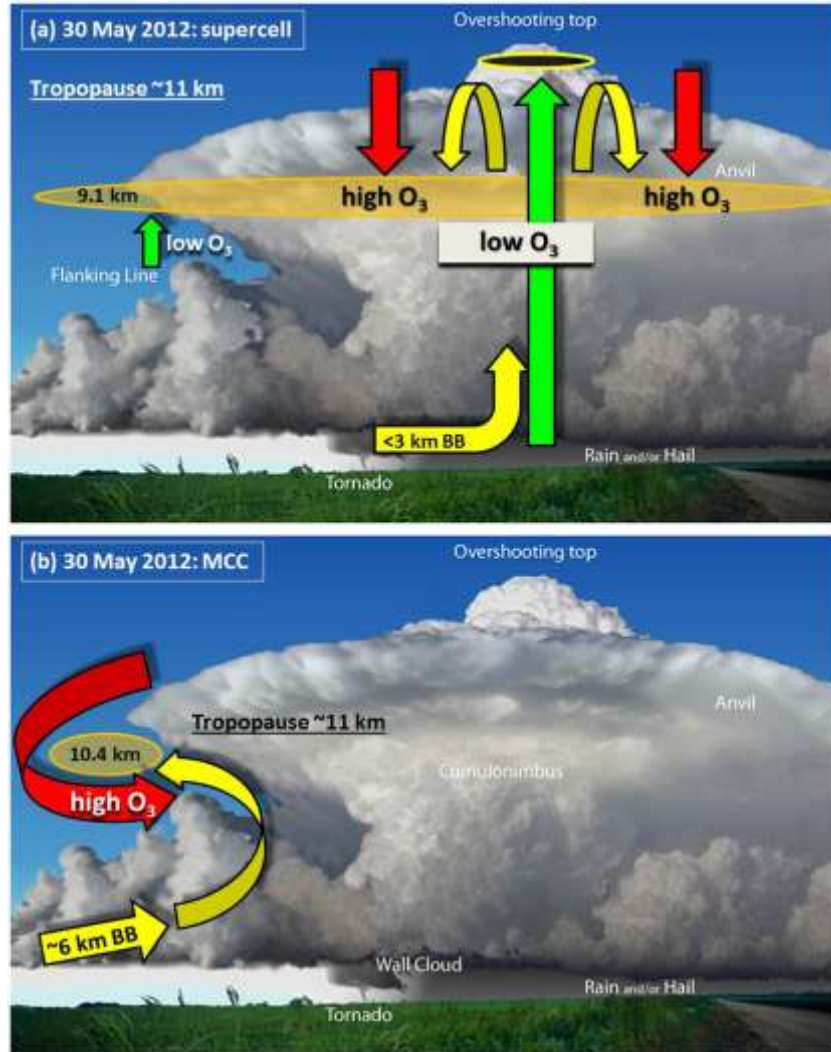


**Figure 7.** Schematic of an isolated, overshooting thunderstorm cell (credit: NOAA National Weather Service, <http://www.srh.noaa.gov/jetstream/tstorms/tstrmtypes.htm>). Superimposed are the major air mass transport pathways (colored arrows) observed during the Falcon flight on May 30, 2012 based on in-situ trace gas measurements (CO and O<sub>3</sub>) in the lower boundary of the outflow from a supercell (a) and below the outflow from a MCC (b) (orange shaded areas). In (a) emissions from wildfires (BB) and low O<sub>3</sub> mixing ratios are ingested into the supercell (yellow and green). Strong up- and downdrafts within the storm redistribute the ingested pollution (accumulation at the cloud top, black shaded area). As a response to the overshooting top, stratospheric air masses are transported downwards into the anvil outflow (red). In (b) emissions from wildfires (BB, yellow) are ingested into towering cumulus along the flanking line of the overshooting MCC and mix with a stratospheric intrusion wrapped around the anvil outflow (red).

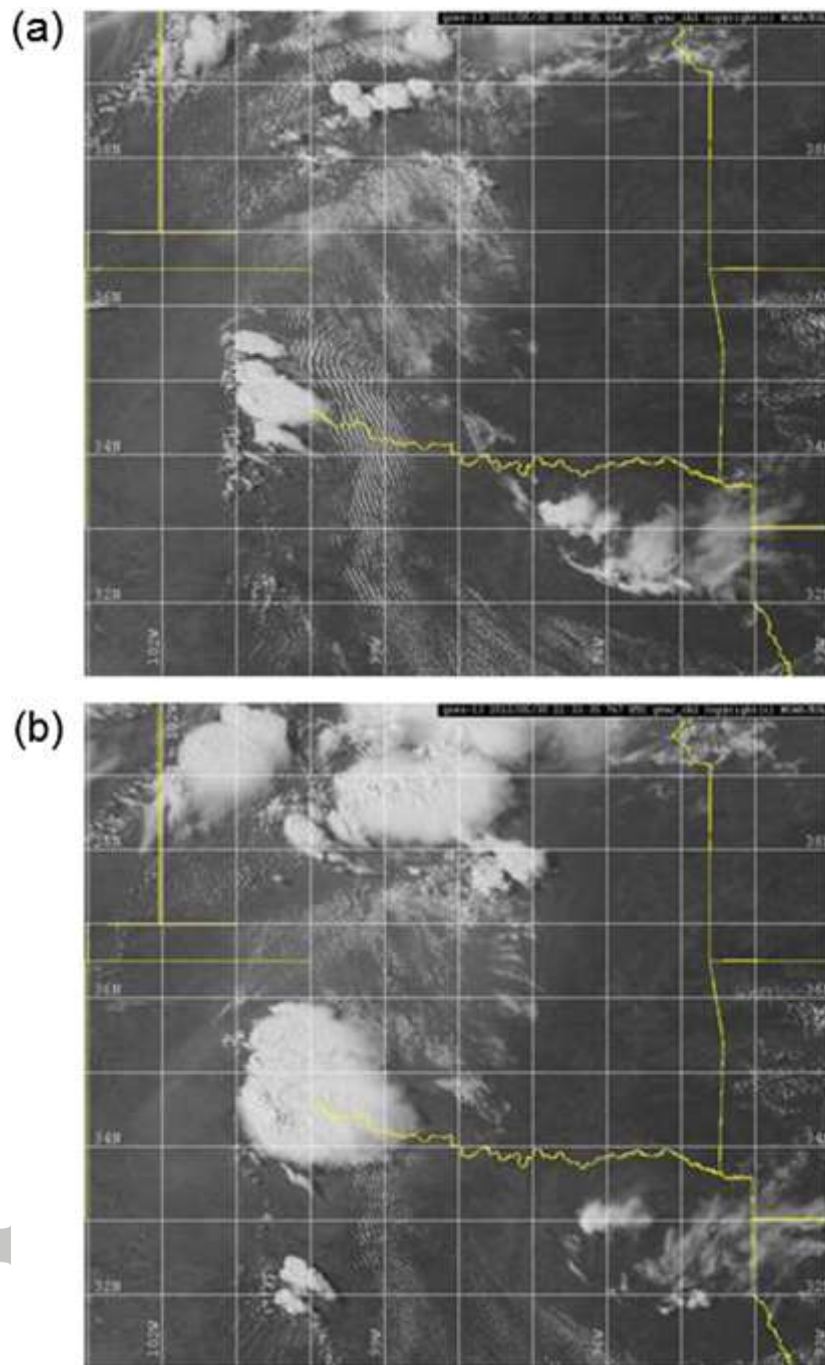


**Figure 8.** GOES visible satellite images on (a) May 30, 2012 at 20:33 UTC and (b) May 30, 2012 at 21:33 UTC (© NCAR/EOL). Along the flanking line of the probed thunderstorms extended wave cloud formations are visible in (a) which are later in (b) covered by the anvil outflow.

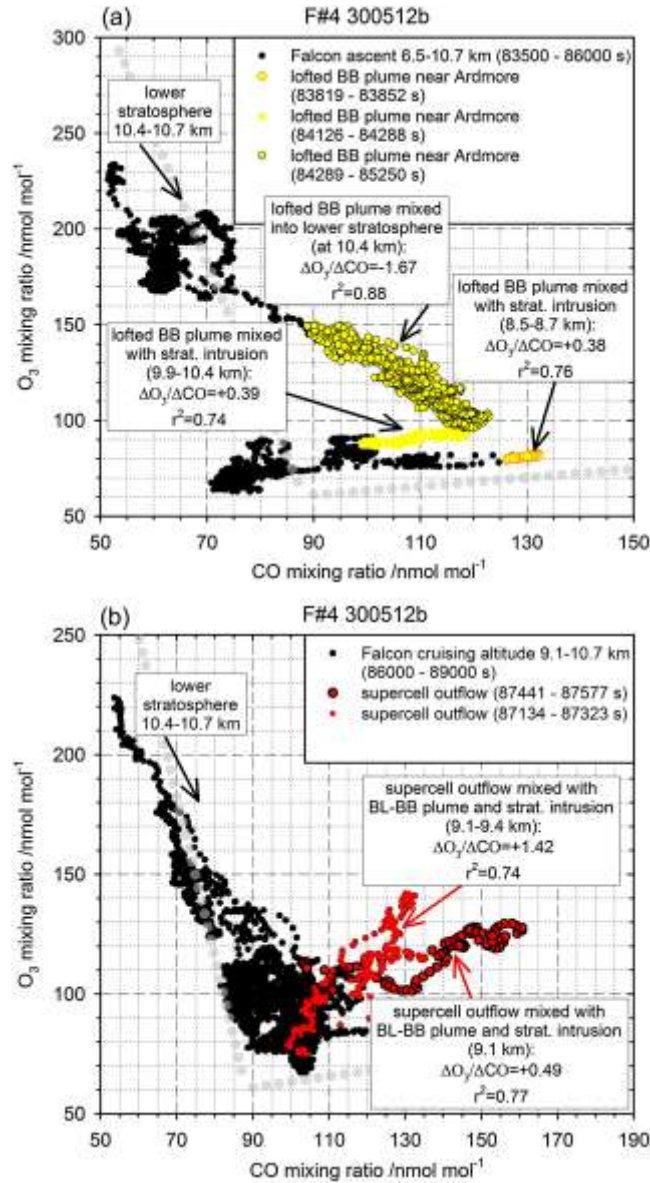


**Figure 9.**  $O_3$ -CO correlations during the Falcon flight on May 30, 2012 for the time period of the ascent from Ardmore (a). The correlations in the lofted BB plume are marked with yellow dots.  $O_3$ -CO correlations during the Falcon flight on May 30, 2012 for the time period of the cruising at 9.1-10.7 km (b). The correlations within the anvil outflow of the supercell are marked with red dots. The correlation in the free tropospheric and stratospheric background is marked with light gray dots.



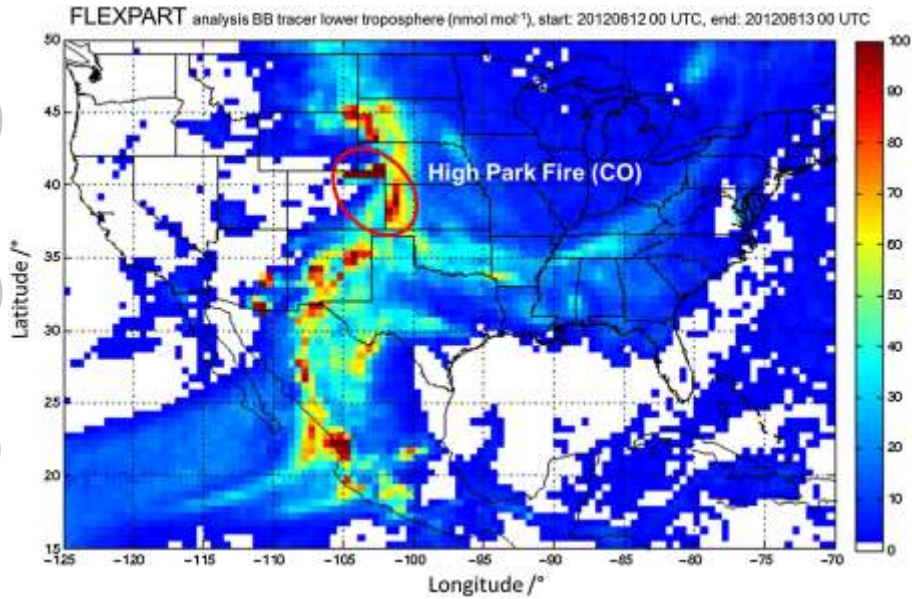


**Figure 10.** FLEXPART BB tracer analysis for the lower troposphere over U.S. and Mexico. Begin and end of the simulation: June 12 at 00 UTC and June 13 at 00 UTC, 2012, respectively. Simulated BB-CO mixing ratios (in color) are given in  $\text{nmol mol}^{-1}$ . The red circle indicates the High Park fire in Colorado and the advection of the smoke plume towards the south along the border between Colorado and Kansas.

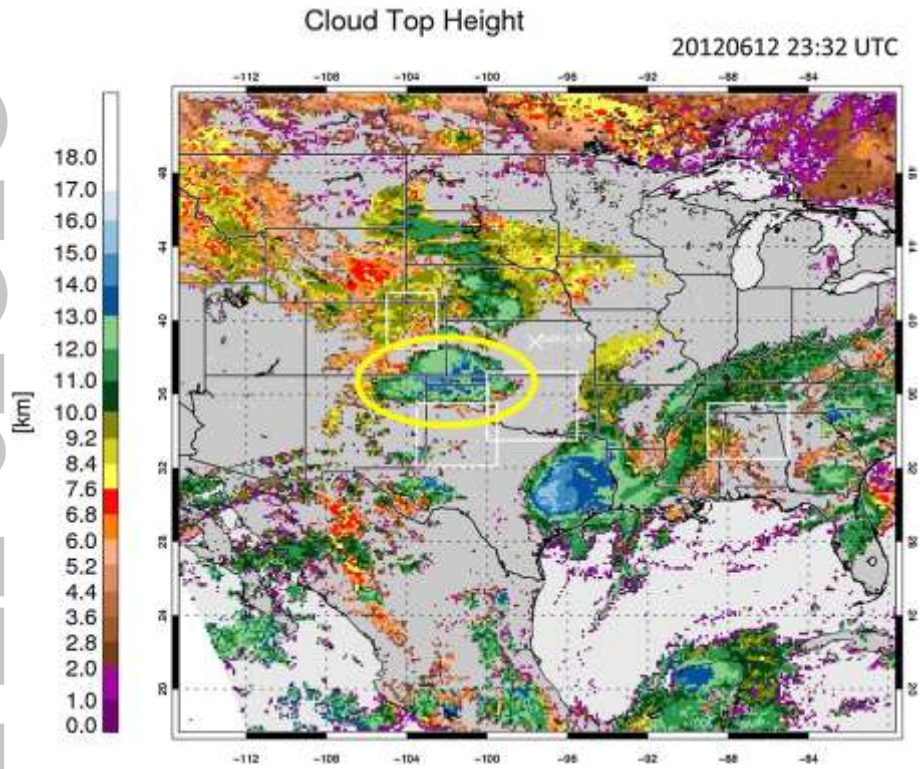


**Figure 11.** Cloud top heights (in km) derived from GOES data on June 12, 2012 at 23:32 UTC (© NCAR/EOL). The yellow circle shows the area of the Falcon operations (squall line probed). The white squares mark the selected DC3 operation areas and the white cross the campaign base in Salina (KS).

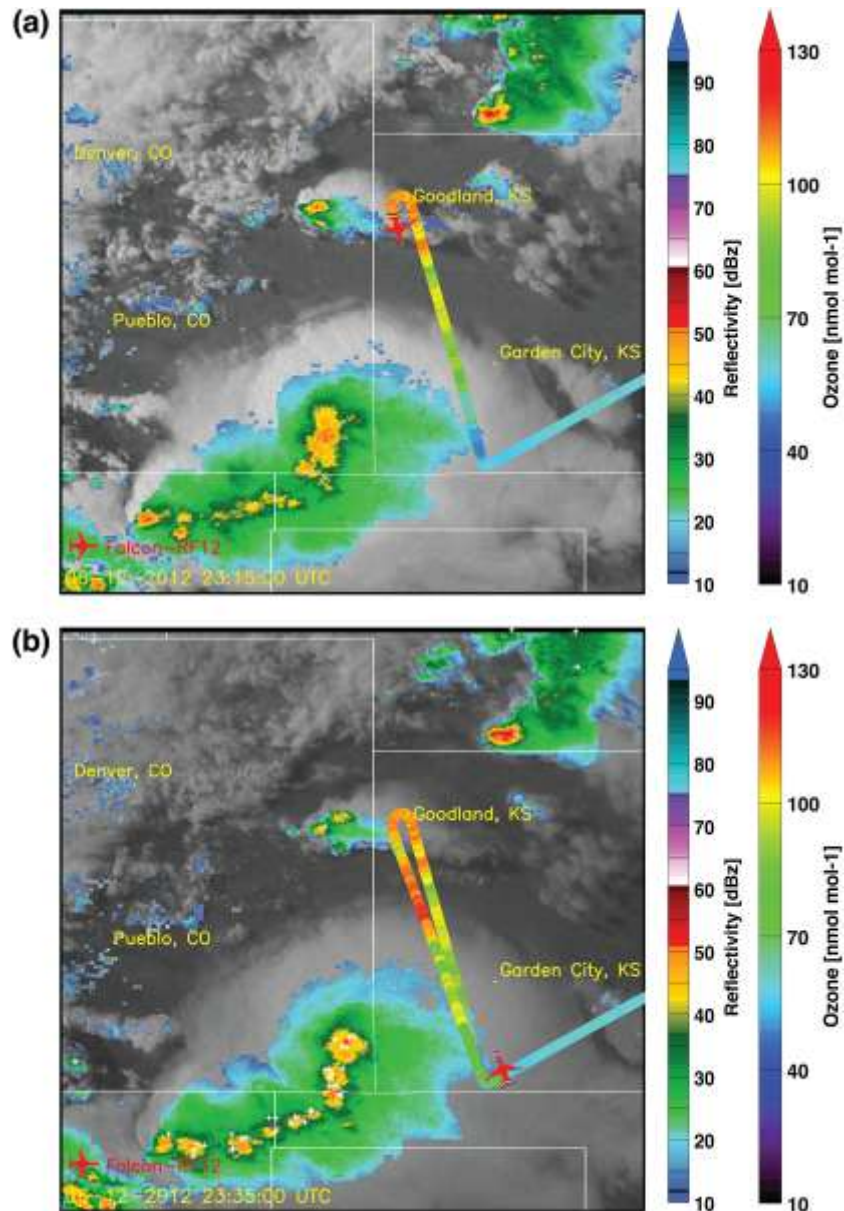


**Figure 12.** Flight tracks of the Falcon (red aircraft) in the evening on June 12, 2012 at 23:15 UTC **(a)** and at 23:35 UTC **(b)**. After the start in Salina, the Falcon approached a squall line, located along the border between Kansas, Oklahoma and Colorado, at low altitudes. Below the anvil outflow the aircraft started to ascend in northerly direction and several cross sections in north-southerly direction followed at different altitudes below, inside and outside the anvil outflow. The flight tracks (color-coded) are superimposed on a GOES IR satellite image (grey), NEXRAD radar reflectivity (colored clouds), and NLDN lightning data (white/pink plus/minus sign for positive/negative flashes). The flight tracks are color-coded according to  $O_3$  mixing ratios along the flight.

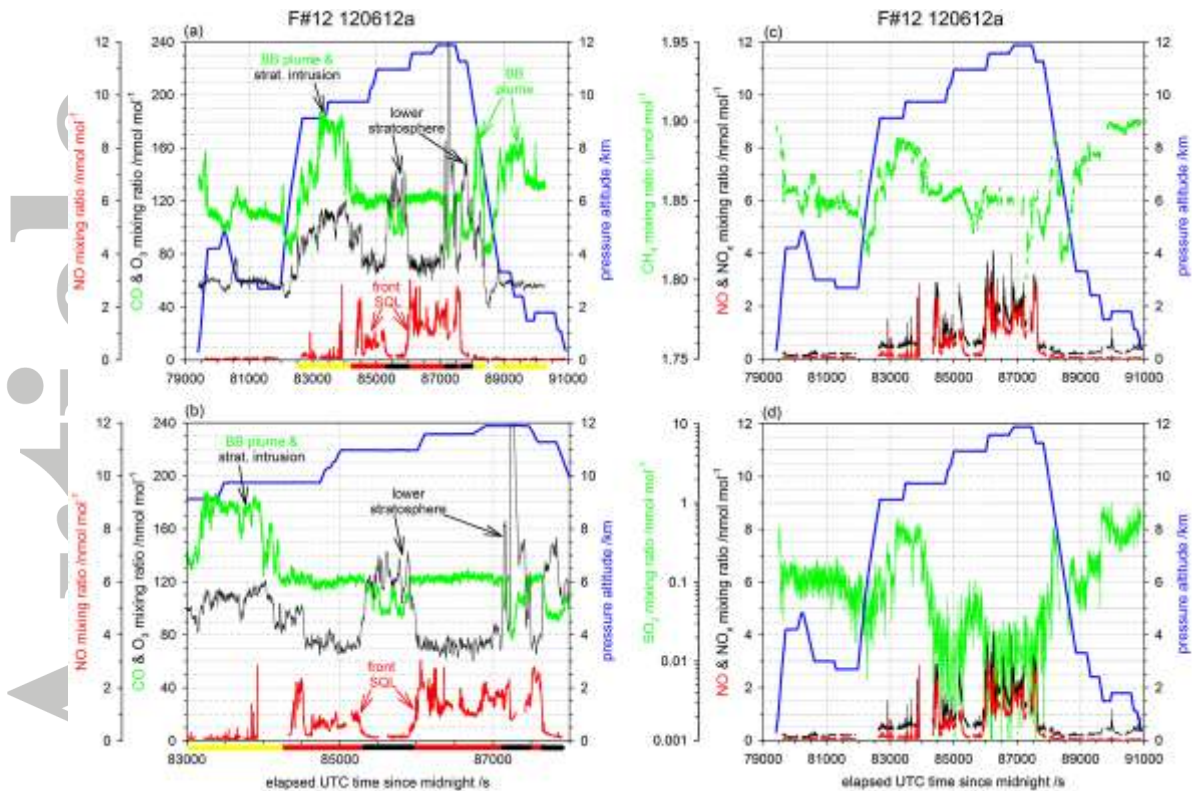


**Figure 13.** Time series of NO, NO<sub>x</sub>, CO, O<sub>3</sub>, SO<sub>2</sub>, CH<sub>4</sub>, and pressure altitude for the Falcon flight on June 12, 2012: complete flight (**a**, **c**, **d**), and selected time period from 83000-88000 s (**b**). Colored bars in (**a**) and (**b**) indicate selected time sequences of the flight with different air masses: BB plume (yellow), stratospheric intrusion/lower stratosphere (black), and fresh squall line (SQL) outflow (red), see also Fig. 16.

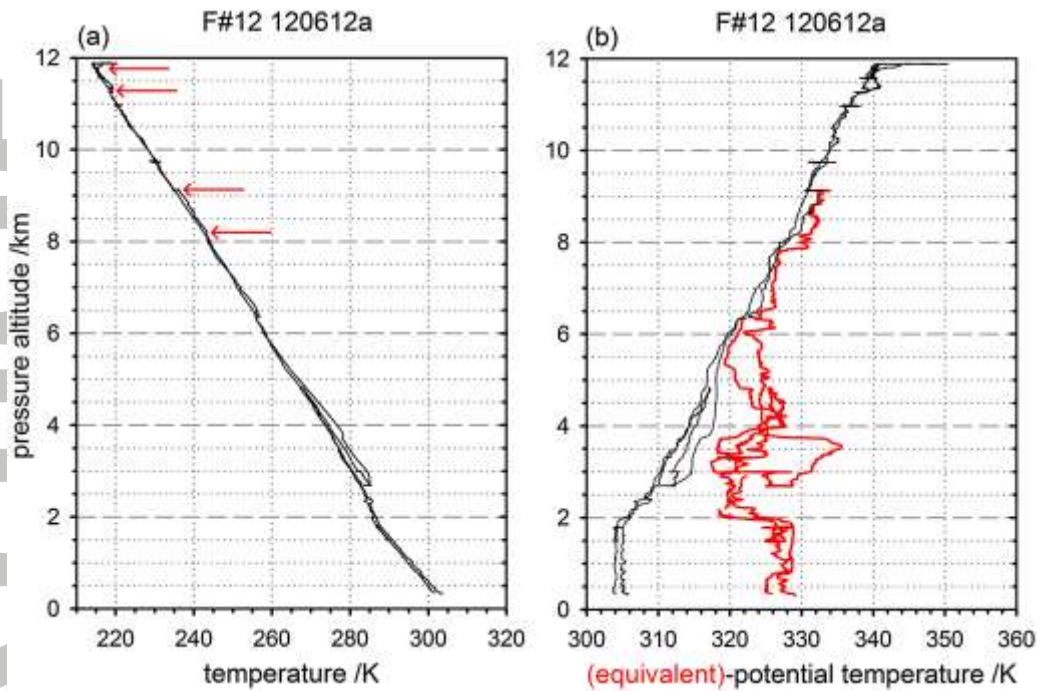


**Figure 14.** Vertical profiles of temperature (a), and (equivalent)-potential temperature (b) derived from Falcon measurements on June 12, 2012. The red arrows indicate two different tropopause levels at 11.2 and 11.8 km, and a stratospheric intrusion between 8.2 and 9.1 km.

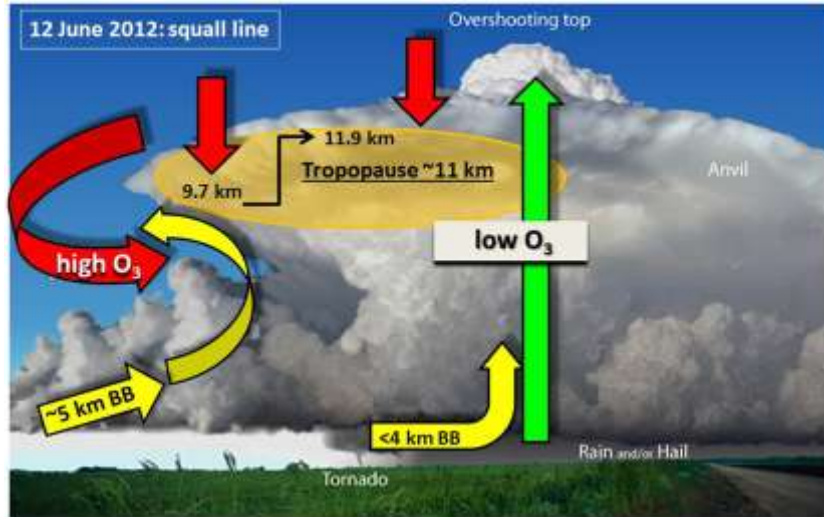


**Figure 15.** Schematic of an isolated, overshooting thunderstorm cell (credit: NOAA National Weather Service, <http://www.srh.noaa.gov/jetstream/tstorms/tstrmtypes.htm>). Superimposed are the major air mass transport pathways (colored arrows) observed during the Falcon flight on June 12, 2012 based on in-situ trace gas measurements (CO and O<sub>3</sub>) within the main vertical (and partly horizontal) extension of the anvil outflow from a squall line (orange shaded area). Emissions from wildfires (BB) and low O<sub>3</sub> mixing ratios are ingested into the overshooting squall line (yellow and green). As a response to the overshooting top, stratospheric air masses are transported downwards along the boundaries of the anvil outflow (red). In addition, emissions from wildfires (BB, yellow) are ingested into towering cumulus along the flanking line of the squall line and mix with a stratospheric intrusion wrapped around the anvil outflow (red).

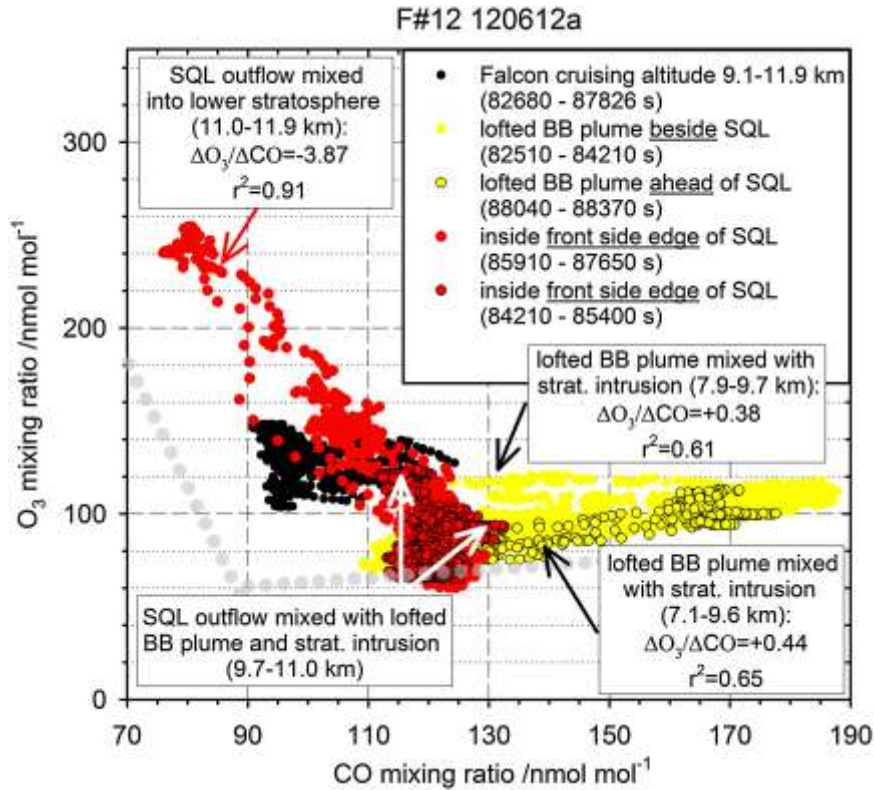


**Figure 16.** O<sub>3</sub>-CO correlations during the Falcon flight on June 12, 2012 for the time period of the stepwise ascent below/inside the squall line (SQL) outflow at cruise altitudes 9.1-11.9 km and the descent to Salina. The correlations in the lofted BB plume and in the anvil outflow of the squall line are marked with yellow and red dots, respectively. The correlation in the free tropospheric and stratospheric background is marked with light gray dots.

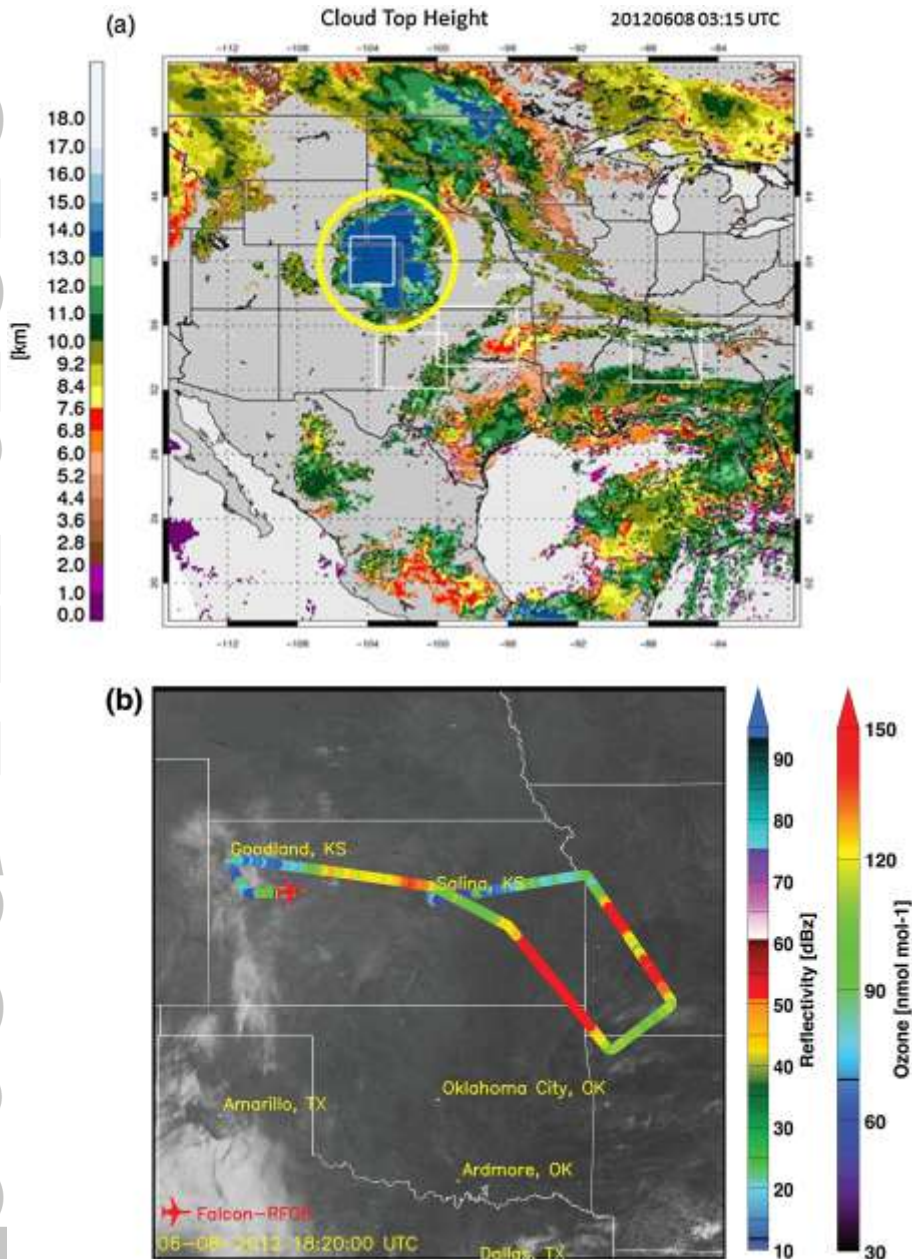


**Figure 17.** Cloud top heights (in km) derived from GOES data on June 8, 2012 at 03:15 UTC over U.S. and Mexico (a) (© NCAR/EOL). The yellow circle marks an extended MCS probed ~15 h later in a decaying stage over Kansas, Missouri and Arkansas (as shown in b). The white squares mark the selected DC3 operation areas and the white cross the campaign base in Salina. In (b) flight tracks of the Falcon (red aircraft) on June 8, 2012 at 18:20 UTC. The flight tracks (color-coded) are superimposed on a GOES IR satellite image (grey) and are color-coded according to O<sub>3</sub> mixing ratios along the flight.



NCAR WRF ARW Forecast ( $\Delta x=3$  km)

8-16 km column LNO<sub>x</sub> Tracer (nmol mol<sup>-1</sup>) 2012-06-08

Wind (in kts) at 11 km 11:00 UTC

2012-06-08

16:00 UTC

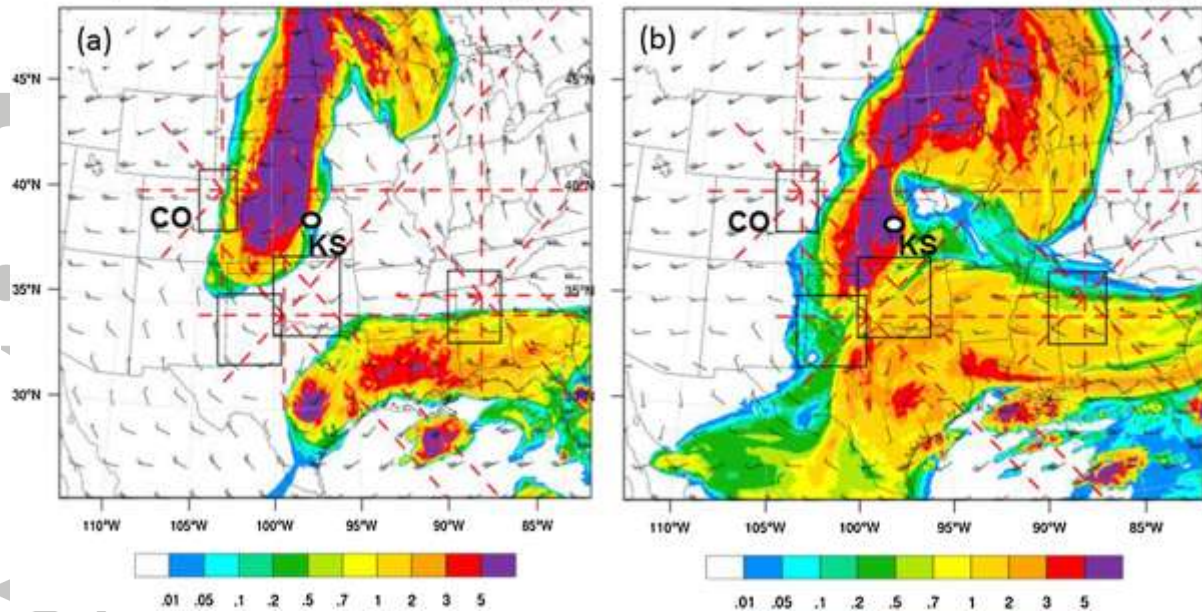


**Figure 18.** NCAR WRF ARW forecast of 8-16 km column LNO<sub>x</sub> tracer (color-coded) and wind barbs at 11 km (black) for June 8, 2012 at 11:00 (a) and 16:00 (b) UTC. The DC3 campaign base (Salina, KS) is marked with a white-black dot. The black squares mark the selected DC3 operation areas and the red dashed lines the available vertical cross sections for the LNO<sub>x</sub> tracer.

Accepted

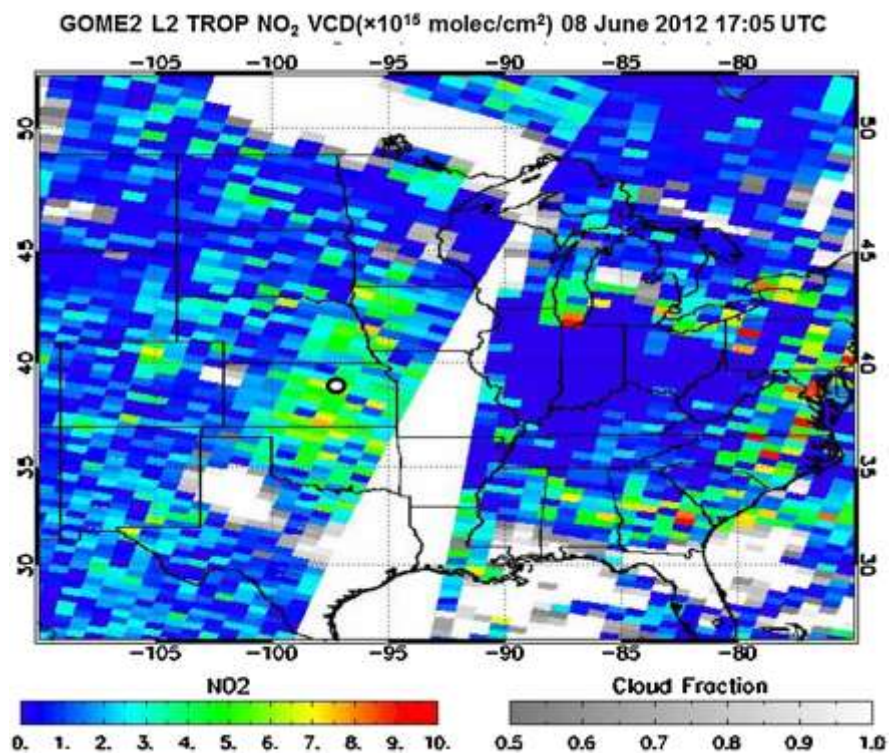


**Figure 19.** Tropospheric NO<sub>2</sub> vertical column densities (VCD) measured by GOME-2 over U.S. and Canada on June 8, 2012 at 17:05 UTC (color-coded). The cloud fraction is superimposed in grey-scales. The DC3 operation site (Salina, KS) is marked with a white-black dot.

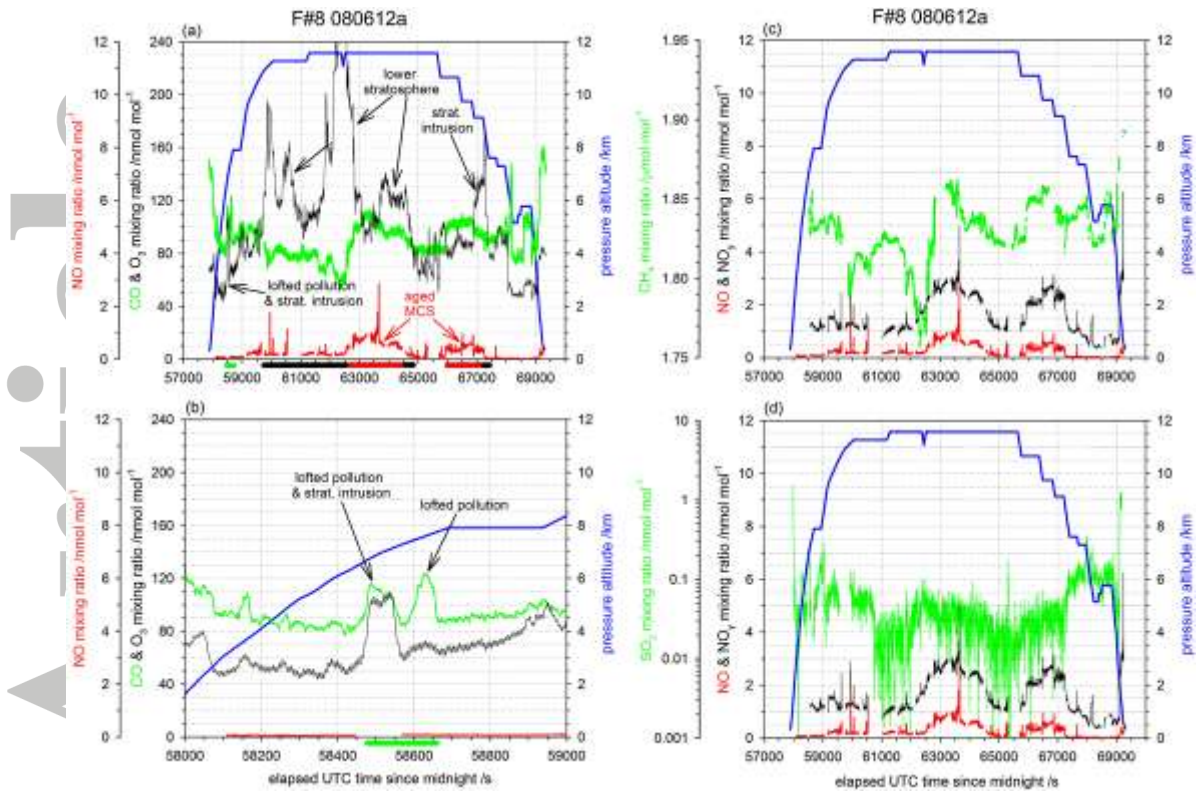


**Figure 20.** Time series of NO, NO<sub>y</sub>, CO, O<sub>3</sub>, SO<sub>2</sub>, CH<sub>4</sub>, and pressure altitude for the Falcon flight on June 8, 2012: complete flight (**a**, **c**, **d**), and selected time period from 58000-59000 s (**b**). Colored bars in (**a**) and (**b**) indicate selected time sequences of the flight with different air masses: lofted pollution (green), stratospheric intrusion/lower stratosphere (black), and aged MCS outflow (red).

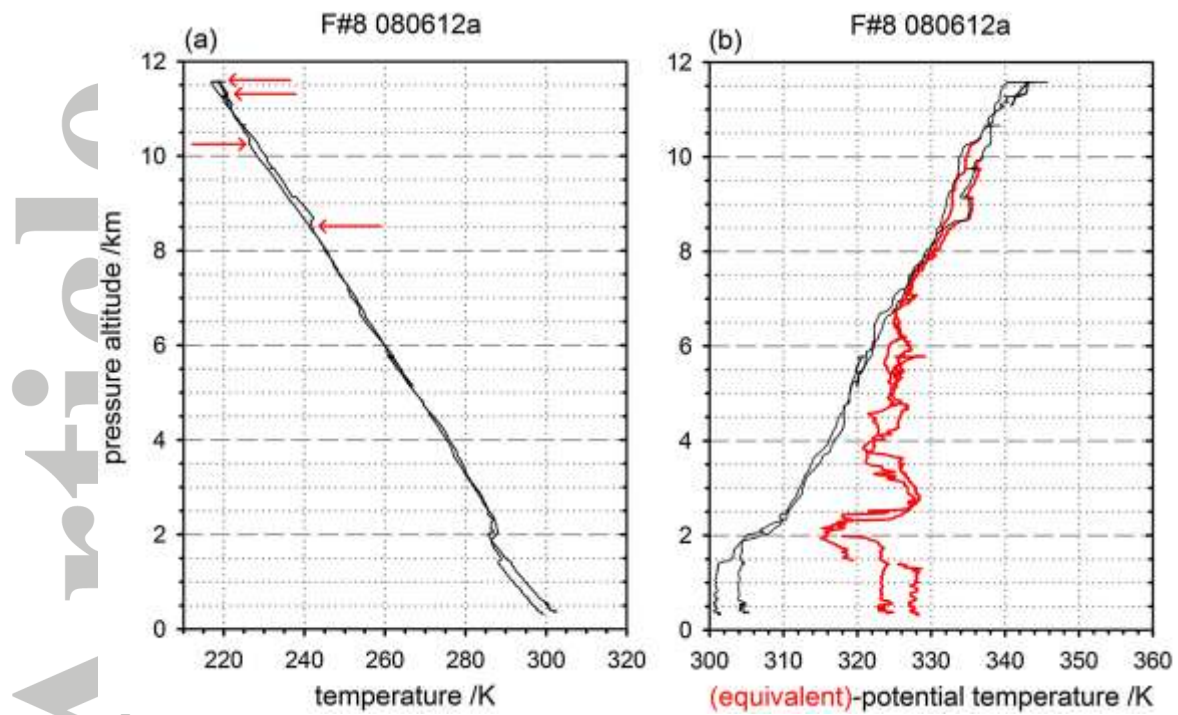


**Figure 21.** Vertical profiles of temperature (a), and (equivalent)-potential temperature (b) derived from Falcon measurements on June 8, 2012. The red arrows indicate two different tropopause levels at 11.2 and 11.6 km, and stratospheric intrusions reaching down to 8.6 and 10.3 km, respectively.

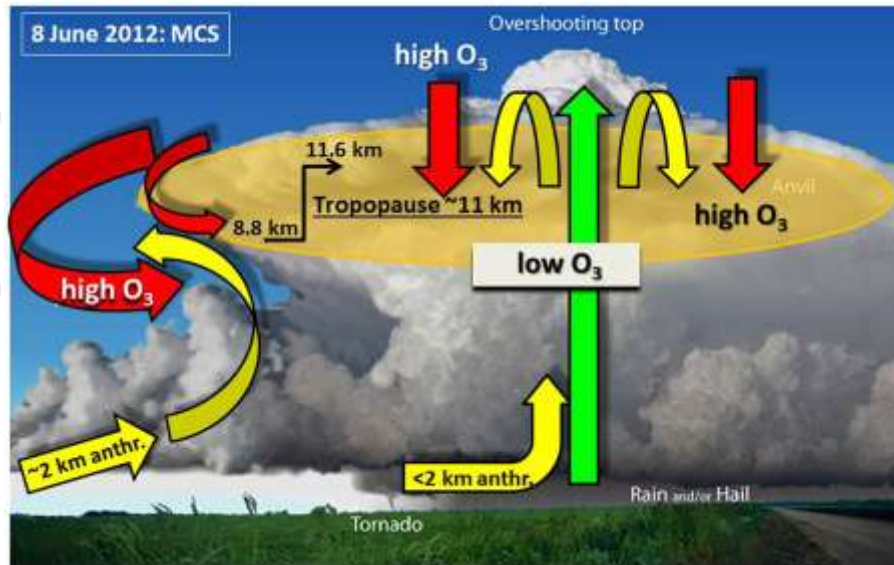


**Figure 22.** Schematic of an isolated, overshooting thunderstorm cell (credit: NOAA National Weather Service, <http://www.srh.noaa.gov/jetstream/tstorms/tstrmtypes.htm>). Superimposed are the major air mass transport pathways (colored arrows) observed during the Falcon flight on June 8, 2012 based on in-situ trace gas measurements (CO and O<sub>3</sub>) within the main vertical and horizontal extension of the anvil outflow from a MCS (orange shaded area). Anthropogenic emissions and low O<sub>3</sub> mixing ratios are ingested into the overshooting MCS (yellow and green). Strong up- and downdrafts within the storm redistribute the ingested pollution. As a response to the overshooting top, stratospheric air masses are transported downwards into the anvil outflow (red). In addition, anthropogenic emissions (yellow) are ingested into towering cumulus along the flanking line of the overshooting MCS and mix with a stratospheric intrusion wrapped around the anvil outflow (red).

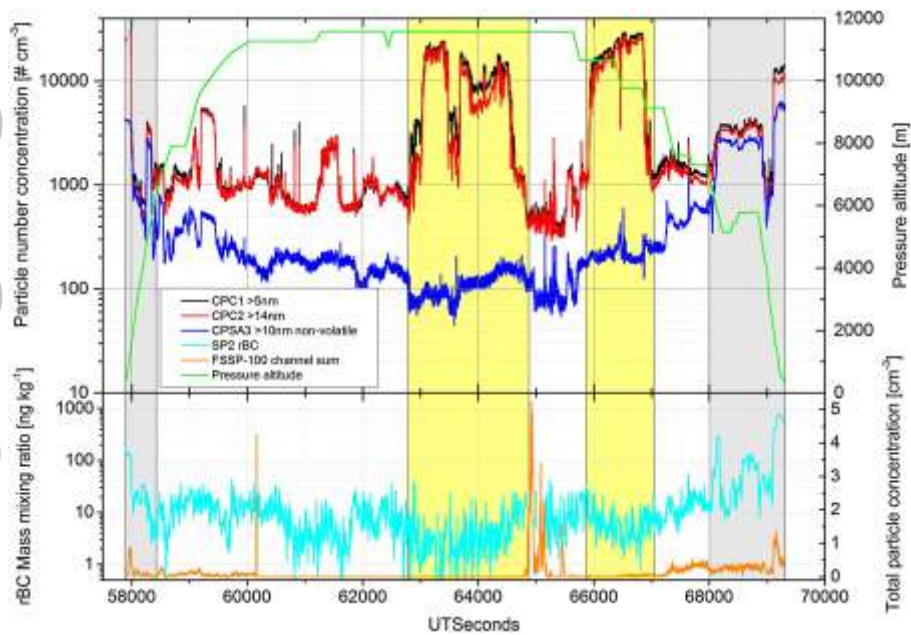


**Figure 23.** Time series of CPC (>5 nm, >14 nm, non-volatile >10 nm), rBC, FSSP-100, and pressure altitude for the Falcon flight on June 8, 2012. Shaded fields (in grey and yellow) indicate time sequences with enhanced concentration of particles >5 nm and >14 nm.

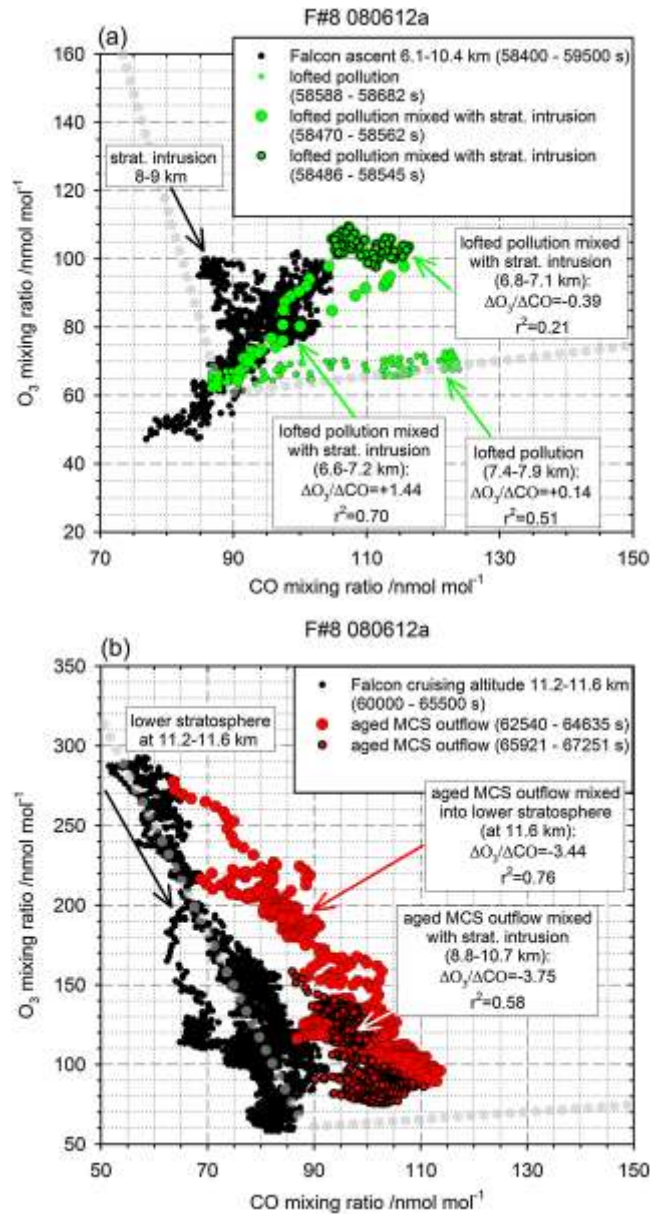


**Figure 24.**  $O_3$ -CO correlations during the Falcon flight on June 8, 2012 for the time period of the ascent from Salina (a). The correlations in lofted pollution plumes are marked with green dots.  $O_3$ -CO correlations during the Falcon flight on June 8, 2012 for the time period of the cruising at 11.2-11.6 km and the descent to Salina (b). The correlations within the anvil outflow of the MCS are marked with red dots. The correlation in the free tropospheric and stratospheric background is marked with light gray dots.